ISSN 1023-9855

Thoracic Medicine

Volume 39 • Number 4 • December 2024

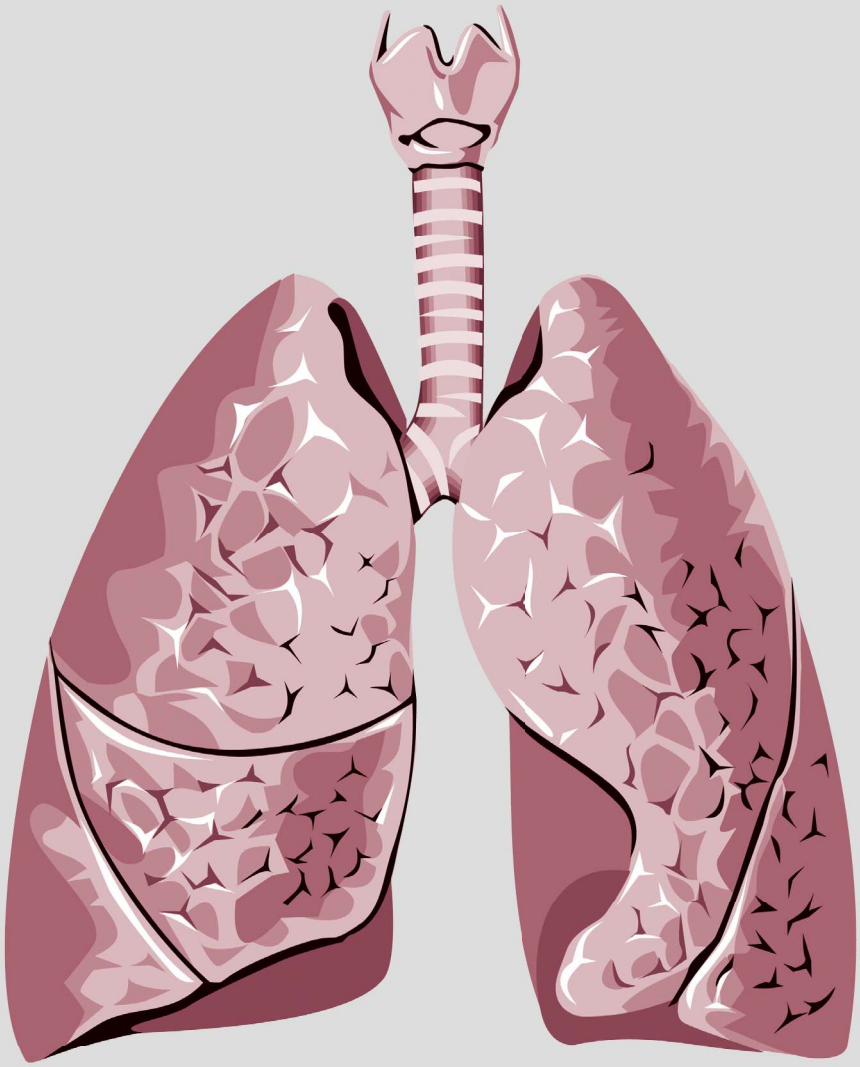

The Official Journal of

Taiwan Society of Pulmonary and Critical Care Medicine

Taiwan Society of Sleep Medicine

Taiwan Society for Respiratory Therapy

Taiwan Society of Tuberculosis and Lung Diseases

Thoracic Medicine

The Official Journal of
Taiwan Society of Pulmonary and Critical Care Medicine
Taiwan Society for Respiratory Therapy
Taiwan Society of Sleep Medicine
Taiwan Society of Tuberculosis and Lung Diseases

Thoracic Medicine

The Official Journal of
Taiwan Society of Pulmonary and Critical Care Medicine
Taiwan Society for Respiratory Therapy
Taiwan Society of Sleep Medicine
Taiwan Society of Tuberculosis and Lung Diseases

Volume 39
Number 4
December 2024

CONTENTS

Orginial Articles

Risk Factors for Hypoxemia in Hospitalized Adult Patients with SARS-CoV-2 Infection ..... 298~309
Jyun-Wei Kang, De-En Lu, I-Ju Chen, Chih-Hsin Lee, Ming-Chia Lee, Yin-Chun Chang

Comparison of Clinical Efficacy of Extended Infusion and Intermittent Bolus Dosing of Piperacillin-Tazobactam in the Treatment of Pneumonia ..... 310~318
Hung-Jui Ko, Kuang-Yao Yang, Wei-Chih Chen, Chia-Hung Chen, Yao-Tung Wang, Pin-Kuei Fu, Li-Kuo Kuo, Chin-Ming Chen, Wen-Feng Fang, Chih-Yen Tu, Shih-Chi Ku, Chuan-Yen Sun

Case Reports

Miliary Tuberculosis and Identification of Tuberculosis-Immune Reconstitution Inflammatory Syndrome (TB-IRIS) – A Case Report ..... 319~326
Chia-Ju Wu Yen-Han Tseng, Sheng-Wei Pan, Jia-Yih Feng, Yuh-Min Chen

Computed Tomography Angiography-Negative Pulmonary Arteriovenous Malformations Diagnosed Using a Lung Perfusion Scan: A Case Report ..... 327~331
Hsin-I Cheng, Chun-Yu Lin, Po-Jui Chang, Horng-Chyuan Lin

An Unusual Presentation of Pulmonary Sequestration: A Case Report ..... 332~335
Yi-Yu Lin, Chin-Feng Wu

MALT Lymphoma Presenting as Bilateral Pulmonary Nodules: A Case Report ..... 336~338
Jen-Hao Chuang

Chylous Effusion in A Patient with Lung Adenocarcinoma Cancer Treated with Rearranged During Transfection-Tyrosine Kinase Inhibitors: A Case Report ..... 339~346
Wei-Hsuan Chang, Gee-Chen Chang

Pulmonary *Trichosporon asahii* Infection in a Patient with Post-COVID-19 Organizing Pneumonia ..... 347~355
Kenneth Yung, Yao-Wen Kuo, Chia-Lin Hsu, Jin-Yuan Shih

Testicular Tuberculosis with Ggeneralized Granuloma – A Case Report ..... 356~358
Che-Min Hsu , Sheng-Wei Pan, Yi-Chen Yeh

Aberrant Lingular Vein-Preserving Left Lower Lobectomy-A Case Report ..... 359~363
Wen-Ruei Tang, Ying-Yuan Chen, Yau-Lin Tseng

Mediastinal Tuberculous Lymphadenitis Diagnosed by EBUS-TBNA – A Case Report ..... 364~368
Tse-Yu Chen, Chung-Kan Peng, Shih-En Tang, Sheng-Huei Wang, Chen-Liang Tsai

Pulmonary Nocardiosis with Multiple Brain Abscesses: A Case Report ..... 369~374
Mei-Yuan Teo, Chen-Yiu Hung, Chun-Hua Wang, Horng-Chyuan Lin

Treatment of Iatrogenic Cervical Esophageal Transection Following Thyroidectomy – A Case Report ..... 375~379
Kai-Yun Hsueh, En-Kuei Tang

Resistance Transformation in Lung Adenocarcinoma Following Targeted Therapy: A Case Study ..... 380~388
Yi-Chen Shao, Wan-Shan Li, Chang-Yao Chu, Sheng-Tsung Chang, Shu-Farn Tey

Risk Factors for Hypoxemia in Hospitalized Adult Patients with SARS-CoV-2 Infection

Jyun-Wei Kang[1], De-En Lu[2,3], I-Ju Chen[4], Chih-Hsin Lee[3,5,6], Ming-Chia Lee[1,7,8,*], Yin-Chun Chang[9,*]

Background: This study identified risk factors for silent hypoxemia in SARS-CoV-2-infected patients, who may have decreased blood oxygen levels, without evident shortness of breath, which complicates diagnosis and treatment.

Methods: This retrospective study included patients with SARS-CoV-2 infection who were hospitalized at 2 facilities from February 1, 2020 to August 31, 2021. First, the patients were categorized based on the presence or absence of hypoxemia at admission. Second, the patients without dyspnea were further divided into groups with and without hypoxemia at admission. We conducted a multivariate logistic regression analysis to identify risk factors for hypoxemia. Finally, we compared the severity of hypoxemia in the patients with and without dyspnea.

Results: Out of 453 patients (excluding those aged under 20 years), 60.9% had hypoxemia. Risk factors included older age, obesity (BMI > 30 mg/m^2), type 2 diabetes mellitus, cough, dyspnea, fever, and muscle weakness. Of the 286 patients without dyspnea, 50.3% had hypoxemia, with hypertension, type 2 diabetes mellitus, cough, fever, and muscle weakness as risk factors. Of the 276 hypoxemic patients, 52.2% lacked dyspnea symptoms. Those with dyspnea tended to need more oxygen therapy, had higher lactate dehydrogenase and D-dimer levels, and had a higher mortality rate.

Conclusion: Older age, obesity, diabetes, cough, fever, and muscle weakness increase hypoxemia risk in SARS-CoV-2 infections. Hypertension, diabetes, cough, fever, and muscle weakness are significant risk factors for silent hypoxemia. ***(Thorac Med 2024; 39: 298-309)***

Key words: COVID-19, SARS-CoV-2, hypoxemia, silent hypoxemia

[1]Department of Pharmacy, New Taipei City Hospital, New Taipei City, Taiwan, [2]Division of Nephrology, Department of Internal Medicine, Wan Fang Hospital, Taipei Medical University, Taipei, Taiwan, [3]Pulmonary Research Center, Wan Fang Hospital, Taipei Medical University, Taipei, Taiwan, [4]Division of Pulmonary Medicine, Department of Internal Medicine, New Taipei City Hospital, New Taipei City, Taiwan, [5]Division of Pulmonary Medicine, Department of Internal Medicine, Wan Fang Hospital, Taipei Medical University, Taipei, Taiwan, [6]Division of Pulmonary Medicine, Department of Internal Medicine, School of Medicine, College of Medicine, Taipei Medical University, Taipei, Taiwan, [7]Department of Nursing, Cardinal Tien College of Healthcare and Management, Taipei, Taiwan, [8]School of Pharmacy, College of Pharmacy, Taipei Medical University, Taipei, Taiwan, [9]Division of Thoracic Surgery, Department of Surgery, Wan Fang Hospital, Taipei Medical University, Taiwan

* Correspondence: Dr. Ming-Chia Lee, Department of Pharmacy, New Taipei City Hospital, New Taipei City, Taiwan, No. 3, Sec. 1, New Taipei Blvd., Sanchong Dist., New Taipei City, Taiwan.
Dr. Yin-Chun Chang, Division of Thoracic Surgery, Department of Surgery, Wan Fang Hospital, Taipei Medical University, Taiwan, No. 111, Sec. 3, Xinglong Rd., Wenshan Dist., Taipei City, Taiwan

Introduction

The emergence of SARS-CoV-2—initially detected in Wuhan, China, in late 2019—marked the onset of a global health crisis unprecedented in recent history [1]. On March 11, 2020, the World Health Organization (WHO) declared COVID-19, caused by SARS-CoV-2, a novel infectious disease, and recognized its potential to have a widespread impact [2]. From 2020 to 2023, the SARS-CoV-2 virus, similar to other RNA viruses, mutated frequently, leading to the emergence of various strains. These variants with differing transmissibility and severity affected the trajectory of the pandemic, posing substantial challenges to healthcare systems worldwide [3]. From January 2020 to March 2021, Taiwan experienced multiple SARS-CoV-2 surges, culminating in its most severe outbreak between May and June 2021, when the case fatality rate reached 5.95%. This severe outbreak was associated with the Alpha variant (B.1.1.7), and was followed by the emergence of the Delta variant, for which the case fatality rate was 0.94% [4].

Common symptoms of SARS-CoV-2 infection include fever, cough, weakness, and dyspnea. Although most cases are mild, a small percentage progress to acute respiratory illness and hypoxia, and require hospitalization, with some cases resulting in death, multiorgan failure, or acute respiratory distress syndrome [5]. Hypoxemia is a common complication in severe COVID-19 cases, and can thus serve as an indicator of disease severity [6]. Some patients with hypoxemia may not have typical signs of respiratory distress, such as dyspnea. This phenomenon is known as "happy" or "silent hypoxemia." This condition can lead to rapid deterioration and increased mortality risk. The primary cause of hypoxemia in patients with SARS-COV-2 infection is a low ratio of ventilation to perfusion in the lungs, exacerbated by right-to-left shunting through consolidated lung areas as the disease progresses [7]. Silent hypoxemia was a major focus in the medical literature between 2019 and 2021 [8-9] and has posed challenges to diagnosing and managing SARS-CoV-2 [10].

Hypoxemia should be identified and monitored carefully in patients with SARS-CoV-2 infection. In this study, we identified risk factors for hypoxemia, particularly in patients with silent hypoxemia, and evaluated whether the absence of dyspnea in patients with hypoxemia correlates with greater disease severity than in those with hypoxemia and dyspnea.

Materials and Methods

Study design

This retrospective study included patients who received a diagnosis of SARS-CoV-2 infection, confirmed through a positive SARS-CoV-2 polymerase chain reaction test from a nasopharyngeal swab, prior to their admission to New Taipei City Hospital or Wan Fang Hospital. The study protocol was reviewed and approved by the Institutional Review Boards of both New Taipei City Hospital (Protocol No.: 111004-E) and Taipei Medical University (Protocol No.: N202109021). We enrolled patients who were aged 20 years or older and hospitalized between February 1, 2021 and August 31, 2021. Demographic, clinical, laboratory, and outcome data were extracted from the patients' electronic medical records from the incident time of admission. All patients were followed until discharge or death.

Hypoxemia was defined as a peripheral

capillary oxygen saturation level below 95% measured by pulse oximetry under ambient air conditions. We categorized patients based on the presence of hypoxemia or the manifestation of dyspnea on admission. In the first analysis, the enrolled patients were split into 2 groups: patients with and those without hypoxemia on admission. In the second analysis, the patients without dyspnea were split into 2 groups: patients with hypoxemia on admission and those without hypoxemia. In the final analysis, the patients with hypoxemia were split into 2 groups: those with dyspnea and those without dyspnea. Several comorbidities—hypertension, type 2 diabetes mellitus, hyperlipidemia, coronary artery disease, chronic kidney disease, chronic viral hepatitis infection, respiratory diseases, and malignancy—were recorded. The respiratory diseases included chronic obstructive pulmonary disease, asthma, and diffuse parenchymal lung diseases.

Statistical analysis

Categorical variables are presented as numbers and percentages (%), and continuous variables are presented as means and standard deviations. The chi-square test or Fisher's exact test was used to analyze categorical variables, and the Student's t-test was employed to evaluate continuous variables. We conducted multivariate logistic regression analysis and calculated adjusted odds ratios (aORs) with 95% confidence intervals (CIs) to identify risk factors for hypoxemia in all the patients and in the group without dyspnea. All variables were included in the multivariate logistic regression analysis, using a backward stepwise approach. We used *p*-values 0.2 as the removal criterion in our automatic selection of variables. We removed variables with *p*-values >0.1 in determining the final model. All tests of significance were 2-tailed, and the α level was set at 0.05. Analyses were performed using R version 4.1 (R Foundation, Indianapolis, IN, USA).

Results

During the study period, a total of 464 patients with confirmed SARS-CoV-2 infection were admitted to 2 hospitals: 184 (39.7%) to Wang Fang Hospital and 280 (60.3%) to New Taipei City Hospital. After excluding 11 patients aged under 20 years, the remaining 453 patients were included in the analysis. Of those 453 patients, 60.9% experienced hypoxemia. The baseline characteristics, symptoms, and mortality of the enrolled patients are listed in Table 1. Significant differences were observed between the patients with and without hypoxemia in terms of baseline characteristics, such as the proportion of those aged ≥65 years (27.1% vs. 49.6%, $p < 0.001$) and the proportion of those with a BMI of ≥30 kg/m^2 (6.2% vs. 15.6%, $p = 0.03$). The Katz index was lower in the hypoxemia group than in the non-hypoxemia group ($p < 0.001$). Furthermore, the prevalence rates of hypertension, type 2 diabetes mellitus, cardiovascular diseases, chronic kidney disease, hepatitis B carrier status, and dyslipidemia were higher in the hypoxemia group than in the non-hypoxemia group ($p < 0.05$). Patients with hypoxemia were significantly more likely to have cough, dyspnea, anorexia, fever, muscle soreness, and muscle weakness. In addition, the mortality rate was significantly higher in the hypoxemia group than in the non-hypoxemia group (1.1% vs. 20.7%, $p < 0.001$).

Table 2 lists the ORs and 95% CIs of the factors associated with hypoxemia in multivariate logistic regression analysis. Hypoxemia was

Table 1. Clinical Characteristics of Hospitalized Patients with SARS-CoV-2 Infection.

	All	Non-hypoxemia $SpO_2 \geqq 95\%$	Hypoxemia $SpO_2 < 95\%$		Absence of dyspnea	Dyspnea	
	n=453	n=177	n=276	*p-value*	n=286	n=167	*p-value*
Age, years	58.45 ± 17.91	50.71 ± 19.03	63.42 ± 15.23	**<0.001**	59.23 ± 18.80	62.26 ± 15.60	**<0.001**
Age group, n (%)				**<0.001**			**0.003**
< 45, n (%)	112 (24.7)	78 (44.1)	34 (12.3)		85 (29.7)	27 (16.2)	
45 ~ 64, n (%)	156 (34.4)	51 (28.8)	105 (38.0)		97 (33.9)	59 (35.3)	
≧65, n (%)	185 (40.8)	48 (27.1)	137 (49.6)	**<0.001**	104 (36.4)	81 (48.5)	**0.011**
Male sex, n (%)	245 (54.1)	91 (51.4)	154 (55.8)	0.361	144 (50.3)	101 (60.5)	**0.037**
Body mass index, kg/m^2	25.22 ± 4.37	24.16 ± 4.0	25.9 ± 4.46	**<0.001**	24.98 ± 4.09	25.63 ± 4.78	0.125
Body mass index group, kg/m^2				**0.01**			0.815
< 18.5	15 (3.5)	7 (4.0)	8 (2.9)		10 (3.5)	5 (3.0)	
≧18.5 to < 24	178 (39.3)	84 (47.5)	94 (34.1)		115 (40.2)	63 (37.7)	
≧24	260 (57.4)	86 (48.9)	174 (63.0)		161 (56.3)	99 (59.3)	
≧30	54 (11.9)	11 (6.2)	43 (15.6)	**0.03**	29 (10.1)	25 (15.0)	0.126
Katz index, score 0-6	5.57 ± 1.45	5.93 ± 0.56	5.34 ± 1.76	**<0.001**	5.77 ± 1.04	5.24 ± 1.91	**0.001**
Smoking, n (%)	61 (13.5)	23 (13.0)	38 (13.8)	0.814	40 (14.0)	21 (12.6)	0.671
Drinking, n (%)	40 (8.8)	13 (7.3)	27 (9.8)	0.372	26 (9.1)	14 (8.4)	0.798
Comorbidities							
Respiratory disease, n (%)	24 (5.3)	6 (3.4)	18 (6.5)	0.147	15 (5.2)	9 (5.4)	0.947
HTN, n (%)	214 (47.2)	61 (34.5)	153 (55.4)	**<0.001**	125 (43.7)	89 (53.3)	**0.049**
T2DM, n (%)	132 (29.1)	29 (16.4)	103 (37.3)	**<0.001**	66 (23.1)	66 (39.5)	**<0.001**
CAD, n (%)	80 (17.7)	23 (13.0)	57 (20.7)	**0.037**	42 (14.7)	38 (22.8)	**0.030**
CKD, n (%)	60 (13.2)	14 (7.9)	46 (16.7)	**0.007**	31 (10.8)	29 (17.4)	**0.048**
HepB, n (%)	52 (11.5)	12 (6.8)	40 (14.5)	**0.012**	29 (10.1)	23 (13.8)	0.242
HepC, n (%)	5 (1.1)	2 (1.1)	3 (1.1)	1.000	2 (0.7)	3 (1.8)	0.281
Dyslipidemia	80 (17.7)	22 (12.4)	58 (21.0)	**0.019**	48 (16.8)	32 (19.2)	0.522
Malignancy, n (%)	29 (6.4)	8 (4.5)	21 (7.6)	0.190	17 (5.9)	12 (7.2)	0.602
Steroid use before COVID, n (%)	3 (0.7)	0 (0.0)	3 (1.1)	0.284	0 (0.0)	3 (1.8)	**0.023**
Symptoms							
Cough, n (%)	307 (67.8)	103 (58.2)	204 (73.9)	**<0.001**	176 (61.5)	131 (78.4)	**<0.001**
Sore throat, n (%)	118 (26.0)	44 (24.9)	74 (26.9)	0.628	80 (28.0)	38 (22.8)	0.222
Dyspnea, n (%)	167 (36.9)	35 (19.8)	132 (47.8)	**<0.001**	NA	NA	
Anosmia, n (%)	42 (9.3)	21 (11.9)	21 (7.6)	0.128	32 (11.2)	10 (6.0)	0.066
Anorexia, n (%)	131 (28.9)	39 (22.0)	92 (33.3)	**0.010**	73 (25.5)	58 (34.7)	**0.037**
Ageusia, n (%)	45 (9.9)	18 (10.2)	27 (9.8)	0.893	29 (10.1)	16 (9.6)	0.848
Fever, n (%)	256 (56.5)	75 (42.4)	181 (65.6)	**<0.001**	148 (51.7)	108 (64.7)	**0.007**
Chillness, n (%)	51 (11.3)	19 (10.7)	32 (11.6)	0.778	28 (9.8)	23 (13.8)	0.196
Headache, n (%)	70 (15.5)	27 (15.3)	43 (15.6)	0.925	41 (14.3)	29 (17.4)	0.389
Diarrhea, n (%)	84 (18.5)	36 (20.3)	48 (17.4)	0.431	48 (16.8)	36 (21.6)	0.207
Chest pain, n (%)	44 (9.7)	13 (7.3)	31 (11.2)	0.173	15 (5.2)	29 (17.4)	**<0.001**
Muscle soreness, n (%)	62 (13.7)	16 (9.0)	46 (16.7)	**0.021**	35 (12.2)	27 (16.2)	0.240
Muscle weakness, n (%)	141 (13.1)	37 (20.9)	104 (37.7)	**<0.001**	82 (28.7)	59 (35.3)	0.140
Hypoxemia, n (%)	276 (60.9)	NA	NA		144 (50.3)	132 (79.0)	**<0.001**
Mortality, n (%)	59 (13.0)	2 (1.1)	57 (20.7)	**<0.001**	17 (5.9)	42 (25.1)	**<0.001**

Acronyms: n, number; CAD, coronary heart disease; CKD, chronic kidney disease; HepB, hepatitis B; HepC hepatitis C; HTN, hypertension; T2DM, type 2 diabetes mellitus.

Table 2. Risk Factors for Hypoxemia in Patients with SARS-CoV-2 Infection, as Determined through Multivariate Logistic Regression

Variables	Adjusted odds ratio	95% Confidence Intervals	*p-value*
Age (≧ 65 years)	1.86	1.17 to 2.95	0.009
BMI (≧ 30 kg/m^2)	2.73	1.27 to 5.59	0.010
Katz index	0.71	0.53 to 0.95	0.020
T2DM	1.81	1.07 to 3.04	0.026
Cough	1.60	1.01 to 2.55	0.046
Dyspnea	2.64	1.64 to 4.24	<0.001
Fever	1.99	1.29 to 3.07	0.002
Muscle weakness	1.84	1.13 to 2.98	0.014

Acronyms: BMI, body mass index; T2DM, type 2 diabetes mellitus

significantly associated with age ≥ 65 years (aOR: 1.86, 95% CI: 1.17 to 2.95, p = 0.009), BMI ≥ 30 kg/m^2 (aOR: 2.73, 95% CI: 1.27 to 5.59, p = 0.01), Katz index (aOR: 0.71, 95% CI: 0.53 to 0.95, p = 0.02), type 2 diabetes mellitus (aOR: 1.81, 95% CI: 1.07 to 3.04, p = 0.026), cough (aOR: 1.60, 95% CI: 1.01 to 2.55, p = 0.046), dyspnea (aOR: 2.64, 95% CI: 1.64 to 4.24, p < 0.001), fever (aOR: 1.99, 95% CI: 1.29 to 3.07, p = 0.002), and muscle weakness (aOR: 1.84, 95% CI: 1.13 to 2.98, p = 0.014).

Of the 286 patients without dyspnea, 49.7% did not experience hypoxemia. The baseline characteristics, symptoms, and mortality of the patients without dyspnea and with or without hypoxemia are presented in Table 3. Significant differences were noted between patients with versus without hypoxemia in terms of the following baseline characteristics: age ≥ 65 years (26.1% vs. 46.5%, p< 0.001), BMI ≥ 30 kg/m^2 (24.32% ± 4.16% vs. 25.63% ± 3.94%, p = 0.007), Katz index (lower in the hypoxemia group; p< 0.001), and prevalence of hypertension, type 2 diabetes mellitus, cardiovascular diseases, chronic kidney disease, hepatitis B carrier status, and dyslipidemia (higher in the hypoxemia group; p< 0.05). Patients with hypoxemia were significantly more likely to have cough, anorexia, fever, muscle soreness, and muscle weakness.

Table 4 lists the ORs and 95% CIs of the factors associated with silent hypoxemia in multivariate logistic regression analysis. Silent hypoxemia was significantly associated with hypertension (aOR: 1.86, 95% CI: 1.08 to 3.23, p= 0.026), type 2 diabetes mellitus (aOR: 2.72, 95% CI: 1.38 to 5.39, p = 0.004), cough (aOR: 1.94, 95% CI: 1.13 to 3.32, p= 0.016), fever (aOR: 2.22, 95% CI: 1.33 to 3.72, p= 0.002), and muscle weakness (aOR: 1.94, 95% CI: 1.08 to 3.48, p= 0.027).

The baseline characteristics of the patients with hypoxemia but with or without dyspnea are presented in Table 5. The results indicated that compared to the patients without dyspnea, patients with dyspnea were more likely to be administered advanced respiratory support, such as a nonrebreathing mask (17.4% vs. 40.9%, p< 0.001), high-flow nasal cannula (6.3% vs. 21.2%, p< 0.001), and mechanical ventilation (13.2% vs. 25.8%, p= 0.008). Furthermore, mortality was higher among patients with dyspnea than among those without (11.1% vs. 31.1%, p< 0.001). Greater percentages

Table 3. Baseline Clinical Characteristics of Hospitalized Patients with SARS-CoV-2 Infection without Dyspnea

	Non-hypoxemia $SpO_2 \geqq 95\%$ n=142	Hypoxemia $SpO_2 < 95\%$ n=144	*p-value*
Age, years	46.69 ± 19.46	62.69 ± 15.69	**<0.001**
Age group, n (%)			**<0.001**
< 45, n (%)	67 (47.2)	18 (12.5)	
45 ~ 64, n (%)	38 (26.8)	59 (41.0)	
≧65, n (%)	37 (26.1)	67 (46.5)	**<0.001**
Male sex, n (%)	70 (49.3)	74 (51.4)	0.723
Body mass index, kg/m^2	24.32 ± 4.16	25.63 ± 3.94	**0.007**
Body mass index group, kg/m^2			0.242
< 18.5	6 (4.2)	4 (2.8)	
≧18.5 to < 24	63 (44.4)	52 (36.1)	
≧24	73 (51.4)	88 (61.1)	
≧30	10 (7.0)	19 (13.2)	0.085
Katz index, score 0-6	5.99 ± 0.168	5.56 ± 1.433	**<0.001**
Smoking, n (%)	18 (12.7)	23 (16.0)	0.426
Drinking, n (%)	12 (8.5)	14 (9.7)	0.708
Comorbidities			
Respiratory disease, n (%)	5 (3.5)	10 (6.9)	0.194
HTN, n (%)	44 (31.0)	81 (56.3)	**<0.001**
T2DM, n (%)	16 (11.3)	50 (34.7)	**<0.001**
CAD, n (%)	14 (9.9)	28 (19.4)	**0.022**
CKD, n (%)	9 (6.3)	22 (15.3)	**0.015**
HepB, n (%)	8 (5.6)	21 (14.6)	**0.012**
HepC, n (%)	1 (0.7)	1 (0.7)	1.000
Dyslipidemia	14 (9.9)	34 (23.6)	**0.002**
Malignancy, n (%)	5 (3.5)	12 (8.3)	0.085
Steroid use before COVID, n (%)	0 (0)	0 (0)	NA
Symptoms			
Cough, n (%)	75 (52.8)	101 (70.1)	**0.003**
Sore throat, n (%)	34 (23.9)	46 (31.9)	0.132
Anosmia, n (%)	19 (13.4)	13 (9.0)	0.243
Anorexia, n (%)	29 (20.4)	44 (30.6)	**0.049**
Ageusia, n (%)	14 (9.9)	15 (10.4)	0.876
Fever, n (%)	55 (38.7)	93 (64.6)	**<0.001**
Chilliness, n (%)	14 (9.9)	14 (9.7)	0.969
Headache, n (%)	24 (16.9)	(11.8)	0.219
Diarrhea, n (%)	27 (19.0)	21 (14.6)	0.316
Chest pain, n (%)	7 (4.9)	8 (5.6)	0.812
Muscle soreness, n (%)	11 (7.7)	24 (16.7)	**0.021**
Muscle weakness, n (%)	28 (19.7)	54 (37.5)	**0.001**

Acronyms: n, number; CAD, coronary heart disease; CKD, chronic kidney disease; HepB, hepatitis B; HepC hepatitis C; HTN, hypertension; T2DM, type 2 diabetes mellitus.

Table 4. Risk Factors for Silent Hypoxemia, as Determined through Multivariate Logistic Regression

Variables	Adjusted odds ratio	95% Confidence Intervals	*p-value*
HTN	1.86	1.08 to 3.23	0.026
T2DM	2.72	1.38 to 5.39	0.004
Cough	1.94	1.13 to 3.32	0.016
Fever	2.22	1.33 to 3.72	0.002
Muscle weakness	1.94	1.08 to 3.48	0.027

Acronyms: HTN, hypertension; T2DM, type 2 diabetes mellitus

Table 5. Clinical Characteristics of Hospitalized Patients with SARS-CoV-2 Infection and Hypoxemia

	Without dyspnea n=144		Dyspnea n=132		*p-value*
Respiratory support					
Nasal cannula, n (%)	136	(94.4)	109	(82.6)	**0.002**
Simple mask, n (%)	45	(31.3)	57	(43.2)	**0.040**
Non-rebreathing mask, n (%)	25	(17.4)	54	(40.9)	**<0.001**
HFNC, n (%)	9	(6.3)	28	(21.2)	**<0.001**
Mechanical ventilation, n (%)	19	(13.2)	34	(25.8)	**0.008**
Medication use					
Remdesivir, n (%)	64	(44.4)	76	(57.6)	**0.029**
Tocilizumab, n (%)	35	(24.3)	44	(33.3)	0.097
NRICM101, n (%)	10	(6.9)	16	(12.1)	0.141
Dexamethasone, n (%)	93	(64.6)	111	(84.1)	**<0.001**
Colchicine, n (%)	13	(9.0)	15	(11.4)	0.521
Monoclonal Ab., n (%)	10	(6.9)	14	(10.6)	0.281
Fluvoxamine, n (%)	4	(2.8)	4	(3.0)	1.000
Laboratory data					
WBC count, x10^3/μL	6.38 ± 3.00	n=143	7.02 ± 4.46	n=132	0.168
Albumin, g/L	3.50 ± 0.51	n=104	3.45 ± 0.57	n=78	0.857
CRP, mg/dL	6.73 ± 6.09	n=131	8.46 ± 8.00	n=124	0.054
Ferritin, ng/mL	1275.90 ± 3158.77	n=94	1306.96 ± 1487.33	n=66	0.941
Procalcitonin, ng/mL	0.34 ± 0.84	n=79	4.07 ± 22.47	n=78	0.147
LDH, U/L	285.82 ± 134.32	n=135	345.45 ± 165.82	n=117	**0.002**
CPK, U/L	176.58 ± 258.37	n=141	235.26 ± 340.55	n=121	0.115
D-dimer, mg/L	1.86 ± 3.45	n=126	3.20 ± 6.59	n=119	**0.049**
Fibrinogen, mg/dL	467.13 ± 188.38	n=52	447.30 ± 185.49	n=38	0.621
Platelet, x10^3/μL	204.69 ± 81.95	n=143	187.38 ± 80.17	n=130	0.079
ESR, mm/hr	31.99 ± 26.40	n=126	33.44 ± 23.50	n=105	0.664
Length of hospitalization, days	18.67 ± 13.36		19.30 ± 14.54		0.711
CVP, n (%)	20	(13.9)	28	(21.2)	0.109
sBSI, n (%)	2	(1.4)	7	(5.3)	0.092
Mortality, n (%)	16	(11.1)	41	(31.1)	**<0.001**

Acronyms: n, number; CRP, C-reactive protein; CPK, creatine kinase; CVP, central venous pressure; ESR, erythrocyte sedimentation rate; HFNC, high flow nasal cannula oxygen; LDH, lactate dehydrogenase; sBSI, secondary bloodstream infection; WBC, white blood count.

of patients with dyspnea received remdesivir (44.4% vs. 57.6%, $p = 0.029$) and dexamethasone (64.6% vs. 84.1%, $p < 0.001$). Patients with dyspnea also had higher levels of lactate dehydrogenase (LDH; 285.82 ± 134.32 vs. 345.45 ± 165.82 U/L, $p = 0.002$) and D-dimer (1.86 ± 3.45 vs. 3.20 ± 6.59 mg/L, $p = 0.049$).

Discussion

This study provides valuable insights into the clinical characteristics and outcomes of patients with SARS-CoV-2 infection, particularly focusing on hypoxemia and its risk factors. Among the enrolled patients, 60.9% experienced hypoxemia on admission. Older age, obesity (BMI > 30 kg/m^2), type 2 diabetes mellitus, cough, dyspnea, fever, and muscle weakness were identified as risk factors for hypoxemia. In addition, 31.8% of patients experienced silent hypoxemia on admission. Hypertension, type 2 diabetes mellitus, cough, fever, and muscle weakness were associated with the occurrence of silent hypoxemia. Finally, our study found that patients with silent hypoxemia did not have worse outcomes than those patients with hypoxemia accompanied by dyspnea.

Hypoxemia is a prognostic indicator of various patient outcomes, including length of hospital stay, intensive care unit (ICU) admission, intubation, and mortality [6]. Thus, understanding the predictors and implications of hypoxemia is crucial for effective managing of SARS-CoV-2 and optimizing of clinical outcomes. One of the key findings of this study is the high prevalence of hypoxemia in patients with SARS-CoV-2 infection -- nearly 60% of the included patients were found to experience this complication. Moreover, the mortality rate was significantly higher in the hypoxemia group than in the non-hypoxemia group, a finding compatible with that of another study [6]. Individuals who are susceptible to hypoxemia should receive early and proactive treatment, including the monitoring of their blood oxygen levels, prompt supplementation of oxygen, and administration of antiviral and steroidal therapies.

Several studies have confirmed that older age is associated with higher disease severity, and a higher risk of mortality in patients with SARS-CoV-2 infection [11-14]. However, the relationship between age and hypoxemia remains controversial. Our study revealed that older age was a significant predictor of hypoxemia; this finding is consistent with those of 2 previous studies [15, 16], but contradicts that of another study [17]. Our cohort's size and age distribution were similar to those in the study conducted by Asleh, *et al* [15]. By contrast, the study conducted by Rai, *et al*. involved a smaller sample of only 73 patients, and the average age of those patients was younger than that in our cohort [17]. In our study, patients aged 65 years and older were more likely to develop hypoxemia, indicating the higher vulnerability of this demographic group to severe SARS-CoV-2 illness. Age-related physiological changes, along with the comorbidities common in older adults, may contribute to this increased susceptibility to hypoxemia and its complications.

We also identified obesity (BMI ≥ 30 kg/m^2) as another independent risk factor for hypoxemia, consistent with the findings of 1 study [15], and corroborating the evidence linking obesity to adverse outcomes in SARS-CoV-2 infection. In another study, BMI was found to increase significantly across acute respiratory distress syndrome severity categories, and was negatively correlated with oxygenation levels

[18]. The mechanistic pathways underlying the aforementioned associations may involve chronic inflammation, impaired respiratory mechanics, and compromised pulmonary function, predisposing individuals with obesity to respiratory compromise during SARS-CoV-2 infection [19-20]. Several studies have indicated that obesity increases the risk of requiring mechanical ventilation [21-23].

The findings regarding comorbidities, such as type 2 diabetes mellitus, hypertension, cardiovascular diseases, chronic kidney disease, hepatitis B carrier status, and dyslipidemia, further indicate the complex interplay between pre-existing health conditions and the clinical course of SARS-CoV-2 infection. These comorbidities, often coexisting in individuals with metabolic syndrome, contribute to systemic inflammation, endothelial dysfunction, and immune dysregulation, thereby exacerbating the severity of SARS-CoV-2 infection and increasing the risk of hypoxemia [24-25]. In addition, type 2 diabetes mellitus was determined to be associated with an increased risk of hypoxemia in patients with SARS-CoV-2 infection in our study; this finding is consistent with those of previous studies [17, 26-27]. Our study revealed that the Katz index, a measure of independence in daily activities, was associated with hypoxemia in patients with SARS-CoV-2 infection. This finding suggests that frailty and functional impairment are indicative of a higher likelihood of severe disease and poor outcomes in such patients.

In this study, symptomatology was determined to play a crucial role in predicting the likelihood of hypoxemia in patients with SARS-CoV-2 infection. Common respiratory symptoms, such as cough and dyspnea, were significantly associated with hypoxemia, consistent with the pathophysiological mechanisms of SARS-CoV-2 infection that primarily affect the respiratory system [6, 17, 27]. In addition, non-respiratory symptoms, such as fever, anorexia, muscle soreness, and muscle weakness, were more prevalent in patients with hypoxemia, indicating the systemic nature of SARS-CoV-2 infection and the diversity of its clinical manifestation [5, 11].

The results of our study revealed that half of the patients without symptoms of dyspnea experienced hypoxemia; this finding is consistent with that of a study conducted in Japan [28]. Furthermore, more than half of the patients who developed hypoxemia did not exhibit dyspnea. Several studies have reported varying prevalence rates of silent hypoxemia, possibly due to differences in the definitions of hypoxemia (the range of oxygen saturation levels measured through pulse oximetry) and the characteristics of the studied populations [28-32]. Silent hypoxemia has been reported in other studies. It indicates the importance of vigilant monitoring and objective assessment of oxygenation status, particularly in asymptomatic or mildly symptomatic patients who may still be at risk of silent hypoxemia [7-9].

Our study indicates that hypertension and type 2 diabetes mellitus are risk factors for silent hypoxemia, a finding that does not entirely align with the results of other research [28]. Few studies have elucidated the association between symptoms of SARS-CoV-2 infection and the occurrence of silent hypoxemia. Our study indicates that symptoms such as cough, fever, and muscle weakness might indicate an increased risk of silent hypoxemia. These findings provide valuable insights for clinical risk stratification and early intervention in this subgroup of patients.

One study reported that asymptomatic hypoxemia was associated with considerably poor outcomes (33.3% of such patients were transferred to the ICU, and 25.9% died) [10]. Still, another study did not find a correlation between silent hypoxemia and more severe disease progression, including mortality [33]. In our study, a comparative analysis of patients with dyspnea versus those without revealed notable differences in disease severity, clinical management, and outcomes. Patients with dyspnea exhibited a more severe disease phenotype, characterized by a higher requirement for advanced respiratory support, a higher likelihood of mortality, and elevated inflammatory markers (LDH and D-dimer). These findings indicate the heterogeneous nature of the presentation of SARS-CoV-2 infection and the importance of tailoring treatment strategies on the basis of an individual patient's profile and disease trajectory.

The major limitation of this study is its retrospective nature. Some parameters were missing in the collected data. The baseline oxygenation demands of these participants were not all presented in the electronic chart, which may lead to systematic bias. The data were collected from only 2 hospitals, limiting the generalizability of our findings. Additional studies are warranted to validate our findings in larger cohorts and to identify more factors affecting the development and progression of hypoxemia in SARS-CoV-2 infection.

Conclusion

This study enhances our understanding of the clinical characteristics and prognostic factors associated with hypoxemia in patients with SARS-CoV-2 infection. The findings underscore the multifactorial nature of hypoxemia, which involves a complex interplay among demographic, clinical, and biochemical factors. Early identification of high-risk patients and targeted interventions to mitigate hypoxemia and its complications are essential for improving outcomes in SARS-CoV-2 infection.

Declarations

Acknowledgments: This manuscript was initially edited by Wallace Academic Editing.

Funding: This study was not funded by any institution.

Ethics approval and consent to participate: The study protocol was reviewed and approved by the Institutional Review Boards of both New Taipei City Hospital (Protocol No.: 111004-E) and Taipei Medical University (Protocol No.: N202109021).

Competing Interests: All authors declare no competing interests.

Author Contributions: J.W.K. wrote the first draft of the manuscript. D.E.L., J.W.K., and I.J.C. reviewed and collected data on patients. J.W.K. and M.C.L. performed statistical analyses. M.C.L. and C.H.L. critically revised the manuscript. All authors contributed to the final version of the manuscript.

References

1. Hui DS, Azhar EI , Madani TA, *et al*. The continuing 2019-nCoV epidemic threat of novel coronaviruses to global health - The latest 2019 novel coronavirus outbreak in Wuhan, China. Int J Infect Dis 2020; 91: 264-66.
2. World Health Organization. Director-General's remarks at the media briefing on 2019-nCoV on 11 February 2020. World Health Organization 2020. 2020; available from: https://www.who.int/dg/speeches/detail/whodirector-general-s-remarks-at-the-media-briefing-on-2019-ncov-

on-11-february-2020.
3. Cascella M, Rajnik M, Aleem A, *et al*. Features, evaluation, and treatment of coronavirus (COVID-19), in StatPearls [Internet]. 2023: Treasure Island (FL): StatPearls Publishing; 2024 Jan.
4. Liu LT, Tsai JJ, Chang K, *et al*. Identification and analysis of SARS-CoV-2 alpha variants in the largest Taiwan COVID-19 outbreak in 2021. Front Med (Lausanne) 2022; 9: 869818.
5. Hu Y, Sun J, Dai Z, *et al*. Prevalence and severity of corona virus disease 2019 (COVID-19): a systematic review and meta-analysis J Clin Virol 2020; 127: 104371.
6. Xie J, Covassin N, Fan Z, *et al*. Association between hypoxemia and mortality in patients with COVID-19. Mayo Clin Proc 2020; 95(6): 1138-47.
7. Dhont S, Derom E, Van Braeckel E, *et al*. The pathophysiology of 'happy' hypoxemia in COVID-19. Respir Res 2020; 21(1): 198.
8. Guo L, Jin Z, Gan TJ, *et al*. Silent hypoxemia in patients with COVID-19 pneumonia: a review. Med Sci Monit 2021; 27: e930776.
9. Cajanding RJM. Silent hypoxia in COVID-19 pneumonia: state of knowledge, pathophysiology, mechanisms, and management. AACN Adv Crit Care 2022; 33(2): 143-53.
10. Brouqui P, Amrane S, Million M, *et al*. Asymptomatic hypoxia in COVID-19 is associated with poor outcome. Int J Infect Dis 2021; 102: 233-38.
11. Izcovich A, Ragusa MA, Tortosa, F, *et al*. Prognostic factors for severity and mortality in patients infected with COVID-19: a systematic review. PLoS One 2020; 15(11): e0241955.
12. Gallo Marin B, Aghagoli G, Lavine K, *et al*. Predictors of COVID-19 severity: a literature review. Rev Med Virol 2021; 31(1): 1-10.
13. Terada M, Ohtsu H, Saito S, *et al*. Risk factors for severity on admission and the disease progression during hospitalisation in a large cohort of patients with COVID-19 in Japan. BMJ Open 2021; 11(6): e047007.
14. Tomidokoro D, Asai Y, Hayakawa K, *et al*. Comparison of the clinical characteristics and outcomes of Japanese patients with COVID-19 treated in primary, secondary, and tertiary care facilities. J Infect Chemother 2023; 29(3): 302-08.
15. Asleh R, Asher E, Yagel O, *et al*. Predictors of hypoxemia and related adverse outcomes in patients hospitalized with COVID-19: a double-center retrospective study. J Clin Med 2021; 10(16).
16. Akinbolagbe YO, Erere O, Ephraim AI, *et al*. Predictors and outcomes of COVID-19 patients with hypoxemia in Lagos, Nigeria. J Pan Afr Thorac Soc 2021; 3(1).
17. Rai DK, Thakur S. Study to identify predictor of hypoxia in COVID-19 infection: a single-center, retrospective study. J Family Med Prim Care 2021; 10(5): 1852-55.
18. Estenssoro E, Loudet CI, Dubin A, *et al*. Clinical characteristics, respiratory management, and determinants of oxygenation in COVID-19 ARDS: a prospective cohort study. J Crit Care 2022; 71: 154021.
19. Malhotra A, Hillman D. Obesity and the lung: 3. Obesity, respiration and intensive care. Thorax 2008; 63(10): 925-31.
20. Luzi L, Radaelli MG. Influenza and obesity: its odd relationship and the lessons for COVID-19 pandemic. Acta Diabetol 2020; 57(6): 759-764.
21. Cai Z, Yang Y, Zhang J. Obesity is associated with severe disease and mortality in patients with coronavirus disease 2019 (COVID-19): a meta-analysis. BMC Public Health 2021; 21(1): 1505.
22. Kalligeros M, Shehadeh F, Mylona EK, *et al*. Association of obesity with disease severity among patients with coronavirus disease 2019. Obesity (Silver Spring) 2020; 28(7): 1200-1204.
23. Hendren NS, de Lemos JA, Ayers C, *et al*. Association of body mass index and age with morbidity and mortality in patients hospitalized with COVID-19: results from the American Heart Association COVID-19 Cardiovascular Disease Registry. Circulation 2021; 143(2): 135-144.
24. de Almeida-Pititto B, Dualib PM, Zajdenverg L, *et al*. Severity and mortality of COVID 19 in patients with diabetes, hypertension and cardiovascular disease: a meta-analysis. Diabetol Metab Syndr 2020; 12: 75.
25. Sen S, Chakraborty R, Kalita P, *et al*. Diabetes mellitus and COVID-19: understanding the association in light of current evidence. World J Clin Cases 2021; 9(28): 8327-39.
26. Estedlal A, Jeddi M, Heydari ST, *et al*. Impacts of diabetes mellitus on clinical and para-clinical parameters among COVID-19 patients. J Diabetes Metab Disord 2021; 20(2): 1211-19.
27. Diendere EA, Sondo KA, Ouédraogo AR, *et al*. Predictors of severe hypoxemia among COVID-19 patients in

Burkina Faso (West Africa): findings from hospital-based cross-sectional study. Int J Infect Dis 2021; 108: 289-95.
28. Akiyama Y, Morioka S, Asai Y, *et al*. Risk factors associated with asymptomatic hypoxemia among COVID-19 patients: a retrospective study using the nationwide Japanese registry, COVIREGI-JP. J Infect Public Health 2022; 15(3): 312-14.
29. Alhusain F, Alromaih A, Alhajress G, *et al*. Predictors and clinical outcomes of silent hypoxia in COVID-19 patients, a single-center retrospective cohort study. J Infect Public Health 2021; 14(11): 1595-99.
30. Garcia-Grimshaw M, Flores-Silva FD, Chiquete E, *et al*. Characteristics and predictors for silent hypoxemia in a cohort of hospitalized COVID-19 patients. Auton Neurosci 2021; 235: 102855.
31. Hayakawa K, Morioka S, Asai Y, *et al*. Predictors of silent hypoxia in hospitalized patients with COVID-19 in Japan. J Infect Chemother 2022; 28(10): 1436-1438.
32. Okuhama A, Ishikane M, Hotta M, *et al*. Clinical and radiological findings of silent hypoxia among COVID-19 patients. J Infect Chemother 2021; 27(10): 1536-38.
33. Sirohiya P, Elavarasi A, Sagiraju HJR, *et al*. Silent hypoxia in coronavirus disease-2019: is it more dangerous? - a retrospective cohort study. Lung India 2022; 39(3): 247-53.

Comparison of Clinical Efficacy of Extended Infusion and Intermittent Bolus Dosing of Piperacillin-Tazobactam in the Treatment of Pneumonia

Hung-Jui Ko[1], Kuang-Yao Yang[1,2], Wei-Chih Chen[1,3], Chia-Hung Chen[4], Yao-Tung Wang[5], Pin-Kuei Fu[6], Li-Kuo Kuo[7], Chin-Ming Chen[8], Wen-Feng Fang[9], Chih-Yen Tu[4], Shih-Chi Ku[10], Chuan-Yen Sun[1,2]

Introduction: Pneumonia is a significant cause of morbidity and mortality worldwide. Beta-lactam antibiotic is a choice as an empirical treatment for pneumonia. Based on pharmacodynamic and pharmacokinetic characteristics, extended infusion beta-lactam antibiotic had a potentially better outcome than intermittent bolus dosing. This study aimed to compare the effectiveness of intermittent bolus dosing of piperacillin-tazobactam (PIP-TAZ) and extended infusion of PIP-TAZ in the treatment of pneumonia patients in Taiwan.

Methods: This retrospective study enrolled adult patients diagnosed with either severe community-acquired pneumonia (SCAP) or nosocomial pneumonia across 9 hospitals in Taiwan from March 1, 2018 to May 30, 2019. Primary outcome was clinical cure rate, while secondary outcomes included clinical effectiveness and in-hospital mortality.

Results: A total 1212 patients with pneumonia were included, of which 639 received intermittent bolus dosing of PIP-TAZ and 34 received extended infusion of PIP-TAZ. After propensity score matching using the Charlson comorbidity index, the clinical cure rate and clinical effectiveness were similar in both groups. However, in the SCAP group, the intermittent bolus group demonstrated higher rates of clinical cure and effectiveness than the extended infusion group (clinical cure rate: 94.4% vs 61.1%, $p = 0.016$; clinical effectiveness: 94.4% vs 66.7%, $p = 0.035$).

Conclusion: For the treatment of nosocomial pneumonia, intermittent bolus dosing of PIP-TAZ was non-inferior to an extended infusion strategy. Moreover, intermittent bolus dosing of PIP-TAZ demonstrated higher potency in treating SCAP than the extended infusion strategy. ***(Thorac Med 2024; 39: 310-318)***

Key words: piperacillin-tazobactam, pneumonia, extended infusion

[1]Department of Chest Medicine, Taipei Veterans General Hospital, Taipei, Taiwan, [2]School of Medicine, National Yang Ming Chiao Tung University, Taipei, Taiwan, [3]Institute of Emergency and Critical Care Medicine, National Yang Ming Chiao Tung University, Taipei, Taiwan, [4]Division of Pulmonary and Critical Care Medicine, Department of Internal Medicine, China Medical University Hospital, Taichung, Taiwan, [5]Division of Pulmonary Medicine, Department of Internal Medicine, Chung Shan Medical University Hospital, Taichung, Taiwan, [6]Department of Medical Research, Taichung Veterans General Hospital, Taichung, Taiwan, [7]Department of Critical Care Medicine, MacKay Memorial Hospital, Taipei, Taiwan, [8]Department of Intensive Care Medicine, Chi Mei Medical Center, Tainan, Taiwan, [9]Division of Pulmonary and Critical Care Medicine, Department of Internal Medicine, Kaohsiung Chang Gung Memorial Hospital, Kaohsiung, Taiwan, [10]Division of Chest Medicine, Department of Internal Medicine, National Taiwan University Hospital, Taipei, Taiwan

Address reprint requests to: Dr. Chuan-Yen Sun, Department of Chest Medicine, 14F, No.201, Sec. 2, Shipai Rd., Beitou District, Taipei City, Taiwan.

Introduction

Community-acquired pneumonia (CAP), acquired outside of health care settings, imposes a significant burden, with 1 million hospitalizations and 100,000 deaths annually in the United States [1]. Hospital-acquired pneumonia (HAP), which develops 48 hours after hospitalization, and ventilator-associated pneumonia (VAP), which occurs in patients on mechanical ventilation for more than 48 hours, are both common causes of nosocomial infections [2]. CAP and nosocomial pneumonia are significant causes of morbidity and mortality worldwide, and are deserving of clinical awareness by healthcare providers.

Antibiotic treatment is the essential means of pneumonia management and plays a crucial role in reducing mortality. Beta-lactam antibiotics are commonly chosen agents for empirical treatment of CAP, HAP, and VAP, due to their potent clinical efficacy. Beta-lactam antibiotics are bactericidal and demonstrate time-dependent killing [3]. Clinical efficacy depends on the duration of free drug concentration exceeding the pathogen's minimum inhibitory concentration.

Piperacillin-tazobactam (PIP-TAZ) is a combination of beta-lactam and beta-lactamase inhibitor that is commonly used in controlling various infections. Previous studies have compared intermittent bolus infusion and extended infusion of PIP-TAZ. Some observational studies showed the mortality benefit of extended infusion [4-6]. However, there is still limited comparative data on different administration strategies in the local data in Taiwan. Therefore, this study aimed to evaluate the clinical efficacy of intermittent bolus dosing versus extended infusion of PIP-TAZ for the treatment of patients with severe CAP (SCAP), HAP and VAP.

Materials and methods

Study Design and Data Collection

This study was a retrospective analysis, using clinical information from the BATTLE study. The BATTLE database was implemented between March 2018 and May 2019 at 8 medical centers and 1 regional hospital in Taiwan, and investigated the efficacy and safety of PIP-TAZ and cefoperazone-sulbactam (CFP-SUL) in the management of SCAP and nosocomial pneumonia. Adult patients diagnosed with SCAP, HAP and VAP were treated empirically with PIP-TAZ and CFP-SUL for at least 5 days. The diagnosis of pneumonia was made as: (a) development of new or progressive pulmonary infiltrates on chest radiographs; plus (b) presence of 2 or more of the following: cough, fever, hypothermia, purulent sputum or bronchial aspirate, hypoxemia, and characteristic physical signs [7]. The definition of SCAP was based on the American Thoracic Society and Infectious Disease Society of America guidelines [8]. The dose of PIP-TAZ (2 g/0.25 g) was 4.5 g every 8 h or 3.375 g every 6 h, and the dose of CFP-SUL (1 g/1 g) was 4 g every 12 h. The infusion duration of extended-infusion PIP-TAZ was at least 3 hours. Patients' baseline characteristics, underlying diseases, pneumonia severity, microbiological information, and clinical outcomes were collected retrospectively after ethical approval by the research ethics committee or institutional review board of each participating site. Informed consent was not required due to the retrospective design. All methods were performed in accordance with the Declaration of Helsinki.

Definitions of clinical outcomes

The primary outcome was clinical cure rate, defined as the proportion of patients in which the clinical signs and symptoms resolved or improved within 7 days of the end of treatment, without additional management. Clinical failure was defined as any 1 of the following: (a) worsening or persistent signs and symptoms and requirement of additional antibiotics; (b) death due to pneumonia after 3 days of antibiotic treatment; (c) progression of pneumonia and development of lung abscess or empyema. The indeterminate outcomes included transferal to another hospital, refusal of further treatment, death due to pneumonia within 2 days of antibiotic treatment, death due to a cause other than pneumonia, incomplete treatment due to allergy, severe adverse events, or other personal reasons.

The secondary outcomes were the clinically effective rate and in-hospital mortality. Clinical effectiveness was defined as the improvement of clinical symptoms and signs, radiographic presentation, and inflammation markers, such as white blood cell counts, C-reactive protein, and procalcitonin levels. Clinical ineffectiveness was defined as when any 1 of the 3 criteria was not met. Indeterminate effectiveness was defined as when the above 3 criteria could not be evaluated.

Statistical analysis

Continuous variables were reported as means with standard deviation or medians with interquartile range. Differences in continuous variables were compared using independent t tests, Kruskal-Wallis tests or 1-way ANOVA. Meanwhile, categorical variables were reported as the number of patients and percentages. Differences in categorical variables were examined using the chi-square test or Fisher's exact test. To balance confounding factors and baseline characteristics, we used propensity score matching (PSM) with the Charlson comorbidity index (CCI) between 2 groups. Statistical significance was set at $p < 0.05$. All statistical analyses were performed using SPSS Version 20.0 (IBM Corp., Armonk, NY, USA).

Results

Baseline characteristics

During the study period, a total of 1212 patients with pneumonia were enrolled. The baseline characteristics of all patients are shown in Table 1. Of these patients, 539 received CFP-SUL, 639 received intermittent bolus dosing of PIP-TAZ, and 34 received extended infusion of PIP-TAZ. The mean age of patients receiving extended infusion of PIP-TAZ was 72.9 ± 16.98 years and 28 (82.4%) were male. Age and gender were similar in the 3 groups (Table 1). Of the patients treated with extended infusion of PIP-TAZ, 18 were diagnosed with SCAP and 16 with nosocomial pneumonia. Following PSM by adjusting the CCI, 34 patients in each group receiving either intermittent bolus dosing of PIP-TAZ or extended infusion of PIP-TAZ were subjected to further analysis. In the overall subjects, there were no significant differences in age, gender, SOFA score and underlying comorbidities between patients receiving intermittent bolus dosing or extended infusion of PIP-TAZ, except that the prevalence of a solid tumor was significantly higher in the extended-infusion PIP-TAZ group (2.9% vs 17.6%, $p = 0.046$) (Table 2). In the SCAP group, the CURB-65 score was higher in those receiving extended infusion of PIP-TAZ than in those with intermittent bolus administration (2.00 ± 0.97 vs 2.94 ± 1.00,

Table 1. Baseline Characteristics of Patients Receiving CFP-SUL, Intermittent Bolus Dosing PIP-TAZ and Extended-Infusion PIP-TAZ

Variables	CFP-SUL n=539	Intermittent bolus dosing PIP-TAZ n=639	Extended-infusion PIP-TAZ n=34	*p*
Age, mean±SD	74.8±14.84	75.1±14.82	72.9±16.98	0.849
Male gender, n (%)	372 (69.0%)	451 (70.6%)	28 (82.4%)	0.246
CCI, mean±SD	6.3±2.83	5.7±2.61	5.6±3.13	<0.001*
SOFA score, mean±SD	5.4±2.99	6.6±3.83	8.0±3.97	0.001*
Underlying disease, n (%)				
Heart failure	88 (16.3%)	97 (15.2%)	4 (11.8%)	0.711
Myocardial infarction	55 (10.2%)	43 (6.7%)	1 (2.9%)	0.050
Cerebrovascular disease	79 (14.7%)	51 (8.0%)	3 (8.8%)	0.001*
Dementia	165 (30.6%)	104 (16.3%)	3 (8.8%)	<0.001*
Chronic pulmonary disease	147 (27.3%)	168 (26.3%)	11 (32.4%)	0.714
Chronic kidney disease	82 (15.2%)	102 (16.0%)	7 (20.6%)	0.691
Solid tumor	50 (9.3%)	52 (8.1%)	6 (17.6%)	0.153
Connective tissue disease	27 (5.0%)	30 (4.7%)	0 (0.0%)	0.408

CFP-SUL = cefoperazone-sulbactam, PIP-TAZ = piperacillin-tazobactam, SD = standard deviation, CCI = Charlson comorbidity index, n = number
* $p < 0.05$

Table 2. Baseline Characteristics of Patients Receiving Intermittent Bolus Dosing PIP-TAZ and extended-infusion PIP-TAZ after Propensity Score Matching with the Charlson Comorbidity index

Variables	Intermittent bolus dosing PIP-TAZ n=34	Extended infusion PIP-TAZ n=34	*p*
Age, mean±SD	72.16±15.64	72.89±16.98	0.853
Male gender, n (%)	24 (70.6%)	28 (82.4%)	0.253
SOFA score, mean±SD	7.00±4.95	8.00±3.97	0.678
Underlying disease, n (%)			
Heart failure	5 (14.7%)	4 (11.8%)	0.720
Myocardial infarction	2 (5.9%)	1 (2.9%)	0.555
Cerebrovascular disease	1 (2.9%)	3 (8.8%)	0.303
Dementia	6 (17.6%)	3 (8.8%)	0.283
Chronic pulmonary disease	7 (20.6%)	11 (32.4%)	0.272
Chronic kidney disease	6 (17.6%)	7 (20.6%)	0.758
Solid tumor	1 (2.9%)	6 (17.6%)	0.046*
Connective tissue disease	3 (8.8%)	0 (0.0%)	0.076

PIP-TAZ = piperacillin-tazobactam, SD = standard deviation, n = number
* $p < 0.05$

Table 3. Clinical Outcomes of Patients Receiving Intermittent Bolus Dosing PIP-TAZ and Extended-Infusion PIP-TAZ

Variables	Intermittent bolus dosing PIP-TAZ n=639	Extended-infusion PIP-TAZ n=34	*p*
Primary outcome, n (%)			
Clinical cure	515 (80.7%)	24 (70.6%)	0.118
Failure or indeterminate	123 (19.3%)	10 (29.4%)	
Secondary outcome, n (%)			
Clinical effectiveness	530 (82.9%)	25 (73.5%)	0.276
Ineffectiveness or indeterminate	109 (17.1%)	9 (26.5%)	
In-hospital mortality, n (%)	118 (18.5%)	8 (23.5%)	0.752

PIP-TAZ = piperacillin-tazobactam, n = number

$p = 0.010$) (Table S1), and the prevalence of a solid tumor was significantly higher in those receiving extended-infusion PIP-TAZ in the HAP/VAP group than in the intermittent bolus group (0% vs 33.3%, $p = 0.014$) (Table S2).

Treatment outcomes

The clinical cure rate of intermittent bolus dosing of PIP-TAZ was 80.7%, which was similar to that of the extended-infusion group (Table 3). Regarding the secondary outcome, the clinical effectiveness rate of the intermittent bolus dosing group was 82.9%, and this was also comparable to that of the extended-infusion group. In addition, there was no significant difference in in-hospital mortality between the intermittent bolus dosing group and the extended-infusion group (18.5% vs 23.5%, $p = 0.752$). After PSM using the CCI, there was no significant difference between the 2 groups in both primary outcome and secondary outcome among the overall subjects (Figure 1 and Table 4). In HAP/VAP patients, there was no difference between 2 groups regardless of clinical cure rate or effective rate after PSM (86.7% vs 80.0%, $p = 0.624$; 86.7% vs 80.0%, $p = 0.624$ (Figure 3). However, the clinical cure rate and clinical effectiveness rate among the

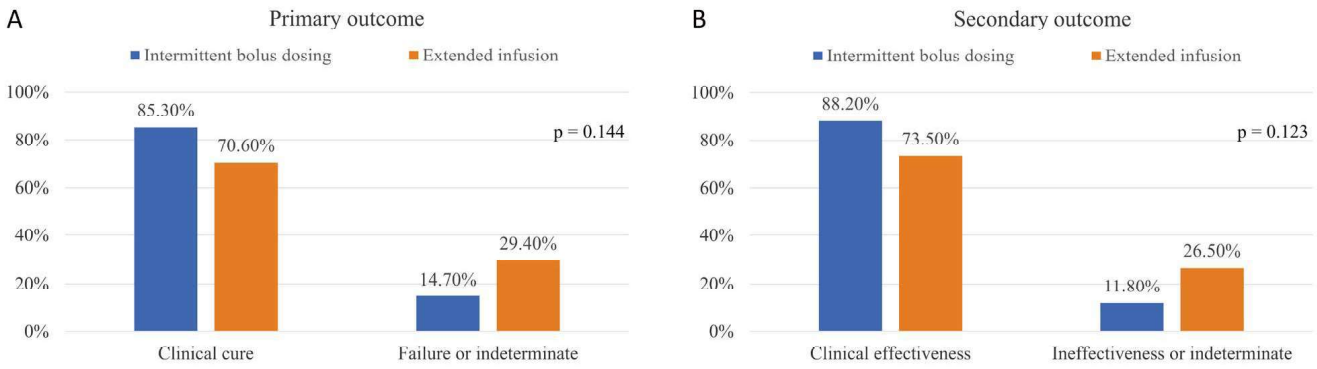

Fig. 1. Primary (A) and secondary (B) outcome of all patients receiving intermittent bolus dosing or extended-infusion piperacillin-tazobactam for pneumonia after propensity score matching with the Charlson comorbidity index.

Table 4. Clinical Outcomes of Patients Receiving Intermittent Bolus Dosing PIP-TAZ and Extended-infusion PIP-TAZ after Propensity Score Matching with the Charlson Comorbidity Index

Variables	Intermittent bolus dosing PIP-TAZ n=34	Extended-infusion PIP-TAZ n=34	*p*
Primary outcome, n (%)			
Clinical cure	29 (85.3%)	24 (70.6%)	0.144
Failure or indeterminate	5 (14.7%)	10 (29.4%)	
Secondary outcome, n (%)			
Clinical effectiveness	30 (88.2%)	25 (73.5%)	0.123
Ineffectiveness or indeterminate	4 (11.8%)	9 (26.5%)	
In-hospital mortality, n (%)	5 (14.7%)	8 (23.5%)	0.355

PIP-TAZ = piperacillin-tazobactam, n = number

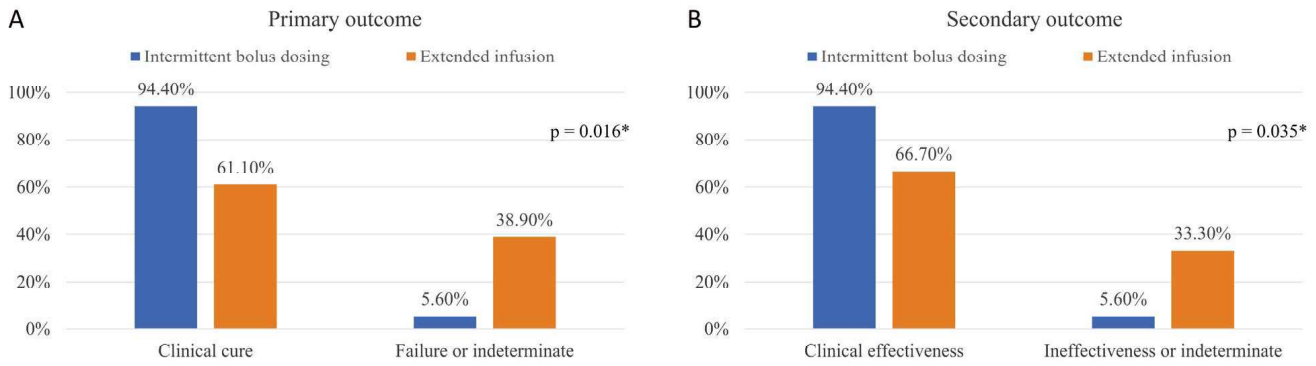

Fig. 2. Primary (A) and secondary (B) outcome of patients receiving intermittent bolus dosing or extended-infusion piperacillin-tazobactam for severe community-acquired pneumonia after propensity score matching with the Charlson comorbidity index.

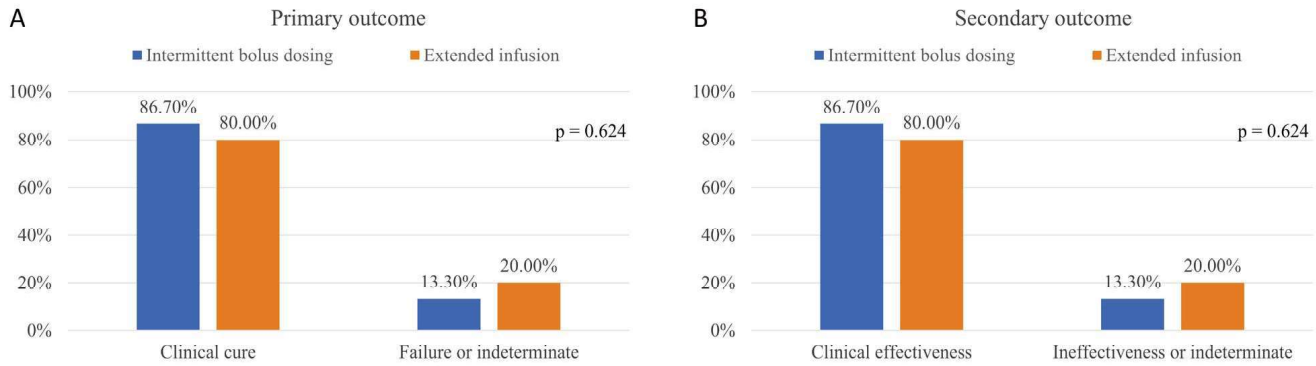

Fig. 3. Primary (A) and secondary (B) outcome of patients receiving intermittent bolus dosing or extended-infusion piperacillin-tazobactam for hospital-acquired pneumonia and ventilator-associated pneumonia after propensity score matching with the Charlson comorbidity index.

SCAP patients were both significantly higher in the intermittent bolus dosing group after PSM (94.4% vs 61.1%, p = 0.016; 94.4% vs 66.7%, $p = 0.035$) (Figure 2).

Discussion

This multicenter retrospective analysis from Taiwan showed that intermittent bolus dosing of PIP-TAZ had rates of clinical cure, effectiveness and in-hospital mortality comparable to extended infusion of PIP-TAZ in treating pneumonia. After adjusting for the CCI, the intermittent bolus dosing group also showed clinical outcomes similar to those of the extended-infusion group. However, in terms of SCAP, the intermittent bolus strategy had higher rates of clinical cure and effectiveness.

A meta-analysis in 2017 that included 18 studies and 3401 patients receiving PIP-TAZ showed that patients treated with extended infusion of PIP-TAZ were associated with lower mortality and a higher clinical cure rate, compared to treatment with an intermittent infusion strategy [9]. Several previous studies have also reported lower mortality rates with extended infusion of PIP-TAZ [10-14]. However, many of these studies included diverse infection sites, not limited to pneumonia, and disease severity also varied. A single-center randomized-controlled trial conducted in China that included 50 patients with HAP showed no significant difference in clinical cure rate between intermittent bolus dosing of PIP-TAZ and extended infusion of PIP-TAZ [15]. A randomized comparative study conducted in Egypt that included 53 patients, of which more than half had respiratory tract infection, also reported a similar clinical cure rate between the intermittent bolus dosing group and the extended-infusion group [16].

Our study focused specifically on pneumonia patients. In our cohort, the mortality rate in patients with intermittent bolus dosing of PIP-TAZ and extended-infusion PIP-TAZ was 18.5% and 23.5%, respectively, which was compatible with previous studies [17-18]. Due to differences in patient numbers, potential bias existed. To balance this, we employed PSM to adjust for the CCI. After matching, there was no difference in clinical cure rate, clinical effectiveness and in-hospital mortality between the intermittent bolus infusion group and the extended-infusion group among the overall subjects. We also conducted subgroup analysis and divided patients into SCAP and HAP/VAP groups. After PSM, the clinical cure rate and clinical effectiveness in SCAP patients were both higher in the intermittent bolus infusion group. One potential explanation could be that within the SCAP group, the extended-infusion patients exhibited greater severity, as evidenced by higher CURB-65 scores (Table S1), resulting in poorer outcomes. The higher CURB-65 score in the extended-infusion group might be attributed to primary physician preference for extended infusion in more severe patients.

Our study has several limitations. First, it was retrospective and not a randomized-controlled trial. Even after propensity score adjusting, residual bias could still exist. Second, the infusion duration of extended-infusion PIP-TAZ was not recorded in the chart, and different durations might have different outcomes. Third, this study was conducted in 9 hospitals, and differences in local epidemiology, drug resistance and empirical antibiotic strategies could influence the outcome. Fourth, the number of patients in the extended-infusion group was relatively small, with a sample size of 34 across all pneumonia patients, including 18 for CAP and 16 for HAP/VAP.

Conclusion

For the treatment of nosocomial pneumo-

nia, intermittent bolus dosing of PIP-TAZ was non-inferior to the extended-infusion strategy. Moreover, intermittent bolus dosing of PIP-TAZ demonstrated higher potency in treating SCAP than the extended-infusion strategy.

Ethical Approval

Taipei Veterans General Hospital (2019-08-006AC), National Taiwan University Hospital (201805123RINB), Mackay Memorial Hospital (19MMHIS282e), Taichung Veterans General Hospital (CE18223A#2), Chung Shan Medical University Hospital (CS18126), Chi Mei Medical Center (10806-008), Chi Mei Medical Centre, Liouying (10808-L01), and Kaohsiung Chang Gung Memorial Hospital (201900932B0C501).

References

1. Ramirez JA, Wiemken TL, Peyrani P, *et al*. Adults hospitalized with pneumonia in the United States: incidence, epidemiology, and mortality. Clin Infect Dis 2017 Nov 13; 65(11): 1806-12.
2. Magill SS, O'Leary E, Janelle SJ, *et al*. Emerging Infections Program Hospital Prevalence Survey Team. Changes in prevalence of health care-associated infections in U.S. hospitals. N Engl J Med 2018 Nov 1; 379(18): 1732-44.
3. Lodise TP, Lomaestro BM, Drusano GL; Society of Infectious Diseases Pharmacists. Application of antimicrobial pharmacodynamic concepts into clinical practice: focus on beta-lactam antibiotics: insights from the Society of Infectious Diseases Pharmacists. Pharmacotherapy 2006 Sep; 26(9): 1320-32.
4. Lodise TP Jr, Lomaestro B, Drusano GL. Piperacillin-tazobactam for Pseudomonas aeruginosa infection: clinical implications of an extended-infusion dosing strategy. Clin Infect Dis 2007 Feb 1; 44(3): 357-63.
5. Yost RJ, Cappelletty DM. The Retrospective Cohort of Extended-Infusion Piperacillin-Tazobactam (RECEIPT) study: a multicenter study. Pharmacotherapy 2011 Aug; 31(8): 767-75.
6. Bartoletti M, Giannella M, Lewis RE, *et al*. Extended infusion of β-lactams for bloodstream infection in patients with liver cirrhosis: an observational multicenter study. Clin Infect Dis 2019 Oct 30; 69(10): 1731-39.
7. Chou CC, Shen CF, Chen SJ, *et al*. Recommendations and guidelines for the treatment of pneumonia in Taiwan. J Microbiol Immunol Infect 2019 Feb; 52(1): 172-99.
8. Mandell LA, Wunderink RG, Anzueto A, *et al*. Infectious Diseases Society of America/American Thoracic Society consensus guidelines on the management of community-acquired pneumonia in adults. Clin Infect Dis 2007 Mar 1; 44 Suppl 2(Suppl 2): S27-72.
9. Rhodes NJ, Liu J, O'Donnell JN, *et al*. Prolonged infusion piperacillin-tazobactam decreases mortality and improves outcomes in severely ill patients: results of a systematic review and meta-analysis. Crit Care Med 2018 Feb; 46(2): 236-43.
10. Chen M, Buurma V, Shah M, *et al*. Evaluation of studies on extended versus standard infusion of beta-lactam antibiotics. Am J Health Syst Pharm 2019 Sep 3; 76(18): 1383-94.
11. Chan AJ, Lebovic G, Wan M, *et al*. Impact of extended-infusion piperacillin-tazobactam in a Canadian community hospital. Infect Med (Beijing) 2023 Feb 6; 2(1): 31-35.
12. Fawaz S, Barton S, Nabhani-Gebara S. Comparing clinical outcomes of piperacillin-tazobactam administration and dosage strategies in critically ill adult patients: a systematic review and meta-analysis. BMC Infect Dis 2020 Jun 20; 20(1): 430.
13. Falagas ME, Tansarli GS, Ikawa K, *et al*. Clinical outcomes with extended or continuous versus short-term intravenous infusion of carbapenems and piperacillin/tazobactam: a systematic review and meta-analysis. Clin Infect Dis 2013 Jan; 56(2): 272-82.
14. Lee GC, Liou H, Yee R, *et al*. Outcomes of extended-infusion piperacillin-tazobactam: a retrospective analysis of critically ill patients. Clin Ther 2012 Dec; 34(12): 2297-300.
15. Bao H, Lv Y, Wang D, *et al*. Clinical outcomes of extended versus intermittent administration of piperacillin/tazobactam for the treatment of hospital-acquired pneumonia: a randomized controlled trial. Eur J

Clin Microbiol Infect Dis 2017 Mar; 36(3): 459-66.
16. Naiim CM, Elmazar MM, Sabri NA, *et al*. Extended infusion of piperacillin-tazobactam versus intermittent infusion in critically ill Egyptian patients: a cost-effectiveness study. Sci Rep 2022 Jun 27; 12(1): 10882.
17. Kollef MH, Nováček M, Kivistik Ü, *et al*. Ceftolozane-tazobactam versus meropenem for treatment of nosocomial pneumonia (ASPECT-NP): a randomised, controlled, double-blind, phase 3, non-inferiority trial. Lancet Infect Dis 2019 Dec; 19(12): 1299-1311.
18. Lai CC, Cheng IL, Chen YH, *et al*. The efficacy and safety of doripenem in the treatment of acute bacterial infections--a systemic review and meta-analysis of randomized controlled trials. J Clin Med 2019 Jul 2; 8(7): 958.

Miliary Tuberculosis and Identification of Tuberculosis-Immune Reconstitution Inflammatory Syndrome (TB-IRIS) – A Case Report

Chia-Ju Wu[1], Yen-Han Tseng[1,2], Sheng-Wei Pan[1,2], Jia-Yih Feng[1,2], Yuh-Min Chen[1,2]

Miliary tuberculosis (TB), an often-fatal infectious disease in the absence of intervention, is increasingly observed among immunocompromised individuals. This case study presented a middle-aged man with rheumatoid arthritis who developed miliary TB following anti-tumor necrosis factor-alpha antibody therapy. Sputum conversion was achieved 3 months after the initiation of therapy, but the patient subsequently experienced TB-immune reconstitution inflammatory syndrome characterized by multi-organ involvement. ***(Thorac Med 2024; 39: 319-326)***

Key words: miliary tuberculosis, tuberculosis-immune reconstitution inflammatory syndrome (TB-IRIS), immunocompromised, rheumatoid arthritis, disease-modifying anti-rheumatic agents (DMARDs), anti-TNF-α antibody

Introduction

Miliary tuberculosis (TB) results from the lymphohematogenous dissemination of Mycobacterium tuberculosis (MTB) bacilli and is inherently life-threatening [1]. Several synonymous terms describe this condition in the medical literature, including hematogenous TB, generalized TB, and disseminated TB. The incidence of miliary TB among all forms of TB ranges from 0.15% to 10% in various studies [2-4]. In the past, prior to the advent of effective antibiotic treatments, miliary TB was predominantly observed in infants and children [5]. However, its prevalence has been increasing among adults with a history of immunocompromising conditions such as human immunodeficiency virus/acquired immunodeficiency syndrome (HIV/AIDS), organ transplantation, use of immunosuppressive drugs including anti-tumor necrosis factor-alpha (anti-TNF-α), and chronic renal failure [6].

The diagnosis of miliary TB is challenging due to its varied and often nonspecific presentations, which may remain obscure until the late stages of the disease. Patients typically present with constitutional symptoms including fever, chills, rigors, night sweats, anorexia,

[1]Department of Chest Medicine, Taipei Veterans General Hospital, Taipei, Taiwan, [2]School of Medicine, National Yang Ming Chiao Tung University, Taipei, Taiwan
Address reprint requests to: Dr. Jia-Yih Feng, Department of Chest Medicine, Taipei Veterans General Hospital #201, Sec. 2, Shih-Pai Road, Taipei 11217, Taiwan

weight loss, weakness, and cough persisting for several weeks [6]. In elderly patients, afebrile progressive wasting, termed cryptic miliary TB, may be observed [7]. Other patients may manifest symptoms related to extrapulmonary organ involvement, such as those involving the skin, eyes, meninges, liver, spleen, heart, pleura, kidneys, spine, and gonads [1]. Diagnosis relies on classical clinical manifestations, a miliary pattern on chest X-ray (CXR), and microbiological, cytopathological, histopathological, or molecular evidence [8]. Guidelines from the American Thoracic Society, Centers for Disease Control and Prevention, and Infectious Disease Society of America recommend a 6-month treatment regimen (2 months of isoniazid, rifampin, pyrazinamide, plus ethambutol or streptomycin, followed by 4 months of isoniazid and rifampin) for newly diagnosed cases of miliary TB without meningeal involvement [9]. Here, we present a case of miliary TB following anti-TNF-α therapy, with the relatively rare occurrence of TB immune reconstitution inflammatory syndrome (TB-IRIS) confirmed by multiple biopsies.

Case Presentation

A 53-year-old man presented to a local medical clinic in 2021 with a chronic, productive cough persisting for 3 months. He reported a weight loss, from 72 kg to 65 kg, over the past 6 months. The patient denied fever, malaise, or decreased appetite, but complained of chronic bilateral metacarpal joint pain. He was an ex-smoker (1 pack per day for 20 years, and had quit for 5 years), and had been undergoing treatment with adalimumab, a fully human anti-TNF-α monoclonal antibody, for rheumatoid arthritis for 5 years. The patient did not undergo pre-TNF-α blocker evaluation for latent TB infection. He had no history of health supplement or herbal medicine use, and there were no remarkable occupational exposures, contacts, or travel histories reported.

Following intermittent empirical antibiotics treatment for 3 months with limited improvement of symptoms, he was referred to the Taiwan Anti-Tuberculosis Association, and subsequently to our hospital. Bilateral multiple clustered centrilobular nodules and consolida-

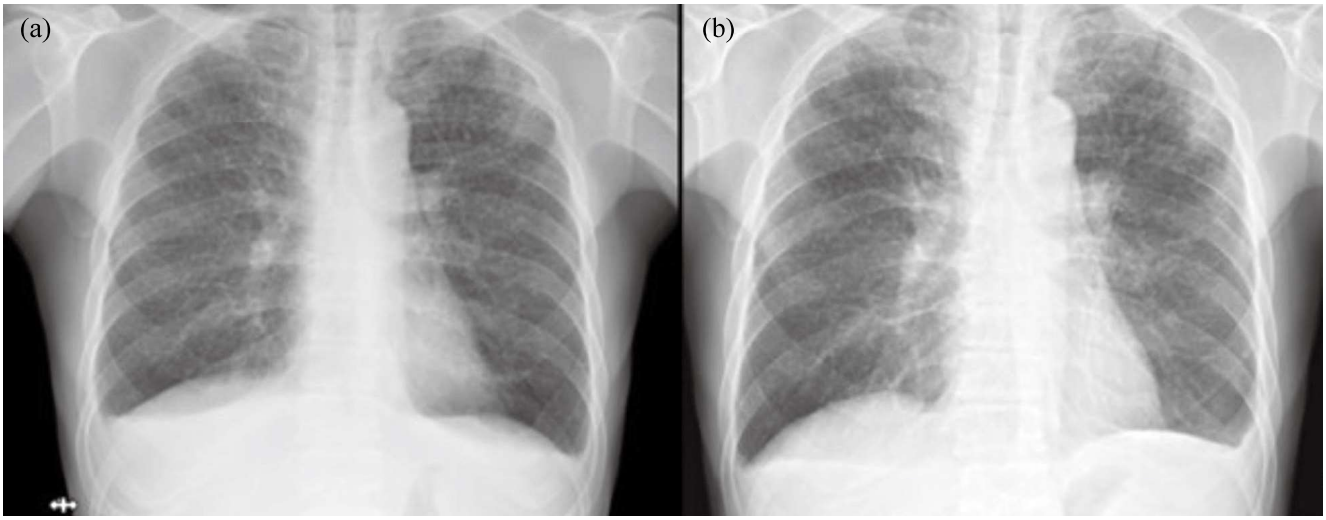

Fig. 1. Chest X-ray images of miliary tuberculosis at diagnosis, and post-sputum conversion following anti-TB treatment.(a) Miliary lesions on CXR (2021/7), (b) CXR after sputum conversion (2021/11)

tions were observed on CXR (Figure 1a) and computed tomography (CT) images (Figure 2a-1). In addition, CT revealed enlarged lymph nodes in the right lower neck, paratracheal region, aortopulmonary (AP) window, and para-aortic regions. Hypodense nodules were

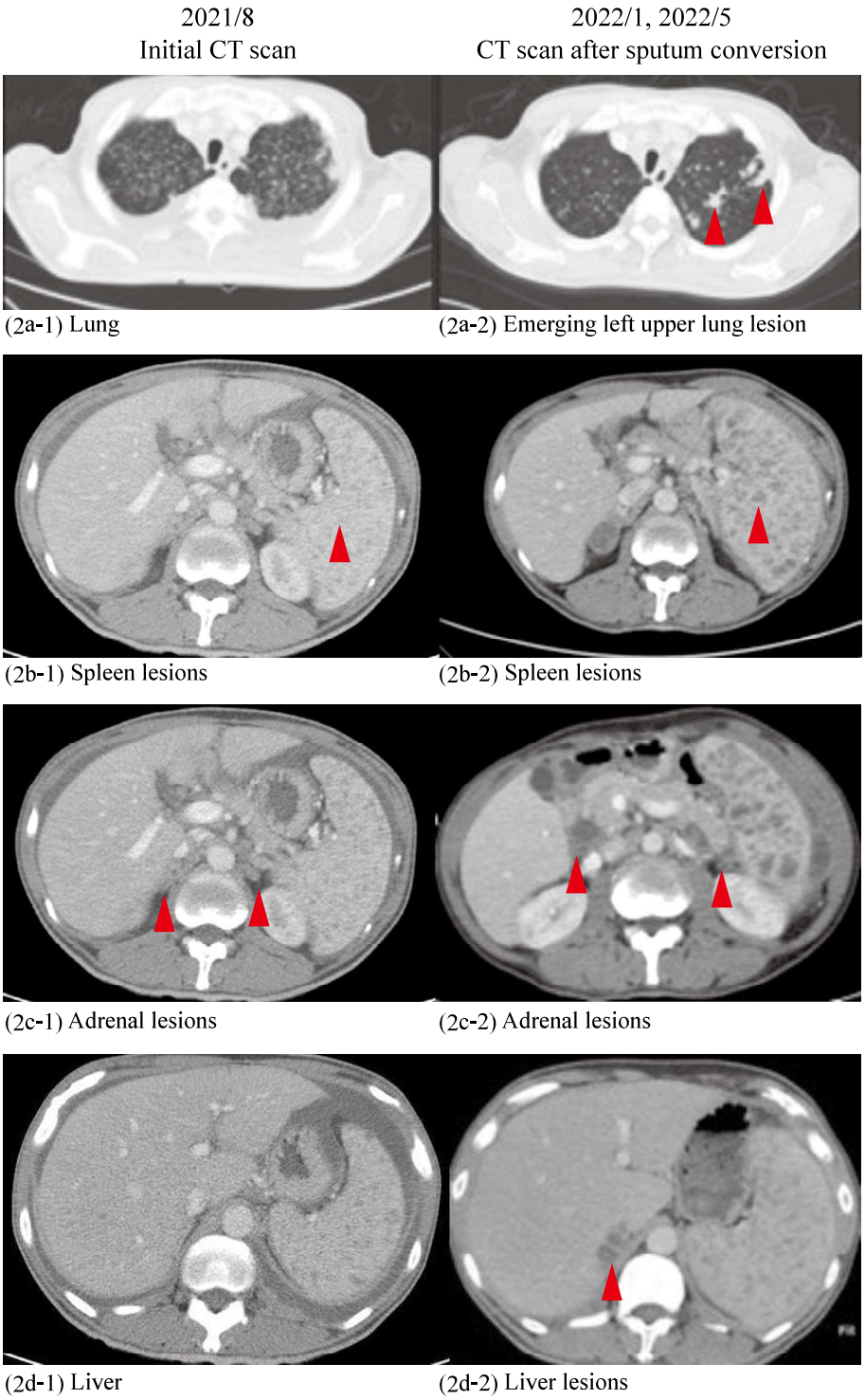

Fig. 2. Computed tomography images of miliary tuberculosis at diagnosis and post-sputum conversion following anti-TB treatment: assorted by lesion sites.

diffusely noted over the spleen and bilateral adrenal glands (Figure 2b-1, 2c-1). Laboratory tests revealed thrombocytopenia (84000/uL), hyponatremia (128 mmol/L), and an increased C-reactive protein (CRP) level (8.45 mg/dL), but no leukocytosis. The HIV Ag/Ab Combo test was negative. Sputum TB polymerase chain reaction (PCR) was positive using the Xpert MTB/RIF test (4.10X105 CFU/mL), and acid-fast stain showed 2+ positivity with culture results of MTB complex. With these findings, miliary TB involving the lymph nodes, spleen, and adrenal glands was diagnosed.

Drug susceptibility testing showed no resistance of the TB bacteria. Anti-TB medications (isoniazid, ethambutol, rifampin, pyrazinamide) were initiated in August 2021. Sputum culture conversion was achieved 3 months after treatment initiation, with the CXR as shown in Figure 1b. The patient remained afebrile with no desaturation or newly emerging symptoms and was kept under outpatient follow-up.

However, follow-up CT scans performed 5 to 9 months after initiation of anti-TB medications showed progression of lymphadenopathy in the right lower neck, paratracheal region, AP window, and para-aortic lymph nodes, as well as progression of the spleen lesions (Figure 2b-2), bilateral adrenal lesions (Figure 2c-2), and newly developed lesions in the lung (Figure 2a-2), liver (Figure 2d-2), and prostate. Sputum culture and serum cryptococcal antigen tests were negative, and serum aspergillus IgG was unremarkable. CT-guided biopsies of the left upper lung nodule, right adrenal gland, spleen, and liver were performed for differential diagnosis. Tissue TB PCR was positive, cultures were negative, and pathology revealed chronic necrotizing granulomatous inflammation (Figure 3). Progression of TB was deemed less likely

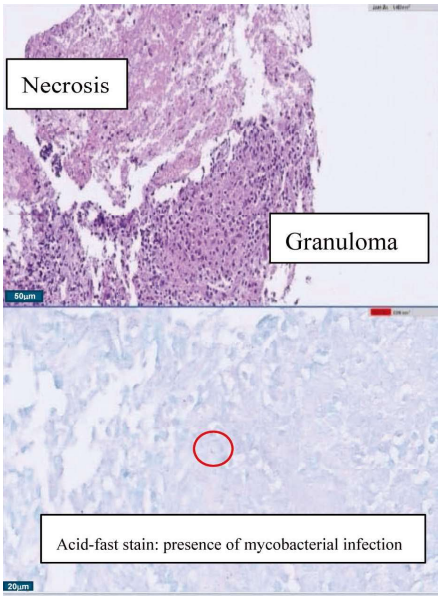

(3a) H&E, ×20; ×60
Left upper lung: Necrotizing granulomatous inflammation and acid-fast bacilli
Sections show a picture of necrotizing granulomatous inflammation. Acid-fast bacilli are shown by acid-fast stain.

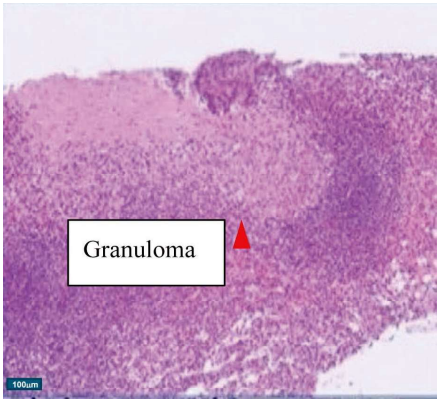

(3b) AFS, ×10
Spleen: chronic granulomatous inflammation
Granulomas composed of epithelioid cells and occasional Langhans' giant cells. Necrosis is not seen.

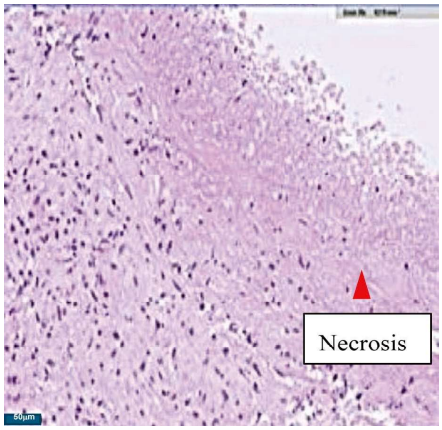

(3c) H&E, ×20
Right adrenal gland: chronic inflammation and necrosis
Sections show fragments of fibro-adipose tissue and adrenocortical tissue with chronic inflammatory cells infiltration. Necrosis is noted. No acid-fast bacilli are observed.

Fig. 3. Pathology slides of lung, spleen, and right adrenal gland from a case of TB-IRIS

due to negative culture results from multiple biopsy samples. Positive TB PCR of the specimens possibly indicated non-viable remains of MTB bacteria. Although the patient did not exhibit fever or rapid worsening in the CXR, typical of TB immune reconstitution inflammatory syndrome (TB-IRIS), the impression of TB-IRIS was still considered after excluding TB progression, other infections, or malignancy. Anti-TB medications were discontinued approximately 16 months after treatment initiation, which also equated to 13 months since sputum conversion.

Discussion

Miliary TB is uniformly fatal if untreated [8]. The prevalence of miliary TB remains uncertain due to difficulties in diagnosis. Studies have shown a positive correlation between the prevalence of extrapulmonary TB and immunosuppression status [10]. Fatal TB, including miliary TB, has been more commonly noted among patients with HIV infection and non-HIV-infected immunocompromised patients, such as those receiving anti-TNF agents like infliximab [11], etanercept [12], or adalimumab [13]. There is a 5-fold increased risk of TB associated with anti-TNF-α therapy in rheumatoid arthritis [13]. Therefore, it is recommended to exclude a latent TB infection prior to starting TNF-a-inhibitor treatment. Any correlation between miliary TB and gender or ethnicity remains controversial. Predisposing factors for miliary TB include childhood infections, malnutrition, HIV/AIDS, alcoholism, tobacco smoking, diabetes mellitus, chronic kidney disease, gastrectomy, organ transplantation, connective tissue disorders, pregnancy, underlying malignancy, and silicosis [1, 6, 14-15].

The immunopathogenesis of miliary TB could be attributed to the inadequate response of effector T-cells, which fail to contain MTB at the pathological site [16]. Mycobacteria hematogenously disseminate to multiple organs, especially those with high blood flow, such as the spleen, liver, lungs, bone marrow, kidneys, and adrenals [8]. Choroidal tubercles are pathognomonic of miliary TB and provide valuable, easily obtained, objective evidence of hematogenous TB [17]. Lumbar puncture should be pursued early, if any clinical suspicions arise, to rule out TB meningitis.

TB-IRIS should be suspected if sudden deterioration of symptoms occurs, despite previous clinical or radiologic improvements during or after completion of anti-TB treatment. Bacterial infections, non-compliance with anti-TB medications, drug resistance, malignancy, and autoimmune diseases should be considered for differential diagnosis [18]. Symptoms commonly include fever, lymphadenopathy, and dyspnea, with pulmonary and lymph node involvement being the most frequently reported signs [19]. Radiologic evaluation may reveal emerging lung lesions or rapid progression of previous lung lesions [18, 20-22]. Acute kidney injury and acute respiratory distress syndrome can develop among patients with miliary TB as a manifestation of IRIS [23-25]. Breen *et al.* reported that the prevalence of TB-IRIS among non-HIV patients is approximately 10% [22]; among HIV-infected patients, it usually occurs after initiation of highly active antiretroviral therapy (HAART), with a prevalence ranging from 4 to 54% (median: 18%) [19, 26], Generally, TB-IRIS tends to manifest more frequently among HIV-positive patients compared to those who are HIV-negative, as noted in our case.

TB-IRIS typically occurs within 3 weeks to

2 months after initiation of anti-TB medication, and the mortality rate is approximately 3% [18, 22]. In our case, TB-IRIS occurred as late as 9 months after the initiation of anti-TB treatment, which is relatively uncommon. Therefore, differential diagnosis, including progression of TB, other bacterial infections, and malignancy, should be considered seriously, and necessary biopsies should be performed before making assumptions. Multiple biopsies of various affected sites in this case aided in the differential diagnosis process. Moreover, a previous review of TB-HIV co-infected patients reminds us that late-onset IRIS needs to be differentiated from antiretroviral treatment failure and HIV progression [27].

The exact pathophysiology of TB-IRIS remains uncertain, but theories suggest an excessive inflammatory response triggered by mycobacterial antigens that are released after initiation of medication. Recent prospective studies have highlighted a correlation between positive sputum cultures, reflective of the heightened antigenic burden, and the activation of inflammatory monocyte markers [28]. Another proposed mechanism is that the reconstitution of the T helper 1 CD4+ immune response after anti-TB treatment triggers excessive systemic inflammation. This proposition finds support in observations of elevated lymphocyte counts and exaggerated tuberculin skin test reactions among patients experiencing paradoxical deterioration during anti-TB therapy [18]. Lederman *et al.* elucidated this concept in a clinical trial where short-term administration of HAART resulted in enhanced CD4 lymphocyte function, characterized by augmented lymphocyte proliferation and expansion of naive and memory CD4 cells. Consequently, among individuals with TB-HIV coinfection, initiation of HIV treatment leads to an increased frequency and/or severity of TB-IRIS. These findings implicate the pivotal role of CD4 cells in the pathophysiology of TB-IRIS.

There is no standard treatment for TB-IRIS. A previous study suggested oral prednisolone 40 mg daily for 14 days, followed by 20 mg daily for another 14 days to alleviate TB-IRIS-related symptoms, without increased risk of infection compared to a placebo [29]. Another study suggested intravenous (IV) methylprednisolone 40 mg every 12 hours until relief of symptoms, followed by maintenance oral prednisolone 20-70 mg/day for 5 to 12 weeks [21]. Potential treatment options for TB-IRIS also include IL-1 receptor antagonist, IL-18BP, small molecule inhibitors targeting inflammasomes, antibodies targeting TNF-α and IL-6, doxycycline, statins, and CCR5 inhibitors [30]. However, there is a lack of evidence from controlled trials for the use of anti-inflammatory agents in IRIS, and the therapeutic benefit of steroid use for TB-IRIS is largely anecdotal. On the other hand, prophylactic treatment for co-infected HIV patients starting ART to prevent TB-IRIS could be considered. The PredART trial showed a decrease of TB-IRIS incidence from 46.7% to 32.5% by administering prophylactic prednisone to patients with TB and HIV co-infection [29].

In summary, TB-IRIS is an abnormal, excessive immune response against live or dead MTB that may occur in either HIV-infected or, more rarely, in HIV-uninfected patients [18]. Sudden worsening of symptoms despite previous clinical or radiologic improvements during or after completion of anti-TB treatment should prompt investigations, which may include further biopsy of the involved site. TB-IRIS should be considered after excluding bacterial infec-

tions, non-compliance to anti-TB medications, drug resistance, malignancy, and autoimmune diseases. Oral steroids could be used to alleviate symptoms related to TB-IRIS.

References

1. Sharma SK, Mohan A, Sharma A. Miliary tuberculosis: A new look at an old foe. J Clin Tuberc Other Mycobact Dis 2016; 3:13-27.
2. Ray S, Talukdar A, Kundu S, *et al*. Diagnosis and management of miliary tuberculosis: current state and future perspectives. Ther Clin Risk Manag 2013; 9:9-26.
3. Toloba Y, Diallo S, Maiga Y, *et al*. [Miliary tuberculosis in Mali during the decade 2000-2009] [Article in French]. Rev Pneumol Clin 2012; 68: 17-22.
4. Toure NO, Cisse MF, Dia Kane Y, *et al*. [Miliary tuberculosis: a report of 49 cases] [Article in French]. Rev Mal Respir 2011; 28: 312-6.
5. Jacques J, Sloan JM. The changing pattern of miliary tuberculosis. Thorax 1970; 25:237-40.
6. Sharma SK, Mohan A, Sharma A. Challenges in the diagnosis & treatment of miliary tuberculosis. Indian J Med Res 2012; 135: 703-30.
7. Proudfoot AT, Akhtar AJ, Douglas AC, *et al*. Miliary tuberculosis in adults. Br Med J 1969; 2: 273-6.
8. Sharma SK, Mohan A. Miliary tuberculosis. Microbiol Spectr 2017; 5(2).
9. Blumberg HM, Burman WJ, Chaisson RE, *et al*. American Thoracic Society/Centers for Disease Control and Prevention/Infectious Diseases Society of America: treatment of tuberculosis. Am J Respir Crit Care Med 2003; 167: 603-62.
10. Sharma SK, Mohan A. Extrapulmonary tuberculosis. Indian J Med Res 2004; 120:316-53.
11. Uthman I, Kanj N, El-Sayad J, *et al*. Miliary tuberculosis after infliximab therapy in Lebanon. Clin Rheumatol 2004; 23: 279-80.
12. Toussirot E, Streit G, Wendling D. Infectious complications with anti-TNFalpha therapy in rheumatic diseases: a review. Recent Pat Inflamm Allergy Drug Discov 2007; 1: 39-47.
13. Malipeddi AS, Rajendran R, Kallarackal G. Disseminated tuberculosis after anti-TNFalpha treatment. Lancet 2007; 369: 162.
14. Sharma SK, Mohan A, Sharma A, *et al*. Miliary tuberculosis: new insights into an old disease. Lancet Infect Dis 2005; 5: 415-30.
15. Sharma SK, Mohan A. Tuberculosis: from an incurable scourge to a curable disease - journey over a millennium. Indian J Med Res 2013; 137: 455-93.
16. Sharma PK, Saha PK, Singh A, *et al*. FoxP3+ regulatory T cells suppress effector T-cell function at pathologic site in miliary tuberculosis. Am J Respir Crit Care Med 2009; 179: 1061-70.
17. Olazabal F, Jr. Choroidal tubercles. A neglected sign. JAMA 1967; 200: 374-7.
18. Lanzafame M, Vento S. Tuberculosis-immune reconstitution inflammatory syndrome. J Clin Tuberc Other Mycobact Dis 2016; 3: 6-9.13.
19. Namale PE, Abdullahi LH, Fine S, *et al*. Paradoxical TB-IRIS in HIV-infected adults: a systematic review and meta-analysis. Future Microbiol 2015; 10: 1077-99.
20. Corral-Gudino L, Rivas-Lamazares A, Gonzalez-Fernandez A, *et al*. Paradoxical deterioration during anti-tuberculous therapy in non-HIV-infected patients with pleural tuberculosis: a pragmatic approach. Eur J Case Rep Intern Med 2016; 3: 000475.
21. Murdoch DM, Venter WD, Van Rie A, *et al*. Immune reconstitution inflammatory syndrome (IRIS): review of common infectious manifestations and treatment options. AIDS Res Ther 2007; 4: 9.
22. Breen RA, Smith CJ, Bettinson H, *et al*. Paradoxical reactions during tuberculosis treatment in patients with and without HIV co-infection. Thorax 2004; 59: 704-7.
23. Goldsack NR, Allen S, Lipman MC. Adult respiratory distress syndrome as a severe immune reconstitution disease following the commencement of highly active antiretroviral therapy. Sex Transm Infect 2003; 79: 337-8.
24. Le Ho H, Barbarot N, Desrues B. Pancytopenia in disseminated tuberculosis: think of macrophage activation syndrome. Rev Mal Respir 2010; 27: 257-60.
25. Jehle AW, Khanna N, Sigle JP, *et al*. Acute renal failure on immune reconstitution in an HIV-positive patient with miliary tuberculosis. Clin Infect Dis 2004; 38: e32-5.
26. Dhasmana DJ, Dheda K, Ravn P, *et al*. Immune reconstitution inflammatory syndrome in HIV-infected patients receiving antiretroviral therapy: pathogenesis, clinical manifestations and management. Drugs 2008; 68:

191-208.
27. Gopalan N, Swaminathan S. Tuberculosis immune reconstitution inflammatory syndrome: Profile of an enigmatic condition. Current Science 2013: 105. 657-65.
28. Andrade BB, Singh A, Narendran G, *et al.* Mycobacterial antigen driven activation of CD14++CD16- monocytes is a predictor of tuberculosis-associated immune reconstitution inflammatory syndrome. PLoS Pathog 2014; 10: e1004433.
29. Meintjes G, Stek C, Blumenthal L, *et al.* Prednisone for the prevention of paradoxical tuberculosis-associated IRIS. N Engl J Med 2018; 379: 1915-25.
30. Cevaal PM, Bekker LG, Hermans S. TB-IRIS pathogenesis and new strategies for intervention: insights from related inflammatory disorders. Tuberculosis (Edinb) 2019; 118: 101863.

Computed Tomography Angiography-Negative Pulmonary Arteriovenous Malformations Diagnosed Using a Lung Perfusion Scan: A Case Report

Hsin-I Cheng[1], Chun-Yu Lin[1], Po-Jui Chang[1], Horng-Chyuan Lin[1]

Pulmonary arteriovenous malformations (PAVMs) are an uncommon and insidious disease caused by abnormal communication between pulmonary arteries and veins. They may remain asymptomatic but can also cause a broad spectrum of symptoms, including dyspnea, hemoptysis, platypnea, hypoxemia, or even neurological insults. Computed tomography angiography (CTA) is a useful tool for establishing the diagnosis in almost all patients with PAVMs. However, a lung perfusion scan may provide some diagnostic benefit when the CTA results are negative. ***(Thorac Med 2024; 39: 327-331)***

Key words: Pulmonary arteriovenous malformations, computed tomography angiography, lung perfusion scan

Introduction

Pulmonary arteriovenous malformations (PAVMs) are a complicated and insidious disease caused by abnormal communication between pulmonary arteries and veins. Here, we report an unusual case of a patient with persistent hypoxemia and a poor response to oxygen therapy, with a negative computed tomography angiography (CTA) finding.

Case Report

A 76-year-old male, diagnosed with coronary artery disease and 2-vessel disease, underwent placement of 3 drug-eluting stents 3 years ago. He presented with recurrent gastrointestinal bleeding episodes and later visited the emergency department due to a cough, and pneumonia was diagnosed. Due to persistent pancytopenia, he was referred for a bone marrow biopsy. On initial examination, the patient's heart rate was 96 beats per minute, blood pressure was 120/64 mmHg, body temperature was 35.3oC, and respiratory rate was 30 breaths per minute while breathing ambient air. At that time, the saturation rate was 78%, as measured by finger pulse oximeter. Saturation by pulse oximeter was still 87-89% under a non-rebreathing mask. Therefore, a high-flow oxygen nasal cannula was given to the patient.

Laboratory tests, including carboxyhemo-

[1]Department of Thoracic Medicine, Chang Gung Memorial Hospital, Taoyuan, Taiwan
Address reprint requests to: Dr. Horng-Chyuan Lin, Department of Thoracic Medicine, Chang Gung Memorial Hospital, No.5, Fuxing St., Guishan Dist., Taoyuan City 333, Taiwan

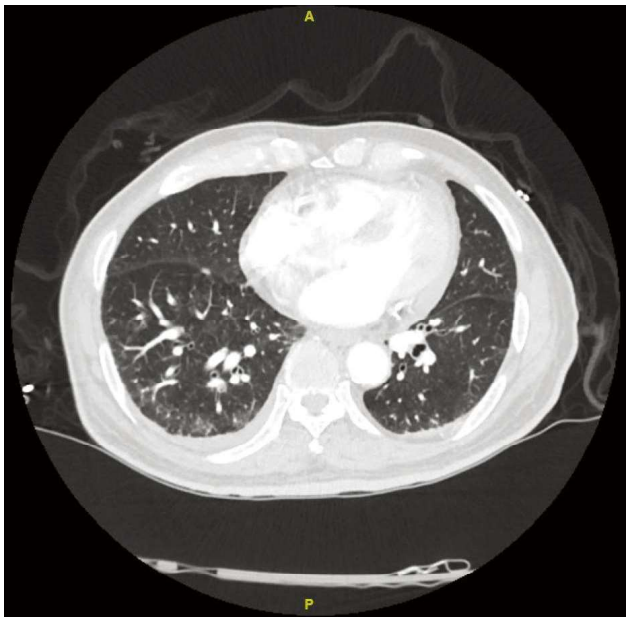

Fig. 1. Diffuse tiny ground-glass opacities (GGOs)

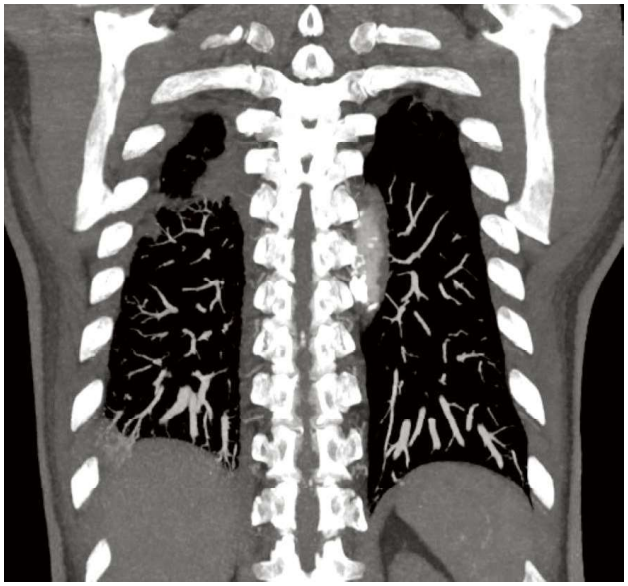

Fig. 2. Diffuse dilation of the pulmonary artery, lower lung-predominate.

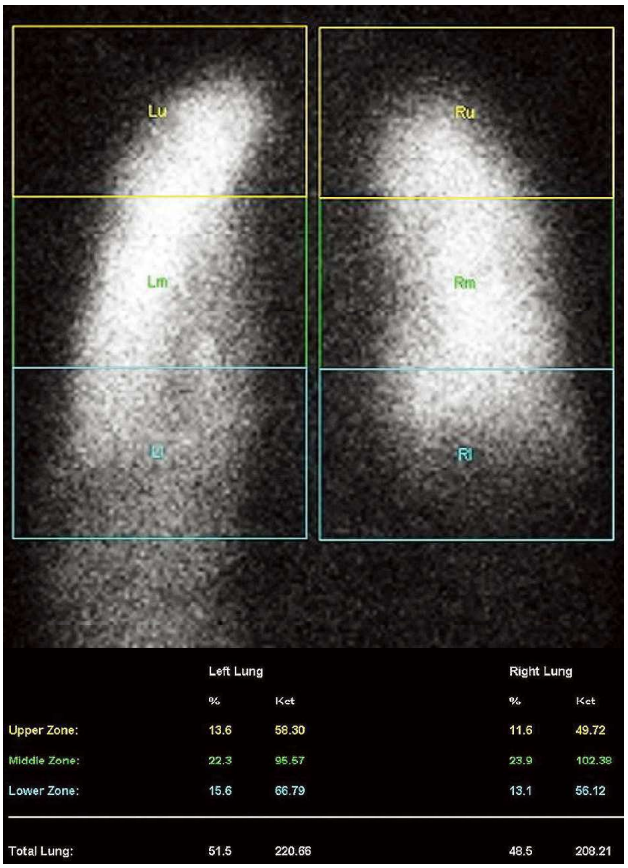

	Left Lung		Right Lung	
	%	Ket	%	Ket
Upper Zone:	13.6	58.30	11.6	49.72
Middle Zone:	22.3	95.57	23.9	102.38
Lower Zone:	15.6	66.79	13.1	56.12
Total Lung:	51.5	220.66	48.5	208.21

Fig. 3. Lung perfusion scan revealed 48% extrapulmonary intake.

globin and methemoglobin, showed no significant findings except for pancytopenia. CTA of the chest showed no evidence of pulmonary embolism. Only a few tiny ground-glass opacities (GGOs) were noted in the bilateral lung parenchyma (Figure 1). Diffuse dilation of the pulmonary artery was also noted (Figure 2). An echocardiogram revealed normal left ventricular systolic function without valvular heart disease. A lung perfusion ventilation scan showed extrapulmonary uptake, which suggested the presence of a right-to-left shunt. The shunt was about 48% (Figure 3). A contrast echocardiogram revealed a strong positive result (Figure 4). Bubbles appeared in the left ventricle at the fourth to fifth beat after a left forearm injection, which suggested intrapulmonary shunts. Cardiac and pulmonary artery angiography showed a high cardiac output (5.76 L/min/m2), with normal pulmonary vascular resistance (0.95 wood units). Multiple arteriovenous malformations were found at the bilateral lower lobes (Figure 5).

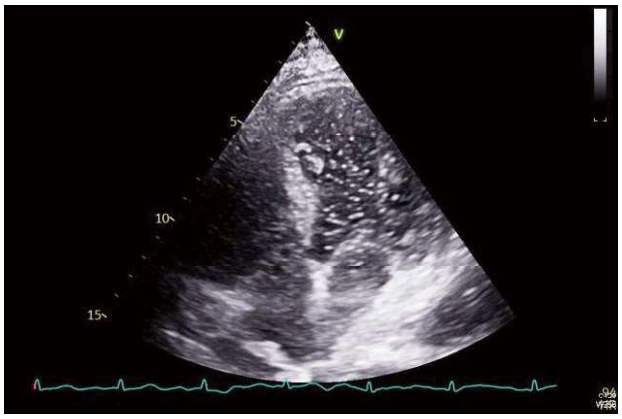

Fig. 4. Air bubbles in the left ventricle, which indicated a positive finding in the contrast echocardiogram.

Fig. 5. Multiple tiny pulmonary arteriovenous malformations were seen at the bilateral lower lung.

After discussion with the cardiologist, pediatric cardiologist and chest surgeon, staged embolization was suggested. An abdominal echogram showed no evidence of liver cirrhosis or ascites. Gastroscopy showed chronic erosive duodenitis. Colonoscopy revealed a colonic ulcer. No angiodysplasia or telangiectasia was found. His saturation was still around 70-80% under ambient air after cardio angiography with embolization therapy for the left lower lung with vascular plugs. Lobectomy, which may provide more benefits, was suggested. In consideration of the patient's poor pulmonary function test and old age, he had a right lower lung lobectomy. The pathology showed clusters of dilated and thick-walled blood vessels, which is consistent with arteriovenous malformation. After the operation, his O_2 saturation improved to 85-88%. However, the patient was lost to follow-up after the second pulmonary embolization.

Discussion

PAVMs are uncommon in the general population, with a prevalence of around 1 in 2600 [1]. About 80-90% of PAVMs are associated with hereditary hemorrhagic telangiectasia (HHT, also known as Osler-Weber-Rendu syndrome), an autosomal-dominant inherited disease [2-5]. A small number are linked to systemic diseases such as anemia or hepatopulmonary syndrome. However, PAVMs can occur in a variety of medical conditions, including hepatic cirrhosis [6], while others are classified as idiopathic. HHT is a vascular disorder characterized by frequent nosebleeds, gastrointestinal bleeding, and distinctive mucocutaneous telangiectasia. The Second International Guidelines on HHT recommend using the Curaçao criteria for diag-

nosis. Approximately 30-50% of patients with HHT will have PAVMs.

Most PAVMs are asymptomatic but can be associated with a variety of clinical manifestations, and in some cases, they may lead to life-threatening complications [7-8]. The size of the PAVM and the degree of right-to-left shunting correlate with the severity of these complications. Patients may experience dyspnea, cyanosis, or chest pain [8]. Serious complications include brain abscesses, paradoxical embolism events such as ischemic strokes or transient ischemic attacks, and, less frequently, hemoptysis or hemothorax [8]. PAVMs should be suspected in patients who present with pulmonary nodules that have a smooth surface, signs of right-to-left shunting such as dyspnea, hypoxemia, cyanosis, cerebral embolism, unexplained hemoptysis or hemothorax, and platypnea or orthodeoxia [5, 9].

The diagnostic approaches for hypoxemia may include patient history and physical examinations, hemogram and biochemical tests, blood gas analysis, chest plain film, chest computed tomography (CT) or CTA, and carboxyhemoglobin or methemoglobin tests. If a definitive diagnosis cannot be established by these examinations, a lung perfusion scan may provide some information on abnormal shunting or V/Q mismatch [10]. An echocardiogram is a useful tool to estimate shunting caused by intra-cardiac shunt. Bubble contrast echocardiography may provide clues to detect shunting and identify intra-cardiac or extra-cardiac shunts [11]. If bubbles appear in the left atrium or left heart more than 5 heartbeats after right heart opacification, this suggests intrapulmonary shunting [11]. Pulmonary angiography is the gold standard for diagnosing PAVMs [7].

Returning to our patient, this individual had confirmed PAVMs, yet the CT results were negative. A case report published in 1993 documented a similar instance where the CT scan was negative, but the diagnosis of PAVMs was established by a radionuclide method [12]. Another study indicated that the sensitivity of CTA was 98% [13]. Only a few patients with PAVMs will be misdiagnosed by CTA.

Conclusion

This case presents a rare instance of PAVMs with a negative pulmonary CTA. It is important to consider PAVMs even when the examination results are negative. A lung perfusion ventilation scan may provide insight into the cause of hypoxemia.

References

1. Shovlin CL. Pulmonary arteriovenous malformations. Am J Respir Crit Care Med 2014; 190(11): 1217-28.
2. Kaufman CS, McDonald J, Balch H, *et al.* Pulmonary arteriovenous malformations: what the interventional radiologist should know. Semin Intervent Radiol 2022; 39(3): 261-70.
3. Shovlin CL. Hereditary haemorrhagic telangiectasia: pathophysiology, diagnosis and treatment. Blood Rev 2010; 24(6): 203-19.
4. Faughnan ME, Palda VA, Garcia-Tsao G, *et al.* International guidelines for the diagnosis and management of hereditary haemorrhagic telangiectasia. J Med Genet 2011; 48(2): 73-87.
5. Dunphy L, Talwar A, Patel N, *et al.* Hereditary haemorrhagic telangiectasia and pulmonary arteriovenous malformations. BMJ Case Rep 2021; 14(1): e238385.
6. Krowka MJ. Hepatopulmonary syndrome and portopulmonary hypertension. Curr Treat Options Cardiovasc Med 2002; 4(3): 267-73.
7. Majumdar S, McWilliams JP. Approach to pulmonary arteriovenous malformations: a comprehensive update. J Clin Med 2020; 9(6): 1927.

8. Salibe-Filho W, Oliveira FR, Terra-Filho M. Update on pulmonary arteriovenous malformations. J Bras Pneumol 2023; 49(2): e20220359.
9. Agrawal A, Palkar A, Talwar A. The multiple dimensions of Platypnea-Orthodeoxia syndrome: a review. Respir Med 2017; 129: 31-8.
10. Bajc M, Lindqvist A. Ventilation/perfusion SPECT imaging-diagnosing other cardiopulmonary diseases beyond pulmonary embolism. Semin Nucl Med 2019; 49(1): 4-10.
11. Bernard S, Churchill TW, Namasivayam M, *et al*. Agitated saline contrast echocardiography in the identification of intra- and extracardiac shunts: connecting the dots. J Am Soc Echocardiogr 2020 Oct 23: S0894-7317(20)30615-5.
12. Trent, C., Tupler RH, Wildenhain P, *et al*. Macrovascular pulmonary arteriovenous malformations demonstrated by radionuclide method. Clin Nucl Med 1993; 18(3): 231-3.
13. Remy J, Remy-Jardine M, Wattinne L, *et al*. Pulmonary arteriovenous malformations: evaluation with CT of the chest before and after treatment. Radiology 1992; 182(3): 809-16.

An Unusual Presentation of Pulmonary Sequestration: A Case Report

Yi-Yu Lin[1], Chin-Feng Wu[1,2]

Pulmonary sequestration is a rare congenital malformation of the lung, and is divided into 2 types: intralobar sequestration and extralobar sequestration. Unique clinical symptoms and radiological findings have been reported by researchers. In our case, a healthy 71-year-old male patient came to our Thoracic Surgery Outpatient Department in June 2023, due to a 2.7-cm left lower lung solid mass, which was found accidently. During operation, an unsuspected pulmonary sequestration was noted, and the final pathology of the resected lung mass was adenocarcinoma in situ within pulmonary sequestration. Adenocarcinoma associated with pulmonary sequestration is rare. To confirm the diagnosis, angiography is necessary. The treatment of choice is lobectomy, but sublobar resection could be an alternative modality. Video-assisted thoracoscopic or da Vinci assisted lung mass resection by an experienced surgeon are feasible, with awareness of the potential risk of vascular injury. ***(Thorac Med 2024; 39: 332-335)***

Key words: Pulmonary sequestration, adenocarcinoma-associated pulmonary sequestration

Background

Pulmonary sequestration (PS) is a malformation of the lower respiratory tract, accounting for 0.15% to 6.4% of all congenital pulmonary malformations [1]. Based on the pleural involvement of the sequestered lung parenchyma, PS can be categorized into either intralobar or extralobar types. Intralobar sequestration (ILS), representing 75% of PS cases, is distinguished by sharing the same visceral pleural lining as the native lung and having venous drainage into the pulmonary veins. In contrast, extralobar sequestration (ELS) possesses its own visceral pleural investment external to the normal lung, and drains into a systemic vein, resulting in the formation of an accessory lobe referred to as a "Rokitansky lobe." Clinical manifestations can vary in PS, ranging from asymptomatic cases to recurrent respiratory infections or hemoptysis [2-4]. Common radiological findings on CT scans often include ground-glass opacity,

[1]College of Medicine, Chang Gung University, Division of Thoracic and Cardiovascular Surgery, Department of Surgery, Chang Gung Memorial Hospital, Taoyuan. [2]Department of Thoracic Surgery, Minimally Invasive Thoracic Surgery Unit (UCTMI), Coruña University Hospital, Coruña, Spain.
Address reprint requests to: Dr. Yi-Yu, Lin, Division of Thoracic Surgery, Chang Gung Memorial Hospital-Linkou, 5 Fuxing Street, Guishan District, Taoyuan 333, Taiwan.

cavitation with or without an air-fluid level, irregular cystic spaces, or bronchiectasis [5]. Due to its peculiarity, we would like to report the following case.

Case Presentation

A 71-year-old male patient visited our Thoracic Surgery Outpatient Department (OPD) on 7 June 2023 for the first time, due to a 2.7-cm solid mass at the left lower lobe (LLL) that was discovered in a regular health examination 1 month previous (Figures 1, 2, red arrows). He had no history of smoking, chronic exposure to passive smoking or poisonous gas, pulmonary infection, or previous surgical procedure. He denied a cough, hemoptysis, fever, chest tightness, chest pain, and dyspnea. No family history of lung cancer was mentioned. Based on the morphology of the tumor on chest computed tomography (CT), malignancy was highly suspected. The patient preferred to receive CT-guided biopsy to confirm the diagnosis.

Fig. 1. Initial chest CT, indicating a solid mass in the LLL.

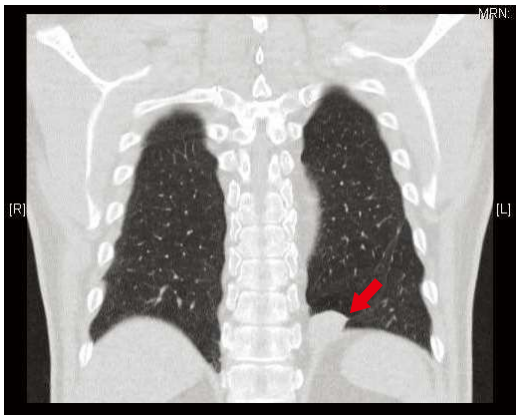

Fig. 2. Initial chest CT, indicating a solid mass in the LLL.

Fig. 3. Chest CT in the CT-guided biopsy, showing a feeding vessel from the thoracic aorta.

The CT-guided biopsy was performed on 12 June, and the pathology report revealed adenocarcinoma in situ (AIS). In the chest CT biopsy series, the feeding vessel was determined to be the thoracic aorta (Figure 3, blue arrow). Regular imaging examinations, including a positon emission tomography scan and brain magnetic resonance imaging, for complete tumor staging, reported neither brain metastasis nor distant structural metastases. The follow-up pulmonary function test showed normal baseline spirometry with FVC 3.19 L (100%) and FEV1 2.53 L (101%).

Under the impression of LLL AIS, tentative clinical stage T1N0M0, surgical resection was indicated. Therefore, he was admitted to the ward on 28 July 2023, and da Vinci-assisted LLL lobectomy was arranged for 29 July 2023.

Fig. 4. Resected PS, about 3 cm in diameter.

During operation, we unexpectedly noticed an ELS, about 3 cm in diameter, below the LLL. With an adequate safety margin, we resected the PS and sent it to the pathology department (Figure 4). The final pathological report was AIS within the PS. Due to the early stage, further systemic treatment was not indicated.

Discussion

PS accounts for 0.15% to 6.4% of all congenital lung malformations [14]. PS was first reported by Huber in 1877, and was named as "sequestration" by Pryce in 1946 [8]. Approximately 60% of cases are diagnosed before the age of 20; diagnosis in adults over 50 is very rare [15]. Zener *et al*. reported in 2017 a 4:1 male:female ratio for ELS prevalence, and 30% of cases had incidental findings [16]. The pathogenesis was that a part of the lung tissue developed into a separate lesion in the embryonic period, and had no respiratory function, but had aberrant arteries [9]. The supplying arteries arise from the thoracic artery in 74% of cases [6], and may stem from the abdominal artery, celiac aorta, splenic artery or even a coronary artery [7]. PS is mainly located in the LLL (71.5%) [10].

Symptoms of PS vary. ILS presents mostly as acquired pulmonary infection; in contrast, ELS is generally asymptomatic. It is accidentally found on routine health examination, and is often misdiagnosed as lung cancer [11], pulmonary cysts, or mediastinal tumors [10]. The average incorrect preoperative diagnosis rate of SP is 58.6% [10].

Adenocarcinoma associated with PS is extremely rare [18-20]. To our knowledge, fewer than 10 cases have been reported until now. Whether full tumor workup is necessary before arrangement of intervention or not is still controversial. If there is any suspicion of PS, angiography is necessary to identify aberrant arteries connected to the systemic artery and confirm the diagnosis. Pulmonary lobectomy is the recommended treatment for PS, even in asymptomatic patients, to avoid infection and lung parenchyma inflammation. However, in a large retrospective case series among adults, there did not appear to be any proof of a significant difference in outcomes between performing surgery and opting for conservative treatment in asymptomatic patients [17]. Sublobar resection is an alternative to lobectomy for peripheral or small lesions in terms of lung function preservation [21]. In our case, we performed wedge resection for the peripheral mass.

Conclusion

This report described a case of AIS associated with PS, mimicking lung cancer in preoperative surveys. Video-assisted thoracoscope or da Vinci-assisted lung mass resection by an experienced surgeon with awareness of the potential risk of vascular injury would be feasible.

References

1. Abbey P, Das CJ, Pangtey GS, *et al*. Imaging in bronchopulmonary sequestration. J Med Imaging Radiat Oncol 2009; 53: 22-31.
2. Liu C, MD, Pu Q, MD, Ma L, MD, *et al*. Video-assisted thoracic surgery for pulmonary sequestration compared with posterolateral thoracotomy. J Thorac Cardiovasc Surg 2013; 146: 557-61.
3. Tanaka T, Ueda K, Sakano H, *et al*. Video-assisted thoracoscopic surgery for intralobar pulmonary sequestration. Surgery 2003; 133: 216-8.
4. Fabre OH, Porte HL, Godart FR, *et al*. Long-term cardiovascular consequences of undiagnosed intralobar pulmonary sequestration. Ann Thorac Surg 1998; 65: 1144-46.
5. Gabelloni M, Faggioni L, Accogli S, *et al*. Pulmonary sequestration: what the radiologist should know. Clin Imaging 2012; 73: 61-72.
6. Savic B, Birtel FJ, Tholen W, *et al*. Lung sequestration: report of seven cases and review of 540 published cases. Thorax 1973; (1): 96-101
7. Walker CM, Wu CC, Gilman MD, *et al*. The imaging spectrum of bronchopulmonary sequestration. Curr Probl Diagn Radiol 2014; 43(3): 100-14.
8. Pryce DM. Lower lobe accessory pulmonary artery with intralobar sequestration of lung: report of 7 cases. J Pathol Bacteriol 1946; 58: 457-67.
9. Markes C, Wiener SN, Reydman M. Pulmonary sequestration. Chest 1972; 61: 253-57.
10. Wei Y, Li F. Pulmonary sequestration: a retrospective analysis of 2625 cases in China. Eur J Cardiothorac Surg 2011; 40: 39-42.
11. Matsuoka H, Nohara H. Pulmonary sequestration with high levels of tumor markers tending to be misdiagnosed as lung cancer. Jpn J Thorac Cardiovasc Surg 2006; 54: 117-19.
12. Yucel O, Gurkok S, Gozubuyuk A, *et al*. Diagnosis and surgical treatment of pulmonary sequestration. Thorac Cardiovasc Surg 2008; 56: 154-57.
13. Salmons S. Pulmonary sequestration. Neonatal Netw 2000; 19: 27-31.
14. Chakraborty RK, Modi P, Sharma S. Pulmonary sequestration. StatPearls [Internet]. Treasure Island (FL): StatPearls Publishing 2024.
15. Montjoy C, Hadique S, Graeber G, *et al*. Intralobar bronchopulmonary sequestra in adults over age 50: case series and review. W V Med J 2012 Sep-Oct; 108(5): 8-13.
16. Zener R, Bottoni D, Zaleski A, *et al*. Transarterial embolization of intralobar pulmonary sequestration in a young adult with hemoptysis. J Thorac Dis 2017 Mar; 9(3): 188-93.
17. Sun X, Xiang Y. Pulmonary sequestration in adult patients: a retrospective study. Eur J Cardiothorac Surg 2015 Aug; 48(2): 279-82.
18. Gatzinsky P, Olling S. A case of carcinoma in intralobar pulmonary sequestration. Thorac Cardiovasc Surg 1988; 36: 290-91.
19. Bell-Thomson J., Missier P., Sommers S.C. Lung carcinoma arising in bronchopulmonary sequestration. Cancer 1979; 44: 334-39.
20. Wang TKM, Oh T, Ramanathan T. Thoracoscopic lobectomy for synchronous intralobar pulmonary sequestration and lung cancer. Ann Thorac Surg 2013; 96: 683-85.
21. Lin TH, Huang WL, Chang CC, *et al*. Uniportal video-assisted thoracoscopic surgery lobectomy and segmentectomy for pulmonary sequestration. J Thorac Dis 2018; 10(6): 3722-28.

MALT Lymphoma Presenting as Bilateral Pulmonary Nodules: A Case Report

Jen-Hao Chuang[1,2]

Mucosa-associated lymphoid tissue (MALT) lymphoma, a subtype of non-Hodgkin lymphoma, typically arises in the stomach, but can also present in various extranodal sites, including the lung. Lung involvement of MALT lymphoma is rare, and bilateral single pulmonary nodules as a presentation are even rarer. This report details a unique case of MALT lymphoma presenting as bilateral lung tumors in a 53-year-old male. ***(Thorac Med 2024; 39: 336-338)***

Key words: lung tumor, uniportal VATS, mucosa-associated lymphoid tissue (MALT) lymphoma

Introduction

Mucosa-associated lymphoid tissue (MALT) lymphoma, a subtype of non-Hodgkin lymphoma, typically arises in the stomach but can also present in various extranodal sites, including the lung [1-3]. Lung involvement of MALT lymphoma is rare, and bilateral single pulmonary nodules as a presentation are even rarer. This report details a unique case of MALT lymphoma presenting as bilateral lung tumors in a 53-year-old male.

Case Presentation

A 53-year-old male, with a medical history of anxiety and insomnia disorder, gastroesophageal reflux disease (GERD), and being positive for anti-HBc, was incidentally found to have lung tumors during a routine health check-up. The patient, a non-smoker, sought a second opinion after chest computed tomography revealed nodules in the right upper lobe (RUL) and left lower lobe (LLL) of the lung (Fig.1A, B). Despite the absence of typical symptoms such as weight loss, appetite decrease, fever, chest pain, cough, dyspnea, or hemoptysis, the bilateral lung tumors prompted the decision for surgical intervention.

Diagnostic Assessment

Pre-operative assessments, including pulmonary function tests, bone scans, and brain

[1]Department of Surgery, National Taiwan University Hospital and National Taiwan University College of Medicine, Taipei, Taiwan. [2]Department of Surgical Oncology, National Taiwan University Cancer Center, National Taiwan University College of Medicine, Taipei, Taiwan.
Address reprint requests to: Dr. Jen-Hao Chuang, National Taiwan University Cancer Center, No. 57, Ln. 155, Sec. 3, Keelung Road, Da'an Dist., Taipei City 106, Taiwan.

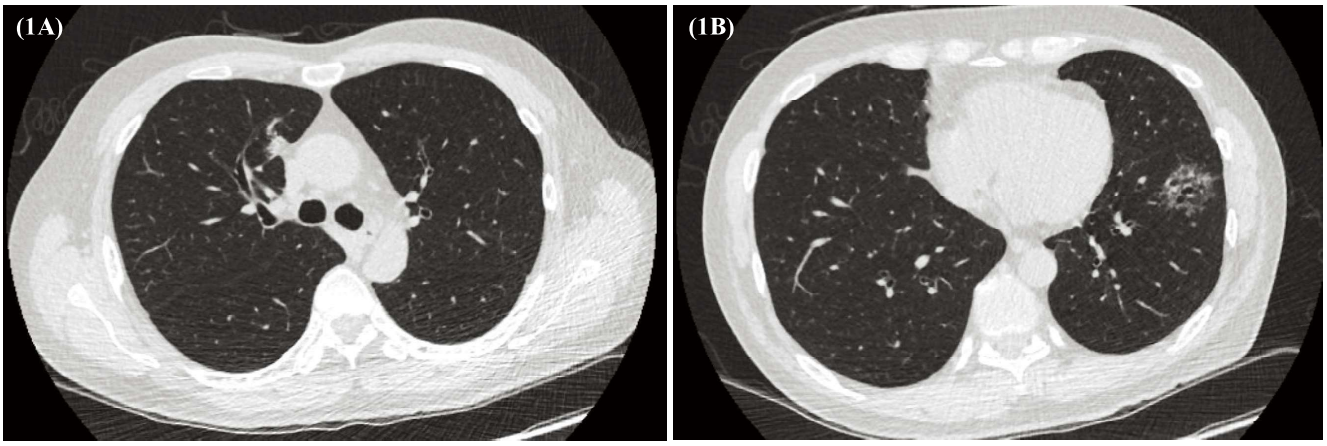

MRI, showed no evidence of distant metastasis. The patient underwent single-port video-assisted thoracoscopic surgery (VATS) for both lobes, followed by lymph node dissection. Pathological examination confirmed extranodal marginal zone lymphoma of MALT (MALT lymphoma) in the wedge resections of both the RUL and LLL.

For the LLL, the wedge resection specimen measured 2.0 x 2.0 x 1.5 cm, and was diagnosed as extranodal marginal zone MALT lymphoma. The RUL specimen measured 1.5 x 0.8 x 0.8 cm and was similarly diagnosed as MALT lymphoma. Microscopically, the RUL and LLL samples both exhibited atypical lymphoid cells characterized by slightly irregular nuclei with moderately dispersed chromatin and inconspicuous nucleoli, and relatively abundant, pale cytoplasm. The cells infiltrated in a marginal zone pattern, forming larger confluent areas with occasional large cells resembling centroblasts or immunoblasts, and lymphoepithelial lesions were occasionally observed.

Immunohistochemistry further supported the diagnosis, with the atypical lymphoid cells testing positive for CD20, CD19, and CD43 (focal), and negative for CD3, CD5, CD30, LEF1, CD10, BCL6, and cyclin D1. These findings were consistent with the histologic diagnosis of extranodal marginal zone MALT lymphoma, as per the WHO classification. The disease was staged as IIE, with an International Prognostic Index (IPI) of 2.

Treatment and Outcome

Post-operative management included prophylactic antibiotics and chest tube drainage. The patient was discharged in a stable condition and planned for outpatient follow-up. Considering the absence of Helicobacter pylori (H. pylori) in the recent gastroscopy, a watchful waiting approach was adopted post-eradication of H. pylori.

Discussion

The bilateral single pulmonary nodules presentation of MALT lymphoma in this case is notable for several reasons. First, lung involvement of MALT lymphoma is uncommon, and bilateral manifestations are even less frequent. Thus, this case emphasizes the importance of considering MALT lymphoma in the differential diagnosis of pulmonary nodules, especially in

patients without a significant smoking history or classic respiratory symptoms [4-7].

The successful management of this patient using VATS highlights the role of minimally invasive surgery in diagnosing and treating pulmonary MALT lymphoma. The absence of H. pylori in later evaluations suggests a complex relationship between H. pylori and MALT lymphoma, not limited to gastric manifestations. This case supports the practice of watchful waiting after H. pylori eradication, especially in pulmonary MALT lymphoma without active gastrointestinal involvement.

Regarding the prognosis, pulmonary MALT lymphoma is generally considered to have a favorable outcome compared to other forms of non-Hodgkin lymphoma. Studies have reported long-term survival rates that are quite encouraging, with a 5-year overall survival rate exceeding 90% in many cases. The indolent nature of MALT lymphoma contributes to a generally good prognosis, although the disease can recur or progress slowly over time. Factors that can influence prognosis include the stage at diagnosis, the patient's age, and the presence of symptoms. In cases where the disease is localized and detected early, as in this patient, surgical resection followed by careful monitoring is often sufficient for management [1-2, 8].

This prognosis is contrasted with other more aggressive lymphomas, highlighting the importance of accurate diagnosis and tailored treatment strategies. It also underscores the potential utility of surgical intervention, not only for therapeutic purposes, but also for comprehensive diagnostic evaluation, which can guide further treatment decisions and surveillance strategies [9-11].

In conclusion, pulmonary MALT lymphoma, especially when presenting as bilateral nodules, as in this case, requires a high degree of clinical suspicion and a multidisciplinary approach for optimal management. The generally favorable prognosis, when combined with effective treatment modalities such as VATS, offers promising outcomes for patients.

References

1. Kelemen K, Rimsza LM, Craig FE, *et al*. Primary pulmonary B-cell lymphoma. Semin Diagn Pathol 2020; 37: 259-67.
2. Cadranel J, Wislez M, Antoine M, *et al*. Primary pulmonary lymphoma. Eur Respir J 2002; 20: 750-62.
3. Graham BB, Mathisen DJ, Mark EJ, *et al*. Primary pulmonary lymphoma. Ann Thorac Surg 2005; 80: 1248-53.
4. Deng W, Wan Y, Yu JQ, *et al*. Pulmonary MALT lymphoma has variable features on CT. Sci Rep 2019; 9: 8657.
5. Wu T, Huang Y, Wang Z, *et al*. Pulmonary MALT lymphoma: imaging findings in 18 cases and the associated pathological correlations. Am J Med Sci 2022; 364: 192-97.
6. King LJ, Padley SP, Wotherspoon AC, *et al*. Pulmonary MALT lymphoma: imaging findings in 24 cases. Eur Radiol 2000; 10: 1932-38.
7. Nakamura D, Kobayashi N, Miyazawa M, *et al*. Pulmonary metastasis with coexisting pulmonary mucosa-associated lymphoid tissue (MALT) lymphoma 20 years after endometrioid adenocarcinoma surgery: a case report. Thorac Cancer 2021; 12: 402-06.
8. McNally E, Cronje L, Fabre A, *et al*. Pulmonary mucosa-associated lymphoid tissue (MALT) lymphoma associated with coeliac disease. BMJ Case Rep 2022; 15.
9. Borie R, Wislez M, Antoine M, *et al*. Pulmonary mucosa-associated lymphoid tissue lymphoma revisited. Eur Respir J 2016; 47: 1244-60.
10. Song Y, Sung YE, Beck KS, *et al*. Radiological and pathological analysis of the galaxy sign in patients with pulmonary mucosa-associated lymphoid tissue (MALT) lymphoma. Thorac Cancer 2023; 14: 2459-66.
11. Guo Z, Hu L, Chen Q, *et al*. Synchronous pulmonary MALT lymphoma and squamous cell lung cancer: a case report. World J Surg Oncol 2023; 21: 182.

Chylous Effusion in A Patient with Lung Adenocarcinoma Cancer Treated with *Rearranged During Transfection*-Tyrosine Kinase Inhibitors: A Case Report

Wei-Hsuan Chang[1], Gee-Chen Chang[1,2,3,4]

Rearranged during transfection (*RET*) rearrangement/fusion-positive non-small cell lung cancer (NSCLC) accounts for 1%–2% of the NSCLC population, and can now be treated effectively with selective RET-tyrosine kinase inhibitors (TKIs), including selpercatinib and pralsetinib. Occasionally, rare side effects can occur with the use of TKIs. Here, we report the case of a 48-year-old man with RET fusion-positive stage IV lung adenocarcinoma who demonstrated a good tumor response to selpercatinib. Unfortunately, the patient developed symptomatic refractory chylous ascites, a rare side effect, 9 months after initiating selpercatinib therapy. Chylous effusion has been reported more frequently with selpercatinib treatment, while pralsetinib-related chylous effusion rarely occurs. In our case report, the patient's chylous effusion persisted even after switching the medication to pralsetinib. We also briefly reviewed various methods that have been successful in treating RET-TKI-induced chylous effusion. ***(Thorac Med 2024; 39: 339-346)***

Key words: RET, lung cancer, selpercatinib, pralsetinib, chylous effusion

Introduction

Lung cancer is the leading cause of cancer-related death worldwide [1]. Non-small cell lung cancer (NSCLC) is the most common type [1]. *Rearranged during transfection* (*RET*) rearrangement is an oncogenic driver in lung cancer [1], and individuals with RET fusion-positive NSCLC account for 1%–2% of the lung cancer population [1-2]. Before the development of selective RET-tyrosine kinase inhibitors (TKIs), multikinase inhibitors (MKIs) with anti-RET activity were used to target RET fusion genes in patients with late-stage lung cancer [2]. The response rates to MKIs have been unappealing, with objective response rates (ORR) of 16-53% [2].

Two selective RET inhibitors, selpercatinib

[1]Division of Pulmonary Medicine, Department of Internal Medicine, Chung Shan Medical University Hospital, Taichung, Taiwan. [2]School of Medicine, Chung Shan Medical University, Taichung, Taiwan. [3]Institute of Medicine, Chung Shan Medical University, Taichung, Taiwan. [4]Institute of Biomedical Sciences, National Chung Hsing University, Taichung, Taiwan
Address reprint requests to: Dr. Gee-Chen Chang, Division of Pulmonary Medicine, Department of Internal Medicine, Chung Shan Medical University Hospital, No. 110, Sec. 1, Jianguo N. Road, Taichung, 402, Taiwan

and pralsetinib, have demonstrated excellent ORRs: 61% and 84% in previously treated and treatment-naïve patients, respectively, for selpercatinib, and 61% and 70% in the same groups, respectively, for pralsetinib [3,4]. In a head-to-head comparison with platinum-based chemotherapy as first-line treatment, selpercatinib demonstrated superiority in ORR and progression-free survival (PFS) [5]. Additionally, both selpercatinib and pralsetinib have shown efficacy in controlling brain metastasis, with intracranial response rates of approximately 85% for selpercatinib and 56% for pralsetinib in patients with brain metastasis [3-4]. Owing to their performance, the National Comprehensive Cancer Network guidelines recommend salpercatinib and pralsetinib as first-line or subsequent treatments for late-stage RET fusion-positive lung cancer [6].

Similar to other TKIs, selective RET-TKIs can have serious adverse effects. The most common serious adverse events (AEs) associated with selective RET-TKIs include hypertension (with both medications) [3-5], elevated alanine aminotransferase (ALT) and aspartate aminotransferase (AST) levels with selpercatinib [3,5], and neutropenia and anemia with pralsetinib [4]. In addition to common AEs, rare AEs may occur and pose significant challenges. Herein, we present the case of a patient who developed refractory chylous effusion after receiving selective RET-TKIs.

Case Presentation

A 48-year-old male patient with a smoking history of 2 packs of cigarettes per day for 20 years presented with left wrist pain and a nontender head mass persisting for 2 months. He experienced unintentional body weight loss of 7 kg within 3 months (from 91 to 84 kg) and occasional hemoptysis. He managed a textile factory in Mainland China and sought medical attention at a hospital in Guangdong for his symptoms. Chest radiography revealed a right upper lobe mass lesion with partial lung collapse, prompting the suspicion of lung cancer. The patient returned to Taiwan in October 2020 for further treatment.

In Taiwan, he underwent contrast-enhanced chest computed tomography (CT), which showed a right upper lobe mass causing upper lobe collapse, multiple diffuse nodules in bilateral lung fields, and mediastinal lymphadenopathy (Figure 1A). Brain magnetic resonance imaging revealed bone metastasis in the frontal skull, while a whole-body bone scan detected bone metastases in the right frontal lobe, left zygomatic bone, and left distal radius. The patient underwent bronchoscopic biopsy, which revealed a tissue pathology that indicated poorly differentiated adenocarcinoma, with positive immunochemical staining for thyroid transcription factor-1 and negative for P40. The final stage was determined to be stage IVB (T4N3M1c). The patient tested negative for programmed cell death-ligand 1 (PD-L1) expression. Hence, molecular sequencing was performed using the Oncomine next-generation sequencing test, which revealed *KIF5B-RET* fusion.

Selpercatinib 80 mg BID was initiated in November 2022. The patient responded well to this treatment, with rapid improvement in wrist pain and head mass. As investigators in the selpercatinib versus chemotherapy trial [5], we had access to the preliminary subgroup analysis prior to the study's publication. We observed 2 groups of patients who did not show a significant PFS benefit from selpercatinib treatment

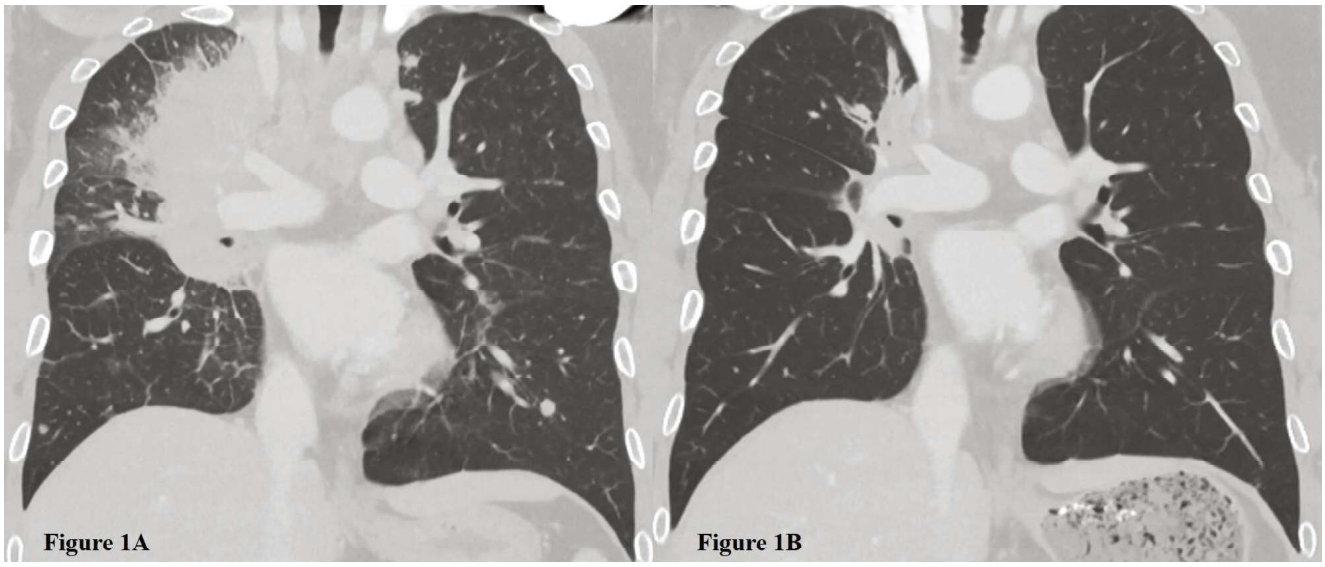

Fig. 1. A: Coronal view of the patient's chest CT at the initial diagnosis of lung cancer. B: Coronal view of the patient's chest CT 6 months after diagnosis after treatment with selpercatinib and local radiotherapy. The primary tumor and lung metastasis are reduced.

compared with chemotherapy. The first group comprised current or former smokers, while the other group comprised patients with negative PD-L1 expression (full forest plot shown in Supplementary Appendix and Figure S2). Our patient exhibited both of these characteristics, suggesting a potentially less favorable outcome and possibly shorter PFS compared with the general population receiving selpercatinib.

After a discussion with our patient, he consented to receive concurrent chemotherapy. Concurrent chemotherapy was initiated on December 13, 2022, with cisplatin + pemetrexed administered for 4 cycles, followed by

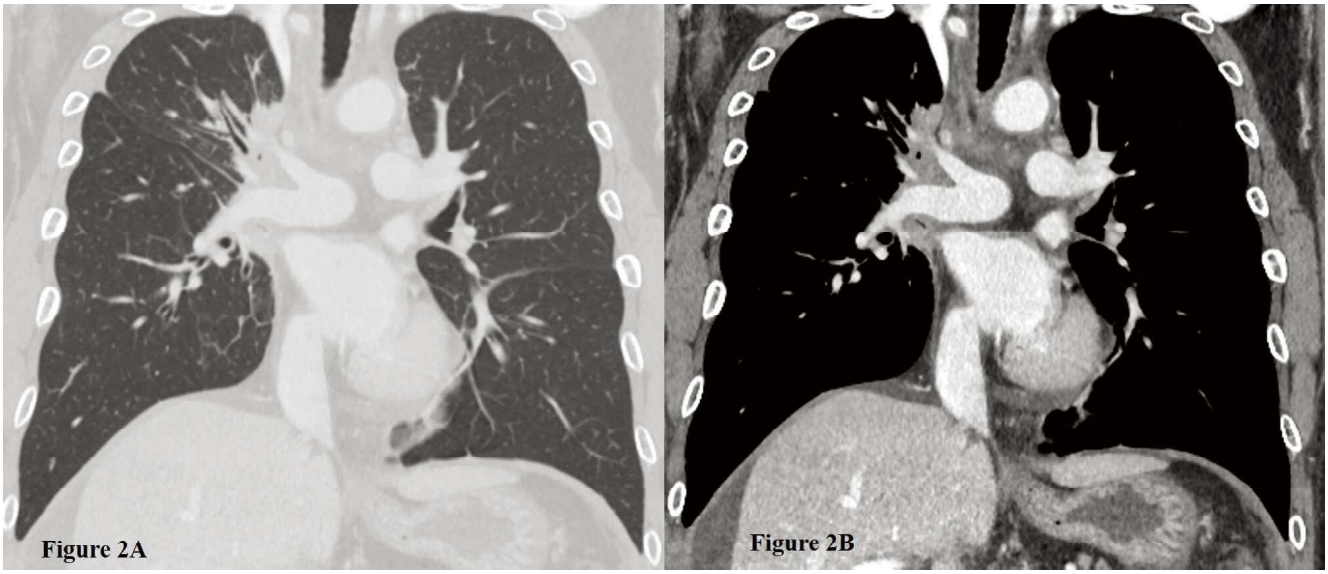

Fig. 2. Coronal view of the lung (A) and mediastinal (B) window of the patient's chest CT at the onset of chylous effusion. No specific sign of lung tumor progression was noted in the lung window, although some ascites was observed in the mediastinal window.

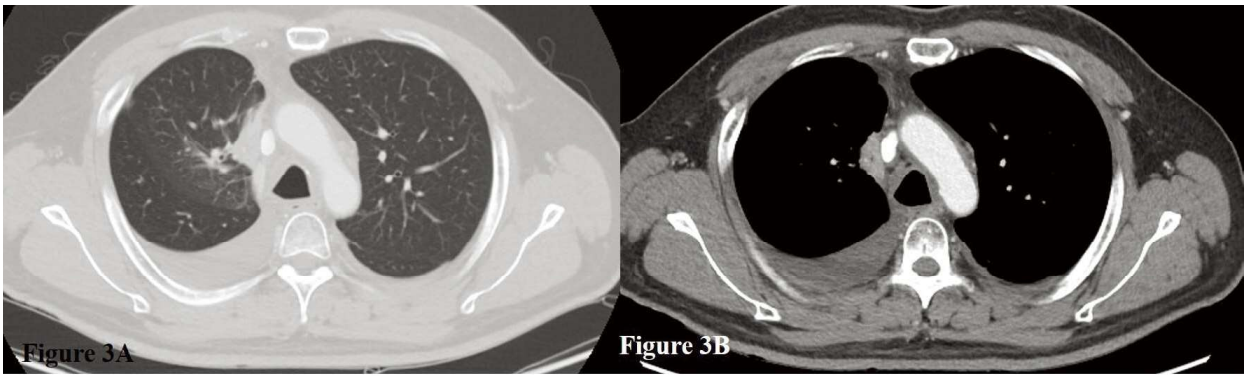

Fig. 3. Axial view of the lung (A) and mediastinal (B) window at the onset of chylous effusion. No obvious signs of perimediastinal pulmonary fibrosis (A) or mediastinal fibrosis (B) were noted. Note that bilateral pleural effusion was evident in the images.

Fig. 4. Chylous effusion when initially drained. The leftmost bottle shows the ascites (triglyceride: 6,736 mg/dL), the middle bottle shows the left pleural effusion (TG: 562 mg/dL), and the rightmost bottle shows the right pleural effusion (TG: 299 mg/dL).

pemetrexed as maintenance therapy (brief treatment timeline shown in Figure 5). On February 13, 2023, local radiotherapy at a dose of 60 Gy was delivered to the primary tumor and mediastinal lymph nodes. This decision was influenced by the findings of the study by Hsu, *et al*. [7], which showed improved PFS and overall survival following curative dose radiotherapy to the primary tumor site in patients with treatment-naïve, stage IIIB–IV lung cancer responding well to epidermal growth factor receptor (EGFR)-TKIs. Although the original

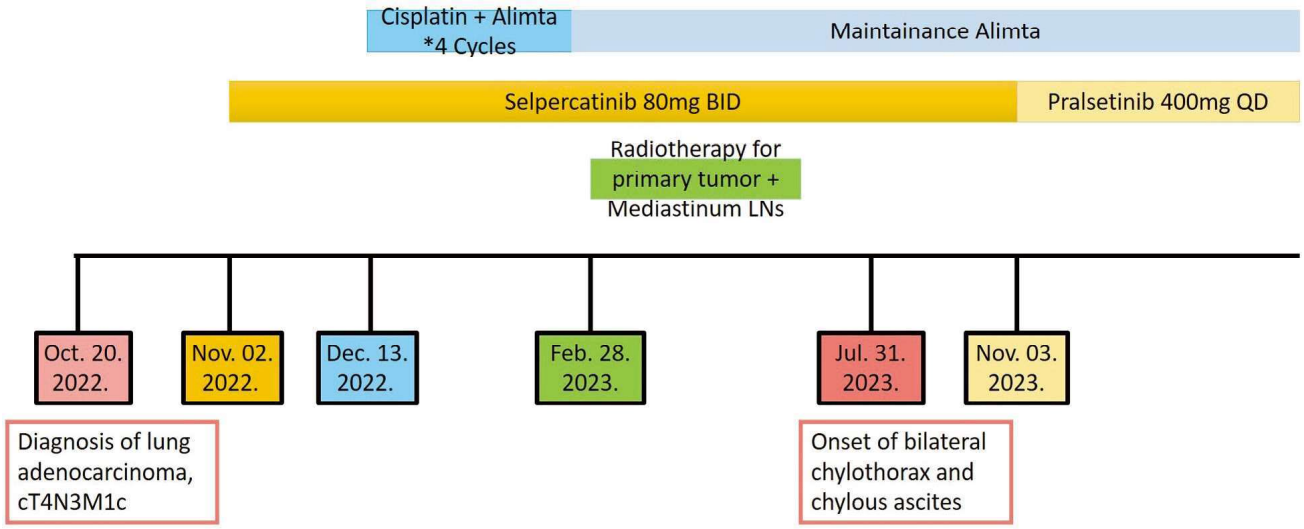

Fig. 5. Brief timeline of the patient's diagnosis of lung cancer and treatments.

study involved an EGFR-TKI population, we hypothesized that the administration of curative dose radiotherapy to our patient, who responded well to RET-TKIs, may yield similar beneficial effects. Six months after treatment, the tumor remained well controlled (Figure 1B), and the patient reported no discomfort.

Nine months after initiating selpercatinib therapy, regular follow-up chest CT revealed bilateral pleural effusion and mild ascites (Figures 2 and 3). Although the patient reported no symptoms at that time, diagnostic tapping was performed, which revealed bilateral chylothorax (triglyceride levels: right = TG 299 mg/dL and left = 562 mg/dL) and abdominal chylous ascites (TG = 6,736 mg/dL) (Figure 4). Cytological results revealed the absence of malignant cells in both the ascites and pleural effusion obtained from the bilateral lung fields. No other evidence of disease progression was noted after a thorough examination. Chylous effusion as a complication associated with selpercatinib therapy was considered.

The patient was advised to consume a high-protein and low-fat diet under the guidance of a nutrition specialist, and selpercatinib therapy was continued. With the continuation of this treatment, the pleural effusion remained constant, while the volume of ascites continuously increased, resulting in progressive abdominal distension, loss of appetite, and weight loss. The patient required therapeutic paracentesis every 1–2 weeks, with each session draining 3000–4000 mL of ascites. Despite maintaining an alipidic diet and taking a regular dose of selpercatinib for 3 months, the volume of ascites did not reduce.

In November 2023, the RET-TKI treatment was switched to pralsetinib (400 mg QD). Eight weeks after switching to pralsetinib, the volume of ascites showed no decrease, requiring weekly abdominal paracentesis despite reporting improvements in abdominal distension and appetite. As grade 3 pancytopenia developed during pralsetinib treatment, pralsetinib was withheld. One week after the discontinuation of pralsetinib, a prominent decrease in ascites was noted. After resuming pralsetinib treatment, ascites recurred. Due to uncontrolled refractory ascites, the treatment was switched to cabozantinib. Three days after initiating carbozantinib therapy, the patient complained of left wrist and skull pain, which were similar to those experienced at the initial diagnosis of lung cancer. The patient discontinued carbozantinib and resumed pralsetinib therapy. Two days later, the skull and wrist pain resolved. The patient remains on pralsetinib therapy.

Discussion

The *RET* gene is located on chromosome 10 and encodes a transmembrane glycoprotein receptor tyrosine kinase [2]. The oncogenic activation of *RET* can occur via mutations or fusions. In NSCLC, only RET fusion/rearrangement has been identified as an oncogenic driver [1-2]. The most common fusion partners in NSCLC are KIF5B and CCDC6, with CCDC6 fusions typically showing better prognosis than KIF5B fusions, regardless of the treatment received [1, 4].

Chylous effusion is a rare complication associated with RET-TKIs [8]. According to a review by Kalchiem-Dekel, *et al*., chylous effusion occurred in 7% of patients taking selpercatinib, but not in patients taking pralsetinib [8]. The presence of chylous effusion had no negative effect on median treatment time, compared with the absence of chylous effusion [8]. More

recently, chylous effusion has been reported following pralsetinib use [9], indicating that this condition is not an isolated AE. In the era of using MKIs to target *RET* fusions, sporadic cases of MKI-related chylous effusion were reported, although the incidence rate was much lower than that with selpercatinib [8].

The mechanism of RET-TKI-induced chylous effusion is not well understood. Chylous effusion typically occurs when the lymphatic flow is disrupted, and is commonly caused by trauma, malignancy, infections, inflammation, cirrhosis, and cardiogenic and congenital conditions [10]. However, RET-TKI-related chylous effusion does not fall into any of these categories. Among salpercatinib-treated patients who develop chylous effusion, no radiological evidence of lymphatic channel invasion or substantial compressive disease has been found [8]. In addition, no chyle leaks have been noted in patients who underwent lymphangiography [8]. Another rare instance of chylothorax, incidentally reported in patients who received mediastinal radiation therapy, is thought to arise from mediastinal fibrosis causing lymphatic drainage obstruction [11-12].

Although our patient received curative dose radiation therapy for the mediastinum and primary tumor, we do not believe that his chylous effusion was related to mediastinal fibrosis, for 2 primary reasons. First, there was no evidence of mediastinal and paramediastinal lung fibrosis or pleural fibrosis on our patient's chest CT at the onset of chylous effusion (Figure 3A, 3B). Second, 1 week after discontinuing pralsetinib due to neutropenia, we observed a significant decrease in the volume of chylous ascites. However, upon resuming pralsetinib, the amount of ascites started to increase (Figure 6), suggesting a strong correlation between ascites and RET-TKI use. Considering this evidence, our patient's chylous effusion was more likely to be a rare side effect of selective RET-TKIs rather than mediastinal fibrosis.

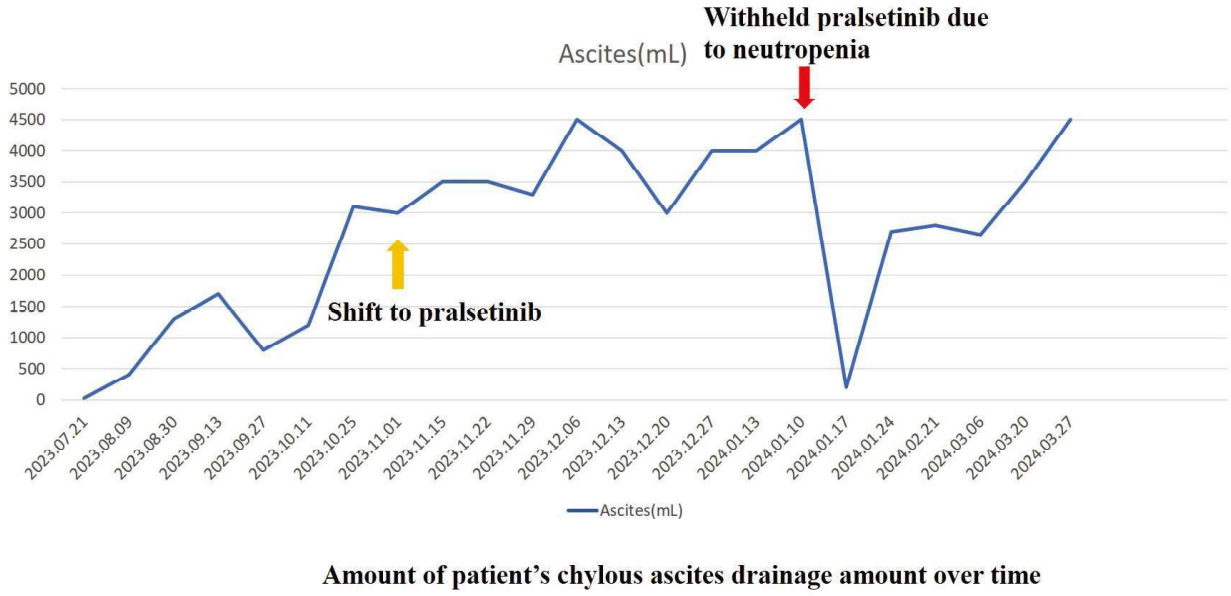

Fig. 6. Records of the amount of ascites drained from the patient. One week after discontinuing pralsetinib treatment, ascites decreased, but then increased after resuming pralsetinib treatment.

The optimal treatment for RET-TKI-induced chylous effusion remains unclear. Although mild asymptomatic effusion can be safely monitored without treatment, symptomatic patients with refractory effusion typically require intensive treatment. Reducing the dose of RET-TKIs has yielded equivocal results. Some studies suggested that reducing the dose decreases the amount of chylous effusion [9, 13], and others reported a correlation between dose reduction and a decrease in effusion [8]. Switching from selpercatinib to pralsetinib or vice versa has been explored as an option, but it did not benefit our patient. Chylous effusion has been attenuated with a low-fat, high-protein diet [9, 14], the use of somatostatin analogs, or any combination of these methods [9]. Bowel rest with total parenteral nutrition, or more invasive treatments such as peritoneovenous shunting, transjugular intrahepatic portosystemic shunt, surgical exploration, and ligation have been employed for the treatment of refractory chylous ascites of other etiologies [9-10, 15]. However, such extreme methods are usually unnecessary and of limited benefit in patients taking RET-TKIs.

In our case, dietary adjustments and switching between selpercatinib and pralsetinib provided limited improvement in chylous ascites. Transitioning his medication to carbozantinib showed minimal control of lung cancer progression with worsening symptoms. Ultimately, the patient opted to continue pralsetinib treatment with regular abdominal paracentesis for optimal lung cancer control.

Chylous effusion is a rare side effect of RET-specific TKIs. As selpercatinib and pralsetinib have shown excellent overall response rates and have been approved for late-stage NSCLC and thyroid cancer [3-4, 16-17], their use is expected to increase in the future. Consequently, more physicians will likely encounter this rare adverse effect. Therefore, it is crucial to avoid misinterpreting the accumulation of pleural effusion and ascites as signs of cancer progression, which could lead to the early discontinuation of effective treatment [7].

Conclusion

Selpercatinib and pralsetinib are 2 selective RET-TKIs approved for first-line treatment of late-stage RET fusion-positive NSCLC [6]. Chylous effusion is a rare side effect of these TKIs, and new-onset effusions in these patients should be carefully interpreted to avoid mistaking AEs for disease progression. TKI dose reduction, dietary adjustments, and the use of somatostatin analogs have shown efficacy in treating RET-TKI-induced chylous effusion. Switching from selpercatinib to pralsetinib may also be considered. Further investigations are needed to elucidate the mechanism behind the occurrence of RET-TKI-induced chylous effusion. Currently, the optimal treatment for this condition remains uncertain, but it should aim at achieving adequate symptom control while maintaining effective TKI treatment.

References

1. Novello S, Califano R, Reinmuth N, *et al*. RET fusion-positive non-small cell lung cancer: the evolving treatment landscape. Oncologist 2023 May 8; 28(5): 402-13.
2. Drilon A, Hu ZI, Lai GGY, *et al*. Targeting RET-driven cancers: lessons from evolving preclinical and clinical landscapes. Nat Rev Clin Oncol 2018 Mar; 15(3): 151-67.
3. Drilon A, Subbiah V, Gautschi O, *et al*. Selpercatinib in patients with RET fusion-positive non-small-cell lung

cancer: updated safety and efficacy from the registrational LIBRETTO-001 phase I/II Trial. J Clin Oncol 2023 Jan 10; 41(2): 385-94.

4. Gainor JF, Curigliano G, Kim DW, *et al*. Pralsetinib for RET fusion-positive non-small-cell lung cancer (ARROW): a multi-cohort, open-label, phase 1/2 study. Lancet Oncol 2021 Jul; 22(7): 959-69.
5. Zhou C, Solomon B, Loong HH, *et al*. First-line selpercatinib or chemotherapy and pembrolizumab in RET fusion–positive NSCLC. N Engl J Med 2023 Nov; 389(20): 1839-50.
6. National Comprehensive Cancer Network ®. Clinical practice guidelines in oncology (NCCN Guidelines®): non-small cell lung cancer (version 2.2024). 2024. https://www.nccn.org/. Accessed 14 February 2024.
7. Hsu KH, Huang JW, Tseng JS, *et al*. Primary tumor radiotherapy during EGFR-TKI disease control improves survival of treatment naïve advanced EGFR- mutant lung adenocarcinoma patients. Onco Targets Ther 2021 Mar 25; 14: 2139-48.
8. Kalchiem-Dekel O, Falcon CJ, Bestvina CM, *et al*. Brief report: chylothorax and chylous ascites during RET tyrosine kinase inhibitor therapy. J Thorac Oncol 2022 September; 17(9): 1130-36.
9. Fricke J, Wang J, Gallego N, *et al*. Selpercatinib and pralsetinib induced chylous ascites in RET-rearranged lung adenocarcinoma: a case series. Clin Lung Cancer 2023 Nov; 24(7): 666-71.
10. Lizaola B, Bonder A, Trivedi HD, *et al*. Review article: the diagnostic approach and current management of chylous ascites. Aliment Pharmacol Ther 2017 Nov; 46(9): 816-24.
11. Lee YC, Tribe AE, Musk AW. Chylothorax from radiation-induced mediastinal fibrosis. Aust N Z J Med 1998 Oct; 28(5): 667-68.
12. Van Renterghem D, Pauwels R. Chylothorax and pleural effusion as late complications of thoracic irradiation. Chest 1995 Sept; 108(3): 886-87.
13. Prete A, Gambale C, Cappagli V, *et al*. Chylous effusions in advanced medullary thyroid cancer patients treated with selpercatinib. Eur J Endocrinol 2022 Nov 29; 187(6): 905-15.
14. Provenzano L, Damian S, Duca M, *et al*. Ascites during selpercatinib treatment: need for a multidisciplinary approach. J Thorac Oncol 2023 Feb; 18(2): e9-e10.
15. Duletzke NT, Kiraly LN, Martindale RG. Chylothorax and chylous ascites: overview, management, and nutrition. Nutr Clin Pract 2023 Jun; 38(3): 557-563.
16. Bradford D, Larkins E, Mushti SL, *et al*. FDA approval summary: selpercatinib for the treatment of lung and thyroid cancers with RET gene mutations or fusions. Clin Cancer Res 2021 Apr 15; 27(8): 2130-35.
17. Kim J, Bradford D, Larkins E, *et al*. FDA approval summary: pralsetinib for the treatment of lung and thyroid cancers with RET gene mutations or fusions. Clin Cancer Res 2021 Oct 15; 27(20): 5452-56.

Pulmonary *Trichosporon Asahii* Infection in a Patient with Post-COVID-19 Organizing Pneumonia

Kenneth Yung[1], Yao-Wen Kuo[2], Chia-Lin Hsu[1], Jin-Yuan Shih[1]

SARS-CoV-2 infection is associated with several sequelae that may occur following the initial infection. We report on the case of an 80-year-old man who developed new onset hypoxia and bilateral pulmonary opacities after his initial mild COVID-19. He was initially treated empirically with broad-spectrum antibiotics, with a poor response. Computed tomography imaging was compatible with organizing pneumonia, so steroids were added. However, oxygen demand and pulmonary opacities showed a poor response to treatment. Sputum culture was later positive for the growth of *Trichosporon asahii*, so voriconazole was added and corticosteroids were tapered. The patient was successfully treated after the addition of voriconazole. Our case highlights that *Trichosporon asahii* superinfection may occur after COVID-19, and its growth from sputum cultures should merit treatment as a true pathogen. ***(Thorac Med 2024; 39: 347-355)***

Key words: SARS-CoV-2, COVID-19, Trichosporon asahii, organizing pneumonia

Background

The spectrum of symptomatic severe acute respiratory syndrome coronavirus 2 (SARS-CoV-2) infection can range from simple upper airway symptoms to severe acute respiratory distress syndrome (ARDS) requiring mechanical ventilation and critical care. In addition to the acute phase of the illness, coronavirus disease 2019 (COVID-19) is also associated with numerous respiratory and systemic sequelae that may persist, even if the initial viral infection has resolved. These may include superinfection or post-COVID interstitial lung diseases (ILDs).

Here, we report the case of a patient who developed acute hypoxemic respiratory failure a week after his initial mild COVID-19 infection, due to post-COVID organizing pneumonia with concurrent *Trichosporon asahii* superinfection.

[1]Division of Pulmonary and Critical Care Medicine, Department of Internal Medicine, National Taiwan University Hospital, Taipei, Taiwan. [2]Department of Integrated Diagnostics and Therapeutics, National Taiwan University Hospital, Taipei, Taiwan
Address reprint requests to: Dr. Kenneth Yung, No. 7, 11th Fl., Lane 48, Section 2, Roosevelt Rd, Zhongzheng District, Taipei City, 100, Taiwan

Case Presentation

An 80-year-old man presented to the emergency room complaining of having had 1 week of progressive dyspnea associated with cough, chest pain, and general malaise that started after recovering from mild COVID-19. He initially presented with fever, sore throat, and cough. COVID-19 infection was confirmed with home SARS-CoV-2 antigen testing. There was no dyspnea at the time, and he only took medications for symptom control from a local clinic. No antiviral medications were prescribed. These upper respiratory airway symptoms and fever then resolved. Afterwards, the patient started experiencing new onset dyspnea and worsening cough that were not initially present.

His past medical history was significant for coronary artery disease previously treated with coronary artery bypass grafting, as well as hypertension, hyperlipidemia, and diabetes mellitus (HbA1c 5.7%), controlled with carvedilol, rosuvastatin, and linagliptin, respectively. He had never been vaccinated against COVID-19. On presentation to our emergency room, his initial oxygen saturation while breathing ambient air, as measured by pulse oximetry, was only 86%. It improved to 94% after receiving oxygen at 3 L/min via nasal cannula. Vital signs were a body temperature of 36.9℃, blood pressure of 110/65 mmHg, heart rate of 76 beats per minute, and respiratory rate of 20 breaths per minute. Blood test results showed a white blood cell count of 9.2 k/μL (78.9% segmented neutrophils) without band form neutrophils or eosinophils. Renal and liver function were unremarkable. High-sensitivity C-reactive protein (hsCRP) was 14.4 ng/mL (normal range <10.0 ng/mL), and procalcitonin was 0.0081 ng/mL (normal range <0.5 ng/mL).

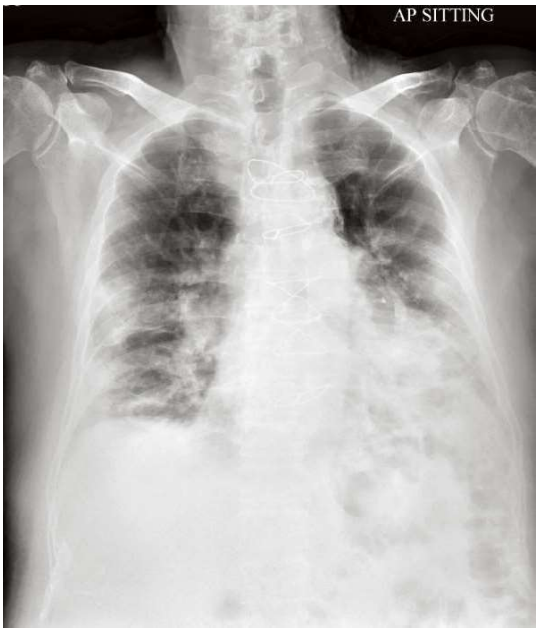

Fig. 1. Admission chest X-ray shows bilateral consolidation.

The SARS-CoV-2 rapid test was negative. Initial chest X-ray showed bilateral subpleural consolidations with bilateral costophrenic angle blunting (Figure 1). The patient was admitted, and a non-contrast computed tomography (CT) scan of the chest showed bilateral subpleural and peribroncho-vascular ground glass opacities and consolidation with bilateral minimal pleural effusion (Figure 2). Based on the imaging, differential diagnoses included community-acquired pneumonia and post-COVID-19 organizing pneumonia. The patient was initially started on broad spectrum antibiotics. However, on the second day of admission, the patient's oxygen demand escalated to FiO_2 60% with a flow of 60 L/min under high-flow nasal cannula (HFNC) usage. His hsCRP level increased to 50.1 ng/mL.

On the eighth day of admission, repeated CT imaging showed worsening bilateral consolidation (Figure 3). Procalcitonin remained low at 0.079 mg/dL. A multi-disciplinary discus-

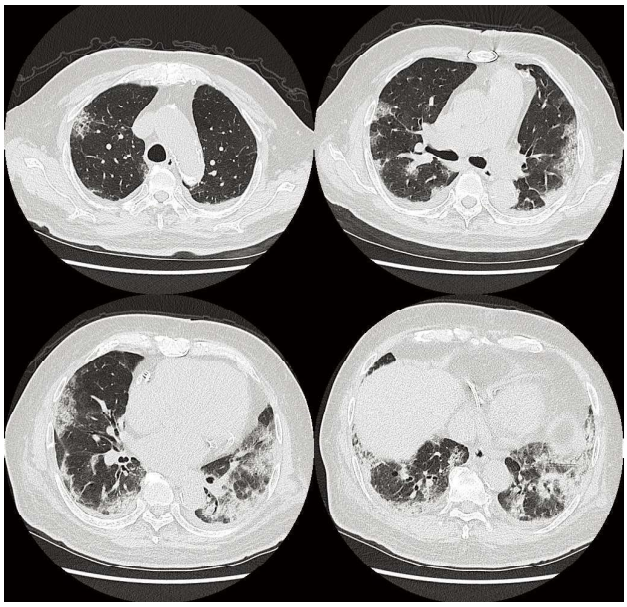

Fig. 2. Admission CT shows bilateral subpleural and peribronchovascular ground glass opacities and consolidation with bilateral minimal amount of pleural effusion.

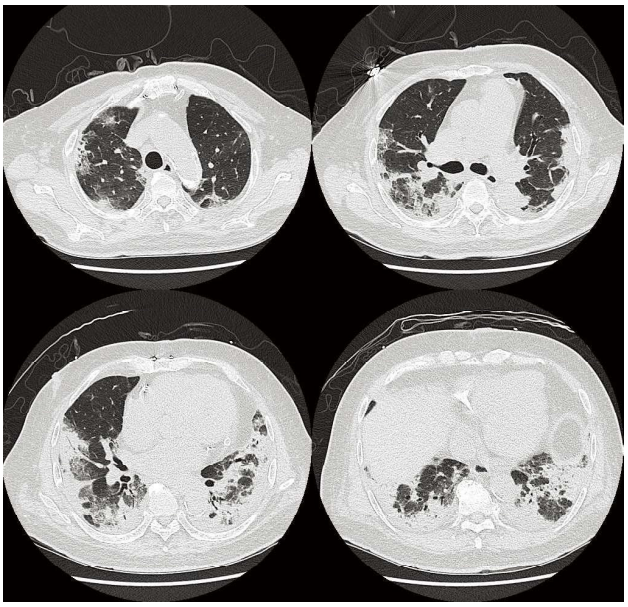

Fig. 3. Day 8 CT shows progression of bilateral consolidation.

sion was then held. Given the patient's imaging and clinical status, as well as his deteriorating oxygenation under broad spectrum antibiotics, it was decided to start corticosteroids for empirical treatment of post-COVID organizing pneumonia. Due to the high oxygen demand at the time and patient refusal, lung biopsy was not considered. Methylprednisolone was initiated at a dose of 1 mg/kg/day. Screening for possible connective tissue disease-related ILD was positive only for antinuclear antibody AC-26. Testing for C3, C4, rheumatoid factor, and other autoantibodies were all within normal limits. After discussion with a rheumatologist, his antinuclear antibody finding was considered incidental since there were no other signs or symptoms of rheumatic disease.

Initial workup for respiratory pathogens was unremarkable; results are shown in Table 1. Even with the use of antibiotics and corticoste-

Table 1. Survey for Infectious Pathogens

Bacteria culture (sputum)	Negative
Acid-fast stain and mycobacterium culture (sputum)	Negative
Aspergillus antigen (expectorated sputum)	Negative
Aspergillus antigen (blood)	Negative
CMV viral load (blood)	Negative
Mycoplasma pneumoniae IgM (blood)	Negative
Chlamydophila pneumoniae IgM Ab	Negative
Legionella urinary antigen	Negative
Pneumococcus urine rapid screen	Negative
Biofire® Filmarray® respiratory panel	Negative

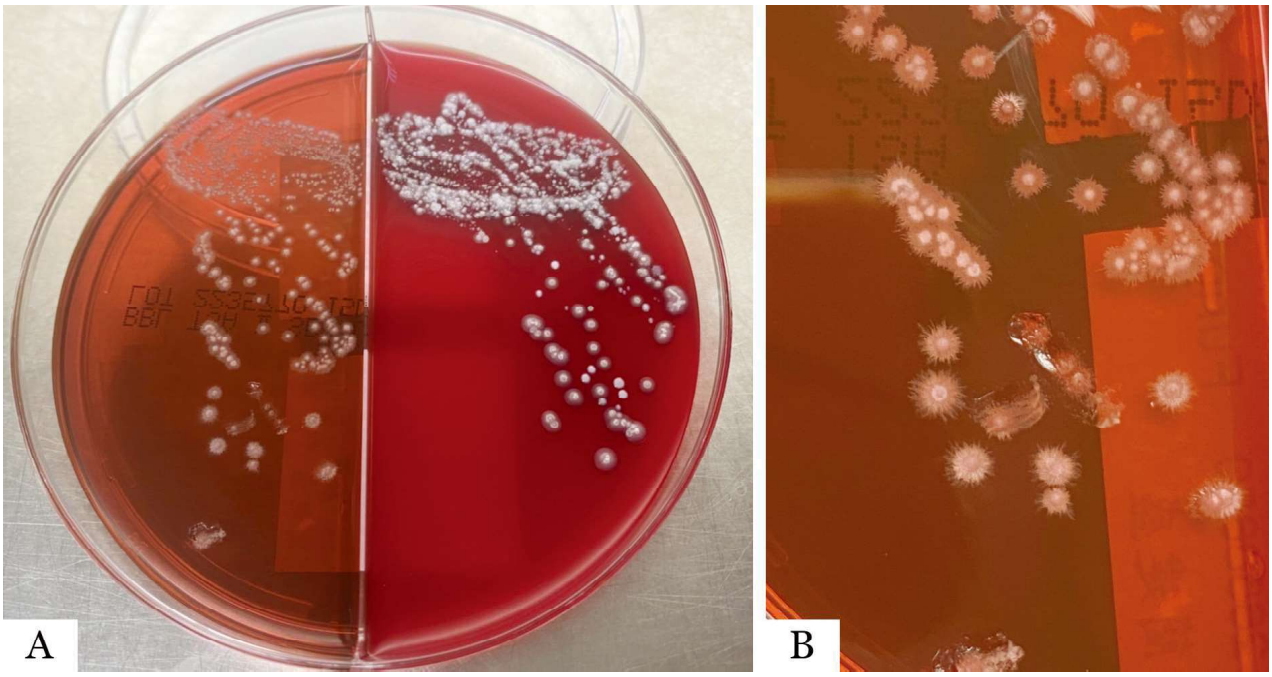

Fig. 4. (A) Numerous cream-colored colonies on EMB agar and blood agar. (B) Enlarged view of colonies on EMB agar shows growth of cream-colored colonies with central heaping and peripheral furrowing with irregular folds typical of *Trichosporon asahii*. The pathogen was confirmed as *Trichosporon asahii* using MALDI-TOF.

roid, the patient's oxygen demand remained at FiO_2 60% under HFNC usage and could not be tapered. However, on hospital day 13, sputum fungal cultures grew *Trichosporon asahii* (Figure 4). Minimal inhibitory concentrations are shown in Table 2. Discussion with our infectious disease specialist was held, and it was decided to treat the Trichosporon growth as a true infection rather than contamination. Intravenous voriconazole was started at 300 mg every 12 hours. Methylprednisolone dosage was tapered to 0.5 mg/kg/day due to a poor therapeutic response and concern for immunosuppression.

After 5 days of voriconazole usage, the patient's FiO_2 could be tapered from 60% under 60 L/min HFNC usage to 50%. During the next 3 weeks under voriconazole, the patient's FiO_2 was continuously tapered along with his steroid dosage. He was transitioned to oral prednisolone at 0.25 mg/kg/day on hospital day 24, and to low-flow nasal cannula usage on hospital day 30. On hospital day 35, the patient's oxygen demand had decreased enough that echo-guided fine needle aspiration could be performed to an area of subpleural consolidation in the lungs. Cytology and cultures for bacteria, fungus, and

Table 2. Minimum Inhibitory Concentration (MIC) for Trichosporon asahii CBS by Broth Microdilution Uusing the Thermo Scientific Sensititre YeastOne® System

Drug	MIC (μg/mL)
5-flucytosine	2
Amphotericin B	1
Fluconazole	8
Itraconazole	0.5
Posaconazole	0.5
Voriconazole	0.25
Anidulafungin	8
Caspofungin	8
Micafungin	8

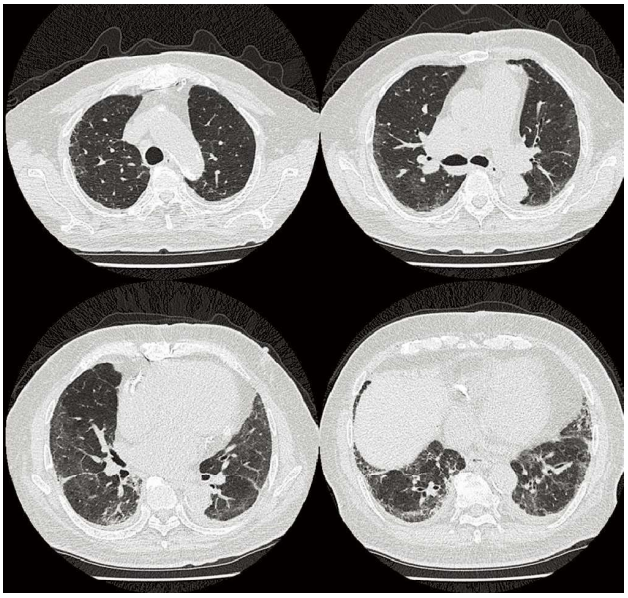

Fig. 5. CT 2 months after discharge shows resolving consolidation, with residual fibrotic changes.

mycobacterium were all negative. The patient was discharged on hospital day 48 after a period of rehabilitation, due to prior deconditioning. Voriconazole was given for a total of 71 days. CT performed 2 months after discharge showed marked improvement in his prior lung consolidation (Figure 5). The patient remained oxygen-free on follow-up.

Discussion

In addition to direct lung injury during the acute phase of illness, long-term pulmonary sequelae have also been described in survivors of COVID-19. These range from symptoms of persistent dyspnea, cough, and thromboembolic disease to post-COVID-19 ILD [1]. Organizing pneumonia is 1 of the presentations of COVID-19-related ILD and has been reported to occur following partial or complete pulmonary recovery from COVID-19 [2]. Definitive diagnosis of organizing pneumonia requires tissue biopsy, but oftentimes a confident clinical diagnosis can be made from a combination of compatible clinical presentation, typical CT imaging patterns, or broncho-alveolar lavage findings. One predominant imaging pattern features the presence of multifocal areas of airspace consolidation that are peripheral and peri-bronchial, with a predisposition for lung bases, and often migrate or change over a matter of weeks [3,4].

For patients who have progressive symptoms, diffuse radiographic involvement, or a need of inpatient management, corticosteroids are the mainstay of treatment [5]. The British Thoracic Society states that a starting dose of 0.75–1 mg/kg prednisolone weaned over 6–12 months is reasonable [6]. The response to steroids is often dramatic, and improvement can occur within days of initiating therapy. When it comes to post-COVID organizing pneumonia, there are no established treatment protocols. In an observational study by Myall, *et al*, 30 patients with symptomatic post-COVID organizing pneumonia were treated with oral prednisolone starting at a maximum dose of 0.5 mg/kg prednisolone tapered over 3 weeks. All patients reported improved symptoms and repeat CT imaging showed improvement [7].

Some patients with organizing pneumonia fail to respond to corticosteroid treatment, which reflects the heterogeneity of the condition [8-9]. These cases may require an increase in corticosteroid dosing or the use of other immunosuppressive agents. In patients treated without biopsy, the diagnosis of organizing pneumonia and possibility of an alternative diagnosis should also be considered. Our patient's history of recent COVID-19 along with typical CT findings led us to suspect a diagnosis of organizing pneumonia. We decided to start corticosteroid treatment due to the poor response to broad spectrum antibiotics and persistently

low procalcitonin levels. However, his oxygen demand and pulmonary imaging showed a less than satisfactory response to methylprednisolone given at 1 mg/kg/day, despite 7 days of therapy.

His sputum culture was later positive for *Trichosporon asahii*. *Trichosporon asahii* is a yeast-like organism found ubiquitously in the environment and as normal flora on human skin and in the gastrointestinal tract [10]. Under microscopy, it can form hyphae, pseudohyphae, and arthroconidia [11]. Fungemia is the most common site of involvement, but isolated pulmonary infection without fungemia has also been reported [12-13]. Risk factors for infection include hematological malignancies, organ transplantation, diabetes, end-stage renal disease, and human immunodeficiency virus infection. Central venous catheter usage and prior antibiotic exposure are also risk factors, as reported by Ruan, *et al* [13]. *Trichosporon asahii* has also been cultured from the sputum and urine of patients without invasive disease, which may reflect colonization [14].

Trichosporon asahii has also been reported as causing secondary infection in otherwise immunocompetent patients with COVID-19. A literature search yielded 13 cases of COVID-19 infection complicated with *Trichosporon asahii* super-infection (Table 3). There were 8 cases of

Table 3. Cases of Trichosporon Asahii Infection in COVID-19 Patients Reported from COVID-19 onset to 2024/5

Ref	Age	Sex	Length of stay	Culture source	Days since admission prior to culture positive	Steroid duration prior to positive culture	Cumulative steroid dose (prednisone equivalent) prior to positive culture (mg)	Anti-fungal used	Outcome
Our case	80	M	48	Sputum	13	7	700	V	Recovery
20	75	M	121	Blood	94	95	447	V	Recovery
21	74	M	40	Urine	18	14	426	E	Death
22	58	F	20	Blood	17	Dose/duration not reported		A	Death
23	58	M	24	Sputum	27	3	470	V	Death
24	73	M	80	Urine	53	Dose/duration not reported		F,V	Death
25	58	M		Blood	11	Dose/duration not reported		V	Recovery
26	57	M	43	Blood	30	30		V	Recovery
26	74	M	32	Blood	30	31		E	Death
26	75	F	45	Blood	26	26		E,A,V	Death
26	73	M	33	Blood	15	16		A,V	Death
27	72	M	21	Blood	10	11		A,V	Death
28	71	M	15	Sputum	7	Dose/duration not reported		V	Death
29	36	F	37	Sputum	22	10		A,V	Death
30	67	M	30	Sputum	24	Dose/duration not reported		E,A,I	Death

V – voriconazole F – fluconazole I – itraconazole A – amphotericin E – echinocandin

fungemia, 3 cases of pulmonary infection, and 2 cases of urinary tract infection. Nine of the reported cases died during admission. COVID-19 coinfection with other opportunistic fungi such as Aspergillus, Mucormycosis, and Candida species has already been well described in the literature [15]. Proposed mechanisms that predispose these patients to opportunistic fungal infection include COVID-19-induced airway epithelial damage, focal lung hypoxia, steroid usage, lymphocyte dysfunction or a decreased type I interferon response [15]. Similar mechanisms may explain why immunocompetent patients may develop invasive *Trichosporon asahii* infection after COVID-19.

Per the European Organization for Research and Treatment of Cancer/Invasive Fungal Infection Cooperative Group definition of opportunistic invasive fungal infections, proven diagnosis of pulmonary trichosporonosis requires identification of *Trichosporon asahii* on biopsy or aspiration specimens from the patient's lung [16]. However, this is often too invasive. A probable diagnosis can be made when there are pulmonary infiltrates and growth of Trichosporon from sputum or bronchoalveolar lavage specimens [17]. Imaging patterns of pulmonary *Trichosporon asahii* infection described in the literature include cavitary lung lesions, and focal or diffuse alveolar consolidation, reticulonodular infiltration, and an interstitial pattern [18,23,29,30]. The optimal antifungal agent for the treatment of *Trichosporon asahii* is not yet defined. Based on in-vitro susceptibility testing and clinical evidence, echinocandins and amphotericin B are poor choices. Azoles have shown the best activity, and amongst them, voriconazole has been shown to have the lowest required minimal inhibitory concentration [19]. Kuo SH reported that in a series of 27 patients infected with Trichosporon receiving either fluconazole, amphotericin B, or voriconazole, those receiving voriconazole treatment had a significantly better rate of survival, at 66% [20].

In the case of our patient, we decided to treat his positive *Trichosporon asahii* sputum cultures as definitive pulmonary infection instead of simply colonization or contamination with normal oral flora. Since he had an unsatisfactory response to corticosteroids and antibacterial agents alone, we believed that *Trichosporon asahii* contributed to his pulmonary condition. In the literature review, *Trichosporon asahii* was not associated with organizing pneumonia, so we suspect that his initial imaging and clinical presentation could be attributed to post-COVID organizing pneumonia. *Trichosporon asahii* infection may then have been precipitated by broad spectrum antibiotics, corticosteroid usage, and COVID-19-induced lung injury. The patient responded well to therapy after a combined approach targeting both organizing pneumonia and *Trichosporon asahii*. To our knowledge, this is the first report of a case of post-COVID 19 complicated with both organizing pneumonia and *Trichosporon asahii* infection.

Conclusion

We reported a case of post-COVID-19 organizing pneumonia complicated with pulmonary *Trichosporon asahii* infection, and successfully treated with voriconazole. Thus, when patients present with respiratory symptoms and abnormal imaging after initial COVID-19, post-COVID-19 organizing pneumonia should be included in the differential diagnoses. If corticosteroid response is poor, other etiologies should be searched for. The pulmonary damage caused

by acute COVID-19 may predispose patients to invasive fungal infection, and *Trichosporon asahii* growth from sputum should potentially be considered a true pathogen.

References

1. Global Burden of Disease Long COVID Collaborators, Wulf Hanson S, Abbafati C, *et al*. Estimated global proportions of individuals with persistent fatigue, cognitive, and respiratory symptom clusters following symptomatic COVID-19 in 2020 and 2021. JAMA 2022; 328(16): 1604-15.
2. Bazdyrev E, Panova M, Zherebtsova V, *et al*. The hidden pandemic of COVID-19-induced organizing pneumonia. Pharmaceuticals (Basel) 2022; 15(12): 1574.
3. Polverosi R, Maffesanti M, Dalpiaz G. Organizing pneumonia: typical and atypical HRCT patterns. Radiol Med 2006; 111(2): 202-12.
4. Miao L, Wang Y, Li Y, *et al*. Lesion with morphologic feature of organizing pneumonia (OP) in CT-guided lung biopsy samples for diagnosis of bronchiolitis obliterans organizing pneumonia (BOOP): a retrospective study of 134 cases in a single center. J Thorac Dis 2014; 6(9): 1251-60.
5. Chandra D, Maini R, Hershberger DM. Cryptogenic organizing pneumonia. [Updated 2022 Sep 12]. In: StatPearls [Internet]. Treasure Island (FL): StatPearls Publishing; 2024 Jan.
6. Bradley B, Branley HM, Egan JJ, *et al*. Interstitial lung disease guideline: the British Thoracic Society in collaboration with the Thoracic Society of Australia and New Zealand and the Irish Thoracic Society. Thorax 2008; 63 Suppl 5:v1-v58.
7. Myall KJ, Mukherjee B, Castanheira AM, *et al*. Persistent post-COVID-19 interstitial lung disease. An observational study of corticosteroid treatment. Ann Am Thorac Soc 2021; 18(5): 799-806.
8. Shitenberg D, Fruchter O, Fridel L, *et al*. Successful rituximab therapy in steroid-resistant, cryptogenic organizing pneumonia: a case series. Respiration 2015; 90(2): 155-59.
9. Purcell IF, Bourke SJ, Marshall SM. Cyclophosphamide in severe steroid-resistant bronchiolitis obliterans organizing pneumonia. Respir Med 1997; 91(3): 175-77.
10. Chander J. Textbook of Medical Mycology. New Delhi: Jaypee Publishers, 2018.
11. Carroll KC, Pfaller MA. Manual of Clinical Microbiology, 4 Volume Set, 13th Edition. ASM Press, 2023.
12. Li H, Guo M, Wang C, *et al*. Epidemiological study of *Trichosporon asahii* infections over the past 23 years. Epidemiol Infect 2020; 148:e169.
13. Ruan SY, Chien JY, Hsueh PR. Invasive trichosporonosis caused by *Trichosporon asahii* and other unusual Trichosporon species at a medical center in Taiwan. Clin Infect Dis 2009; 49(1): e11-e17.
14. Hoy J, Hsu KC, Rolston K, *et al*. Trichosporon beigelii infection: a review. Rev Infect Dis 1986; 8(6): 959-67.
15. Hoenigl M, Seidel D, Sprute R, *et al*. COVID-19-associated fungal infections. Nat Microbiol 7 2022; 1127-40.
16. De Pauw B, Walsh TJ, Donnelly JP, *et al*. Revised definitions of invasive fungal disease from the European Organization for Research and Treatment of Cancer/ Invasive Fungal Infections Cooperative Group and the National Institute of Allergy and Infectious Diseases Mycoses Study Group (EORTC/MSG) Consensus Group. Clin Infect Dis 2008; 46(12): 1813-21.
17. Colombo AL, Padovan AC, Chaves GM. Current knowledge of Trichosporon spp. and trichosporonosis. Clin Microbiol Rev 2011; 24(4): 682-700.
18. Tashiro T, Nagai H, Nagaoka H, *et al*. Trichosporon beigelii pneumonia in patients with hematologic malignancies. Chest 1995; 108(1): 190-95.
19. Hazirolan G, Canton E, Sahin S, *et al*. Head-to-head comparison of inhibitory and fungicidal activities of fluconazole, itraconazole, voriconazole, posaconazole, and isavuconazole against clinical isolates of *Trichosporon asahii*. Antimicrob Agents Chemother 2013; 57(10): 4841-47.
20. Kuo SH, Lu PL, Chen YC, *et al*. The epidemiology, genotypes, antifungal susceptibility of Trichosporon species, and the impact of voriconazole on Trichosporon fungemia patients. J Formos Med Assoc 2021; (9): 1686-94.
21. Cattaneo L, Buonomo AR, Iacovazzo C, *et al*. Invasive

fungal infections in hospitalized patients with COVID-19: a non-intensive care single-centre experience during the first pandemic waves. J Fungi (Basel) 2023; 9(1): 86.

22. Vianello M, Jesus DFF, Sampaio JM, *et al*. Possible *Trichosporon asahii* urinary tract infection in a critically ill COVID-19 patient. Rev Iberoam Micol 2022; 39(2): 54-6.
23. Benelli JL, Basso RP, Grafulha TW, *et al*. Fungal bloodstream co-infection by *Trichosporon asahii* in a COVID-19 critical patient: case report and literature review. Mycopathologia 2022; 187(4): 397-404.
24. Segrelles-Calvo G, Araújo GRS, Llopis-Pastor E, *et al*. *Trichosporon asahii* as cause of nosocomial pneumonia in patient with COVID-19: a triple co-infection. Arch Bronconeumol 2021; 57: 46-48.
25. Cronyn V, Howard J, Chiang L, *et al*. *Trichosporon asahii* urinary tract infection in a patient with severe COVID-19. Case Rep Infect Dis 2021; 2021: 6841393.
26. Ali GA, Husain A, Salah H, *et al*. *Trichosporon asahii* fungemia and COVID-19 co-infection: an emerging fungal pathogen; case report and review of the literature. IDCases 2021; 25: e01244. Doi: 10.1016/j.idcr.2021.e01244
27. Nobrega de Almeida J Jr, Moreno L, Francisco EC, *et al*. *Trichosporon asahii* superinfections in critically ill COVID-19 patients overexposed to antimicrobials and corticosteroids. Mycoses 2021; 64(8): 817-22.
28. Briones-Claudett KH, Briones-Claudett MH, Cordova Loor FJ, *et al*. A 71-year-old man from Ecuador with a history of type 2 diabetes mellitus and severe COVID-19 pneumonia and lung cavitation associated with triple infection with Trichosporon asahii, Klebsiella pneumoniae, and Pseudomonas aeruginosa. J Investig Med High Impact Case Rep 2022; 10: 23247096221140250.
29. Chang DSJ, Harfouch CW, Melendez ML. Trichosporon asahii opportunistic pneumonia after a severe COVID-19 infection. IDCases 2023; 31: e01701.
30. Lopacinski A, Kim C, Khreis M. A case of fatal invasive trichosporonosis in the setting of immunosuppression and post-COVID-19 pneumonia. Cureus 2023; 15(2): e35079. Published 2023 Feb 16.

Testicular Tuberculosis with Ggeneralized Granuloma – A Case Report

Che-Min Hsu[1], Sheng-Wei Pan[1,2], Yi-Chen Yeh[3]

A 65-year-old man presented with a painless left-side scrotal swelling for 6 months. He had urinary urgency, but denied fever, cough or a tuberculosis (TB) history. Physical examination disclosed a normal right testis, but a hard and non-reducible left testis mass. Alpha-fetoprotein and beta-HCG levels were normal. Urinalysis revealed pyuria with a white blood cell count of 10-19/high power fields. Urine acid-fast bacilli smears were negative. Ultrasonography revealed a normal right testis, but an enlarged left testis with heterogeneous echogenicity showing diffuse hypoechoic nodules and increased internal vascularity. Due to concerns regarding testicular cancer, he received a left radical orchiectomy. Cut section of the specimen revealed generalized granuloma involving the testis and epididymis. The histological findings were necrotizing granuloma and multinucleated giant cells. The tissue tested positive for the Mycobacterium tuberculosis-specific IS6110 gene. A urine sample was culture-positive for M. tuberculosis 2 months later, and the sensitivity tests were confirmed. The patient started standard anti-TB chemotherapy. His pyuria resolved and urine samples were culture-negative after 2 months of therapy. The patient completed 6-month treatment smoothly for his testicular TB. ***(Thorac Med 2024; 39: 356-358)***

Key words: Tuberculosis, necrotizing granuloma

Introduction

Isolated testicular and epididymal tuberculosis (TB) disease without involvement of the kidney and lung is a rare extrapulmonary TB disease. Ultrasound images of a testicular mass suggesting diffuse TB granuloma have rarely been reported. Here, we present a sonographic image and a corresponding histologic picture from a patient with testicular TB. Sonographic findings of diffuse hypoechoic nodules in the testis, representing TB granulomas, may alert clinical physicians to the diagnosis of TB and help guide a timely investigation.

[1]Department of Chest Medicine, Taipei Veterans General Hospital, Taipei, Taiwan. [2]School of Medicine, National Yang Ming Chiao Tung University, Taipei, Taiwan. [3]Department of Pathology and Laboratory Medicine, Taipei Veterans General Hospital, Taipei, Taiwan
Address reprint requests to: Dr. Sheng-Wei Pan, Department of Chest Medicine, Taipei Veterans General Hospital, No. 201, Sec. 2, Shih-Pai Rd., Taipei 11217, Taiwan.

Case Report

A 65-year-old man presented with a painless left-side scrotal swelling for 6 months. He had urinary urgency, but denied fever, cough or a TB history. Physical examination disclosed a normal right testis but a hard and non-reducible left testis mass. Alpha-fetoprotein and beta-HCG levels were normal. Urinalysis revealed pyuria with a white blood cell count of 10-19/high power fields. Urine acid-fast bacilli smears were negative. Ultrasonography revealed a normal right testis but an enlarged left testis with heterogeneous echogenicity showing diffuse hypoechoic nodules and increased internal vascularity (Fig. 1. A-B). Due to concerns regarding testicular cancer, he received a left radical orchiectomy.

A cut section of the specimen revealed generalized granuloma involving the testis and epididymis (Fig. 1. C). Histological findings were necrotizing granuloma and multinucleated giant cells (Fig. 1. D-E). The tissue tested positive for the Mycobacterium tuberculosis-specific IS6110 gene. Two months later, a urine sample was culture-positive for M. tuberculosis, but sputum samples were not. His chest radiograph was unremarkable and abdominal computed tomography revealed normal kidneys and prostate. The patient received standard anti-TB treatment for 6 months uneventfully. The pyuria resolved and urine samples were culture-negative.

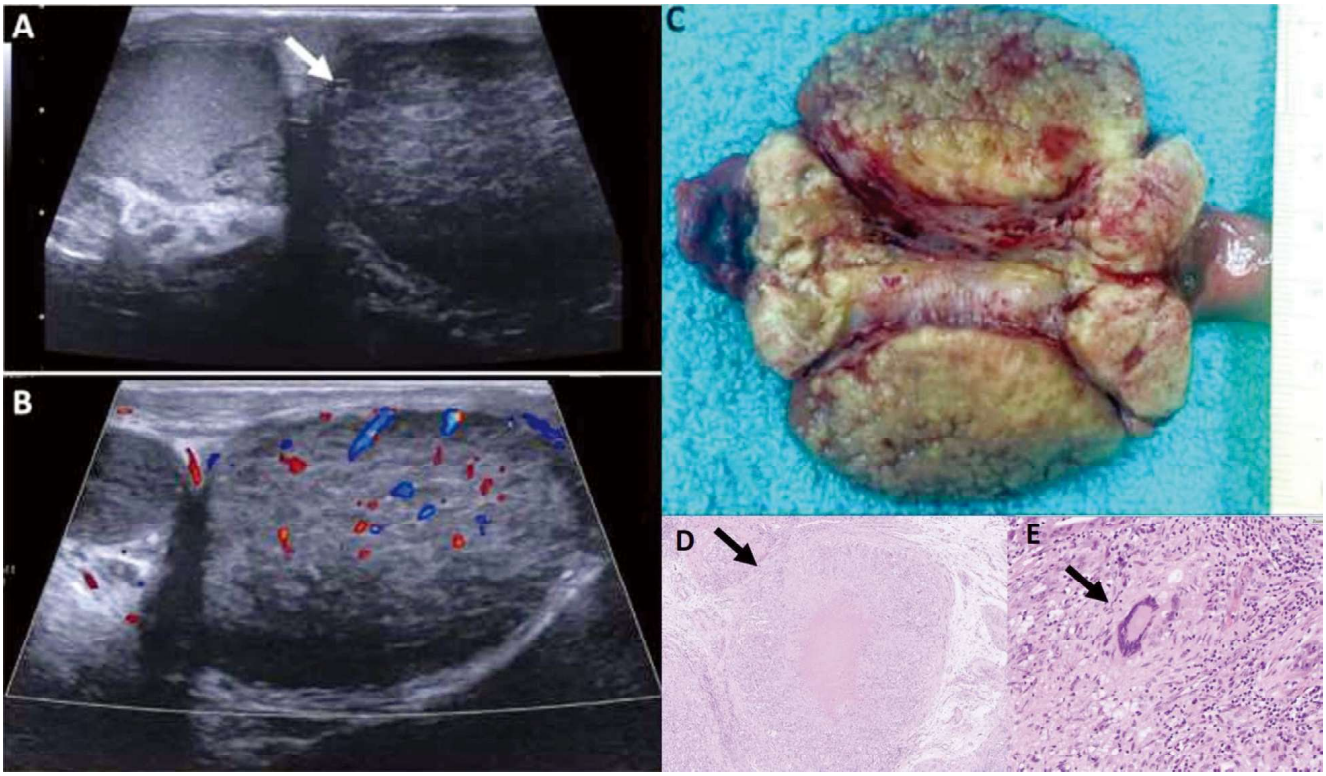

Fig. 1. (A) A scrotal ultrasound reveals an enlarged left testis (arrow, 5.0×3.7×2.7 cm) with diffuse hypoechoic nodules in a heterogeneous background. (B) Color Doppler sonographic image shows increased vascularity sparing the hypoechoic lesions. (C) Cut section of the orchiectomy specimen shows generalized granuloma involving the epididymis and testis. (D) The histological examination revealed chronic granulomatous inflammation and caseous necrosis. (E) A closer examination revealed the presence of multinucleated giant cells.

Discussion

Genitourinary TB accounts for 5% of all extrapulmonary TB diseases. Only 1-2% of cases with genitourinary TB have testis and epididymis involvement, and the patients mostly have concomitant renal or pulmonary disease [1]. Sonography features of testicular TB variously range from a diffusely enlarged heterogeneous hypoechoic pattern to ill-defined tiny hypoechoic nodules, which do not reliably differentiate TB from neoplasm [2]. With regard to diagnostic fine-needle aspiration, there is no consensus on its use in patients with testicular tumor, due to the risk of seeding cancer, although radical orchiectomy can be avoided by aspiration cytology [3]. In our case, the sonographic findings of diffuse hypoechoic nodules, likely representing TB granulomas, may alert a radiologist to the differential diagnosis of TB [2]. Accordingly, for patients with a testicular mass and sonographic findings mimicking diffuse TB granuloma, physicians should start a timely investigation, including acid-fast bacilli smears and nucleic acid amplification testing for M. tuberculosis, and may consider fine-needle aspiration in low-risk patients [1, 4].

Statement of Ethics Approval

Ethical approval was waived because there was no concern that the patient's anonymity could not be maintained in the written text and radiographic images.

References

1. Jacob JT, Nguyen TM, Ray SM. Male genital tuberculosis. Lancet Infect Dis 2008; 8: 335-42.
2. Nepal P, Ojili V, Songmen S, *et al*. "The Great Masquerader": sonographic pictorial review of testicular tuberculosis and its mimics. J Clin Imaging Sci 2019; 9: 27.
3. Abraham S, Izaguirre Anariba DE, *et al*. A case of testicular tuberculosis mimicking malignancy in a healthy young man. Ther Adv Infect Dis 2016; 3: 110-3.
4. Sharma A, Nagalli S, Varughese AT, *et al*. A review of the diagnostic use of fine-needle aspiration cytology for tuberculosis epididymo-orchitis: to do or not to do. Cureus 2020; 12: e6532.

Aberrant Lingular Vein-Preserving Left Lower Lobectomy – A Case Report

Wen-Ruei Tang[1], Ying-Yuan Chen[1], Yau-Lin Tseng[1]

Advances in thin-slice CT and video-assisted thoracoscopic surgery allow for precise thoracic surgeries. We reported the case of a 54-year-old ex-smoker with a 3 cm cavitary lesion in the left lower lung, who opted for direct surgery. Preoperatively, an anomalous left lingular vein draining into the inferior pulmonary vein was noted. Meticulous dissection preserved lingular venous drainage during uniportal video-assisted thoracoscopic surgery-left lower lobectomy. The final pathology suggested IgG4-related disease. The patient's recovery was uneventful, and he was regularly followed up at the outpatient department. ***(Thorac Med 2024; 39: 359-363)***

Key words: anomalous left lingular vein, case report, left lower lobectomy, pulmonary vein, uniportal video-assisted thoracoscopic surgery

Introduction

Recognizing vascular anomalies in thoracic surgery is clinically relevant and important, because these anomalies can significantly impact surgical planning and outcomes. Accurate identification of vascular anomalies helps prevent intraoperative complications, such as excessive bleeding, and ensures the preservation of vital structures, thereby enhancing patient safety and improving surgical success rates.

Thanks to advances in thin-slice computed tomography (CT) and the video-assisted thoracoscopic surgery (VATS) technique, surgeons are now able to comprehensively assess individual patient variations preoperatively and conduct increasingly delicate surgical procedures. In this report, we describe an exceptional case in which the lingular vein drained into the inferior pulmonary vein (IPV), and detail our approach to performing a uniportal VATS left lower lobectomy (LLLobectomy) while preserving aberrant (or uncommon) lingular drainage.

Case Report

Our patient was a 54-year-old man who

[1]Division of Thoracic Surgery, Department of Surgery, National Cheng Kung University Hospital, College of Medicine, National Cheng Kung University, Tainan, Taiwan.
Address reprint requests to: Dr. Ying Yuan Chen, Division of Thoracic Surgery, Department of Surgery National Cheng Kung University Hospital and College of Medicine, National Cheng Kung University, Tainan, Taiwan No.138, Sheng Li Road, Tainan, Taiwan 704, R.O.C..

used to smoke, and had quit 20 years ago. His father had died from colon cancer. He presented to our outpatient clinic with a dry cough lasting for 1 month. The patient did not experience any other symptoms, such as dyspnea, chest tightness, hemoptysis, fever, or significant weight loss.

His chest radiograph revealed a tumor in the left lower lung field. Subsequent CT of the chest identified a 3-cm cavitary lesion with a part-solid nodule in the left lower lobe (LLL). There was no evidence of mediastinal lymphadenopathy or pleural effusion. Due to suspected lung cancer, a CT-guided biopsy was proposed; however, the patient opted for direct surgery, instead. Preoperative assessment indicated localized disease without distant metastasis. An anomalous left lingular vein connecting to the IPV was observed on the CT image preoperatively, and we planned to preserve this uncommon vein during operation (Fig. 1A–1C).

Under general anesthesia and unilateral lung ventilation, the patient was positioned in a right lateral decubitus position. Employing a uniportal VATS approach, we made a 3-cm incision at the 4th intercostal space anterior to the mid-axillary line. Generally, LLLobectomy starts from the loop and transects the entire IPV. However, in this case, upon dividing the pulmonary ligament and incising the pleura surrounding the IPV, we encountered a lingular vein anteriorly crossing the pulmonary artery (PA) (Fig. 2A). Due to its embedded position within the lung parenchyma, the junction with the IPV

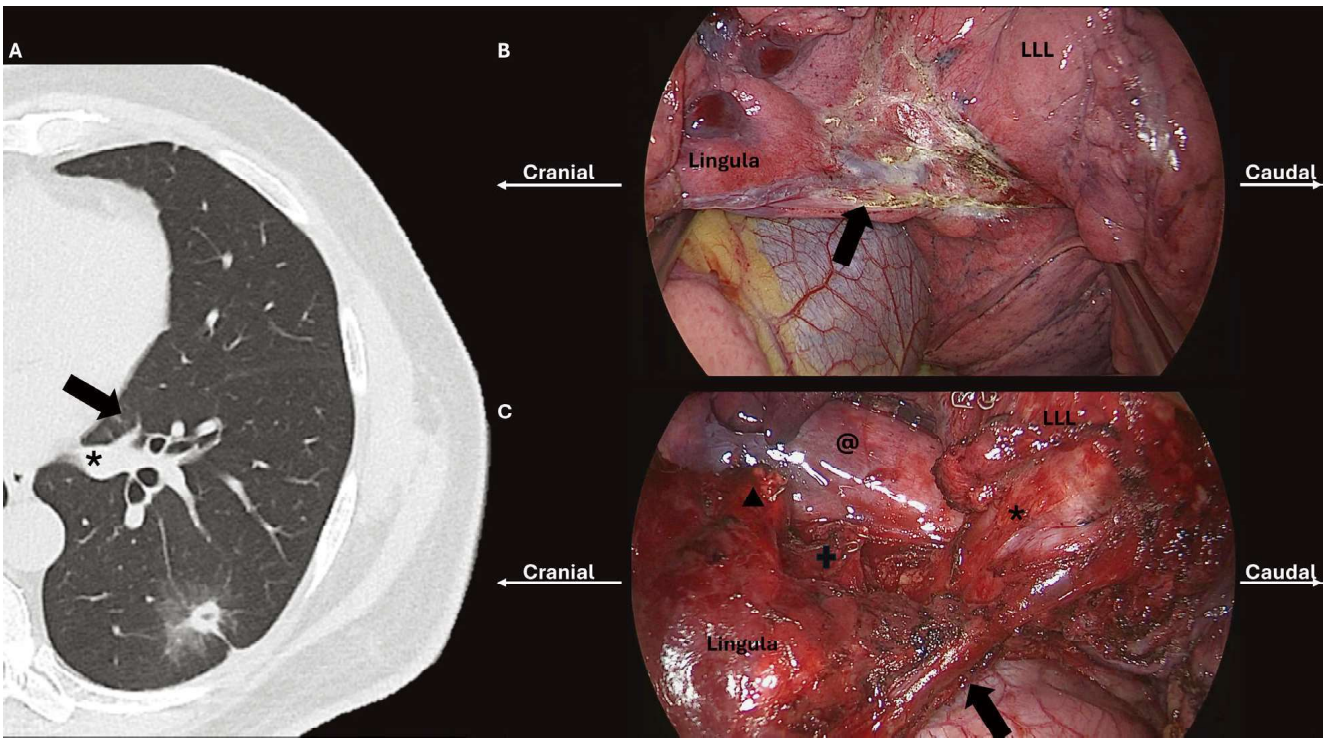

Fig. 1. Anomalous left lingular vein. (A) CT images depicting a single tumor located in the left lower lobe of the lung. (B) Identification of the lingular vein during fissure dissection. (C) Thoracoscopic view showing the lingular vein connecting to the inferior pulmonary vein after meticulous dissection. Key symbols: Arrow indicates the lingular vein; "*" represents the inferior pulmonary veins; cross denotes the inferior pulmonary bronchus; LLL signifies the left lower lobe; triangle marks the inferior pulmonary artery; "@" indicates the thoracic aorta.

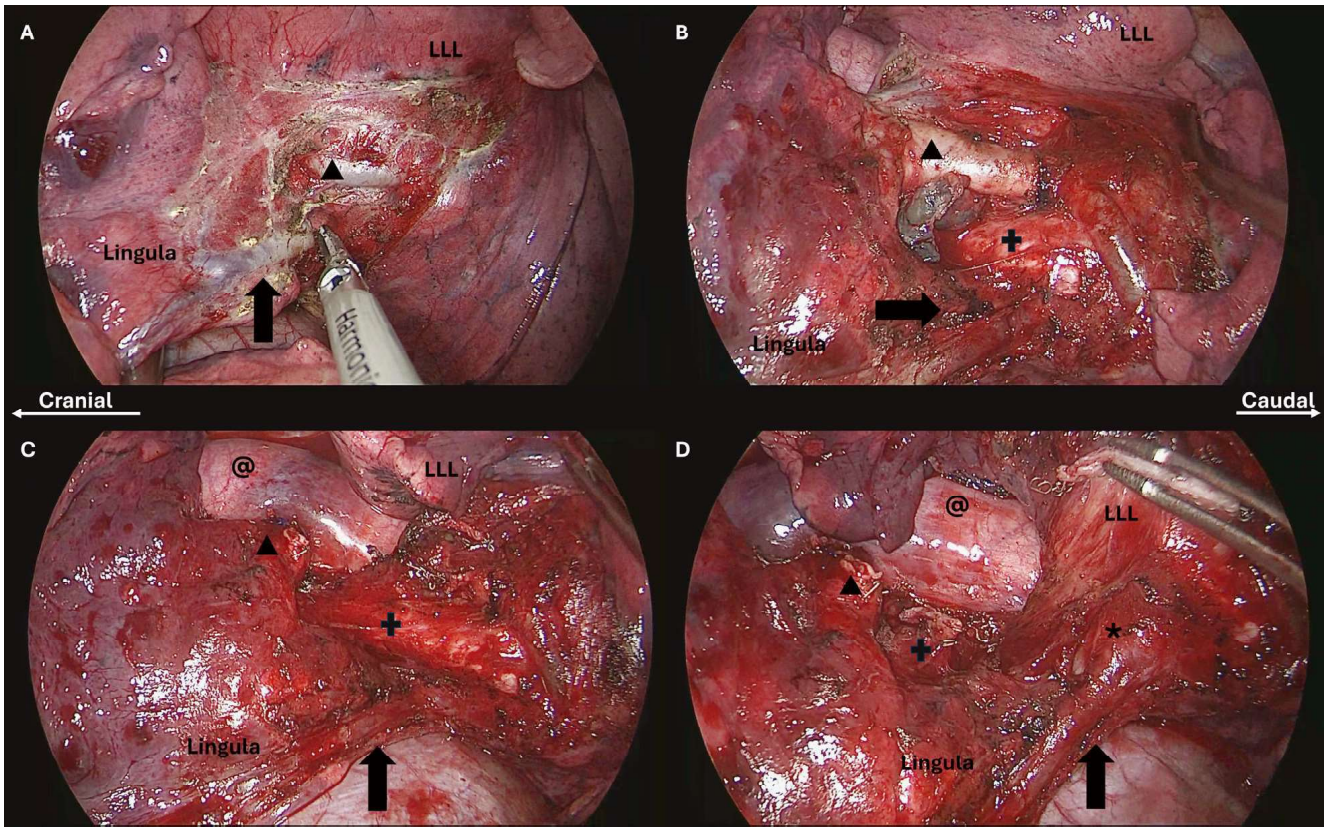

Fig. 2. Detailed steps of lingular vein-preserving left lower lobectomy. (A) Dissection of the major fissure and identification of the lingular vein and basilar arterial trunk. (B) Tracing along the basilar arterial trunk to identify the inferior pulmonary artery and left lower lobe bronchus. (C) Ligation of the inferior pulmonary artery. (D) Transection of the left lower lobe bronchus. Key symbols: Arrow indicates the lingular vein; "*" represents the inferior pulmonary veins; cross denotes the inferior pulmonary bronchus; LLL signifies the left lower lobe; triangle marks the inferior pulmonary artery; "@" indicates the thoracic aorta.

was not readily discernible, necessitating dissection starting from the interlobar fissure and descending PA (Fig. 2B). After cutting off the branches of the PA supplying the LLL and lobar bronchus in sequence, we lifted the distal bronchial stump (Fig. 2C & 2D).

At this juncture, the confluence of the lower lobe pulmonary vein (PV) and the aberrant lingular PV became clearly visible. Following dissection of the surrounding tissue adjacent to the LLL PV, adequate space was obtained to divide the LLL PV with a linear stapler while preserving the flow of the lingular PV (Fig. 3A–3C). Finally, we successfully completed an LLLobectomy using uniportal VATS while preserving the aberrant lingular vein. The patient then regularly took oral analgesics and was able to ambulate without assistance postoperatively. The chest tube was removed on postoperative day 1 and the patient was discharged uneventfully on postoperative day 2. The final pathology suggested IgG4-related disease, and the patient was regularly followed up at the outpatient department.

Discussion

Surgeons should be aware of variations in

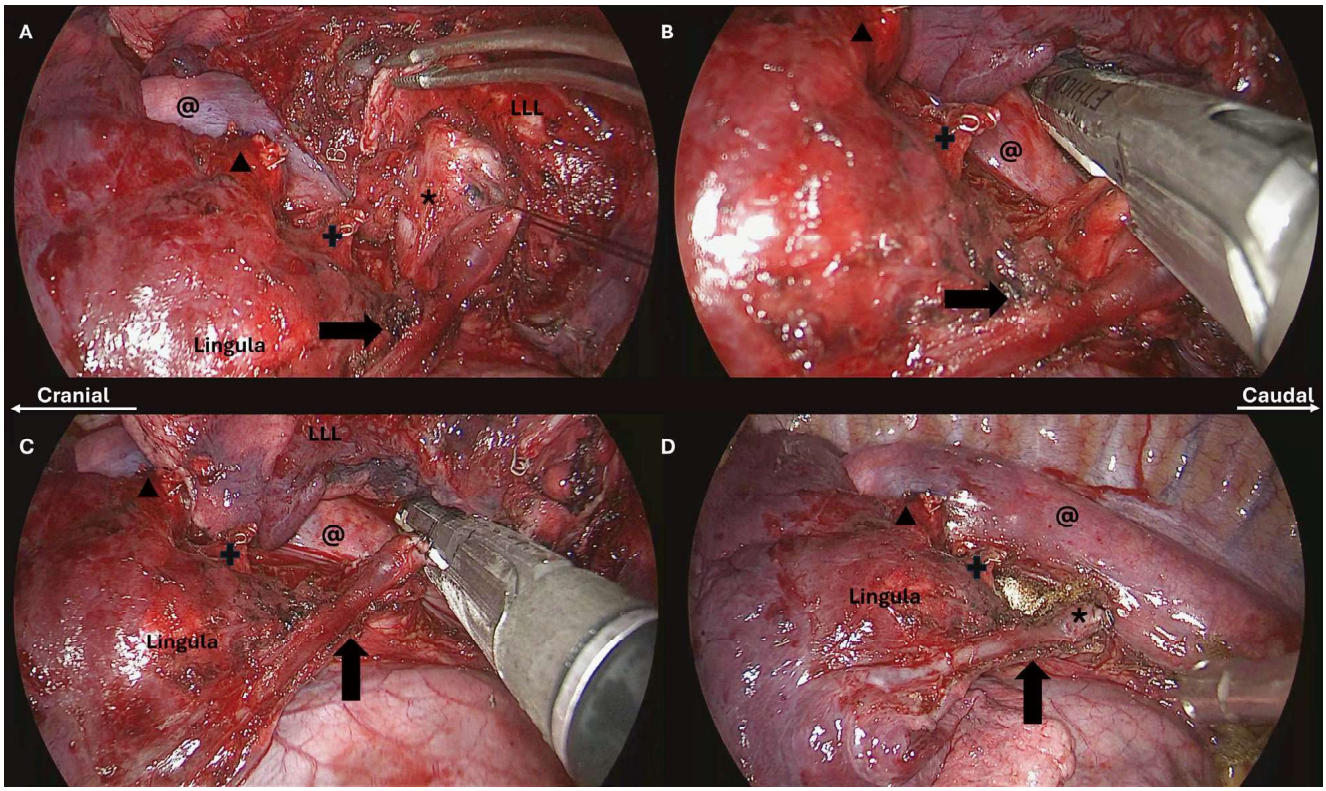

Fig. 3. Detailed steps of dealing with inferior pulmonary veins. (A) Dissection distally to identify trifurcation of inferior pulmonary veins, and then ligation of the anterior basal vein (V8). (B) Stapling of the superior basal vein (V6). (C) Stapling of the inferior basal vein (V9+10). (D) Completion of lingular vein-preserving left lower lobectomy. Key symbols: Arrow indicates the lingular vein; "*" represents the inferior pulmonary veins; cross denotes the inferior pulmonary bronchus; LLL signifies the left lower lobe; triangle marks the inferior pulmonary artery; "@" indicates the thoracic aorta.

PV drainage when doing pulmonary anatomical resection, including lobectomy and segmentectomy. Variation in the PV is not uncommon, and the inadvertent ligation of a PV that should be preserved could result in pulmonary congestion, infection, and even death [1]. Typically, the left superior PV drains the left upper lobe, including the lingula, and courses anteriorly and caudally to the PA, while the left inferior PV drains the left lower lung and traverses inferiorly to the PA [2-3]. In this particular case, a variation in the drainage pattern of the lingular vein was identified on preoperative CT imaging. Specifically, the left lingular vein was observed to loop in front of the PA and bronchi before draining downward into the inferior PV. Such variations were reported in 0.5–10.7% of cases through roentgenologic assessment [4-6]. This anatomical anomaly not only posed challenges for the anterior approach to hilar dissection, but also constrained the working space around the inferior PV.

Previous studies have primarily focused on either carefully ligating the lingular vein from the inferior PV during left upper lobectomy or preserving the lingular vein during left upper lobectomy, particularly in upper trisegmentectomy procedures aimed at conserving the lingula [3, 7-8]. To the best of our knowledge, this report presents the first documentation of a technique focused on preserving lingular drainage during lower lobectomy. Although the

precise clinical ramifications of preserving lingular vein drainage remain uncertain due to the persistence of intersegmental drainage between the lingula and upper trisegment, we posit that this preservation may contribute to better postoperative pulmonary function, reduce the risk of complications such as pulmonary congestion, and facilitate the feasibility of subsequent subsegmental upper trisegmentectomy, should further surgical intervention be required. This case underscores the significance of a meticulous surgical technique and thorough preoperative imaging in managing anatomical anomalies during thoracic surgery.

Practical recommendations for surgeons encountering similar cases include: First, utilizing high-resolution CT angiography or 3D reconstruction software to accurately map vascular anatomy and identify any variations is crucial. Such detailed imaging aids in surgical planning and significantly reduces the risk of intraoperative surprises. Second, during the surgery, using meticulous dissection techniques can help in identifying and preserving critical vascular structures. Surgeons should be prepared for potential variations and have a plan for managing unexpected findings, ensuring that no vital structures are compromised. Last, adopting a multidisciplinary approach by collaborating with radiologists and anesthesiologists optimizes perioperative care and improves surgical outcomes. This teamwork ensures comprehensive management of vascular anomalies, enhancing patient safety and reducing the likelihood of complications. By following these recommendations, surgeons can better navigate the complexities associated with vascular anomalies, ultimately leading to safer and more effective thoracic surgeries.

Conclusion

In conclusion, surgeons performing pulmonary anatomical resections should be mindful of variations in PV drainage, as inadvertent ligation of a crucial vein could lead to severe complications. This case emphasizes the importance of meticulous surgical technique and thorough preoperative imaging in managing anatomical anomalies during thoracic surgery.

References

1. Sugimoto S, Izumiyama O, Yamashita A, *et al*. Anatomy of inferior pulmonary vein should be clarified in lower lobectomy. Ann Thorac Surg 1998; 66(5): 1799-800.
2. Gossot D, Seguin-Givelet A. Anatomical variations and pitfalls to know during thoracoscopic segmentectomies. J Thorac Dis 2018; 10(Suppl 10): S1134-S1144.
3. Gossot D. Left upper lobe: upper segments (S1+2+3) – (lingula-sparing upper lobectomy). In: Gossot D ed. Atlas of Endoscopic Major Pulmonary Resections. France; Springer International Publishing, 2018: 149-56.
4. Yamashita H. Variation in the pulmonary segments and the bronchovascular trees. Roentgenol Anat Lung 1978; 46-58.
5. Shiina N, Kaga K, Hida Y, *et al*. Variations of pulmonary vein drainage critical for lung resection assessed by three-dimensional computed tomography angiography. Thorac Cancer 2018; 9(5): 584-88.
6. Akiba T, Marushima H, Odaka M, *et al*. Pulmonary vein analysis using three-dimensional computed tomography angiography for thoracic surgery. Gen Thorac Cardiovasc Surg 2010; 58(7): 331-5.
7. Lafouasse C, Gossot D, Seguin-Givelet A. Venous concerns after lingula sparing left upper lobectomy. Interdiscip Cardiovasc Thorac Surg 2023; 36(6).
8. Akiba T, Marushima H, Morikawa T. Confirmation of a variant lingular vein anatomy during thoracoscopic surgery. Ann Thorac Cardiovasc Surg 2010; 16(5): 351-53.

Mediastinal Tuberculous Lymphadenitis Diagnosed by EBUS-TBNA – A Case Report

Tse-Yu Chen[1], Chung-Kan Peng[1], Shih-En Tang[1], Sheng-Huei Wang[1]
Chen-Liang Tsai[1]

The neck is the most common site for tuberculous lymphadenitis; however, mediastinal tuberculous lymphadenitis could be underestimated in daily practice. We reported a patient with COVID-19 infection, and mediastinal lymphadenopathy was accidentally found on chest computed tomography and magnetic resonance imaging. The patient received endobronchial ultrasound and transbronchoscopic needle aspiration for a pretracheal retrocaval node with drainage of black fluid. Tuberculous lymphadenitis was diagnosed and confirmed by mycobacterium tuberculosis-polymerase chain reaction. The patient then received anti-tuberculosis medications for treatment of mediastinal tuberculous lymphadenitis. ***(Thorac Med 2024; 39: 364-368)***

Key words: tuberculous lymphadenitis, EBUS-TBNA, endobronchial ultrasound, tuberculosis

Introduction

Tuberculous lymphadenitis (TL), a form of tuberculosis (TB), develops within the lymphatic system. TB is primarily caused by the bacterium *Mycobacterium tuberculosis*, and less commonly by Mycobacterium bovis [1]. TL is the most common form of extrapulmonary TB (EPTB), characterized by the enlargement of lymph nodes. This condition is a manifestation of either a primary infection or reactivation of a latent TB infection, indicating the spread of the bacteria from the initial infection site to the lymph nodes [2].

Case Report

A 90-year-old non-smoking male with a history of aneurysmal dilatation, chronic kidney disease, hypertensive cardiovascular disease, and hyperlipidemia was admitted due to COVID-19 pneumonia. During his admission, the patient received antibiotic treatment with piperacillin/tazobactam 2.25 g q8h IV + doxycycline

[1]Division of Pulmonary and Critical Care Medicine, Department of Internal Medicine, Tri-Service General Hospital, National Defense Medical Center, Taipei, Taiwan.
Address reprint requests to: Dr. Chen-Liang Tsai, Division of Pulmonary and Critical Care Medicine, Department of Internal Medicine, Tri-Service General Hospital, National Defense Medical Center, No. 325, Section 2, Cheng-Gong Rd, Neihu 114, Taipei, Taiwan.

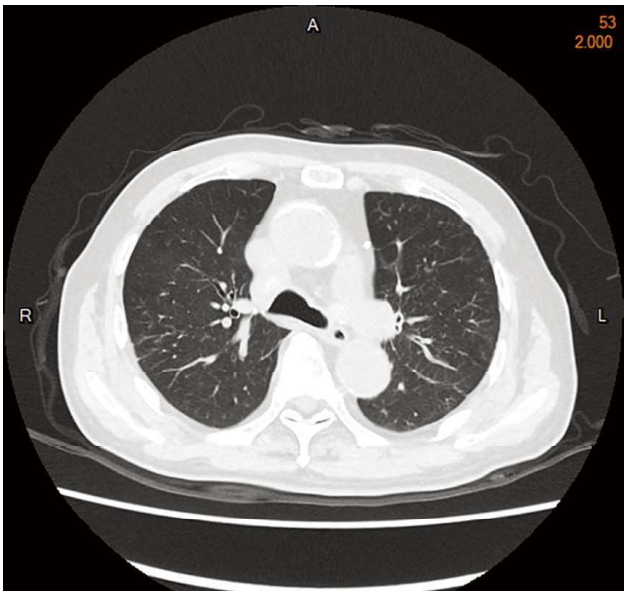

Fig. 1. Non-contrast chest tomography (CT) showed lymphadenopathy in the pretracheal retrocaval (PTRC) region (the patient had chronic kidney disease and did not receive contrast CT).

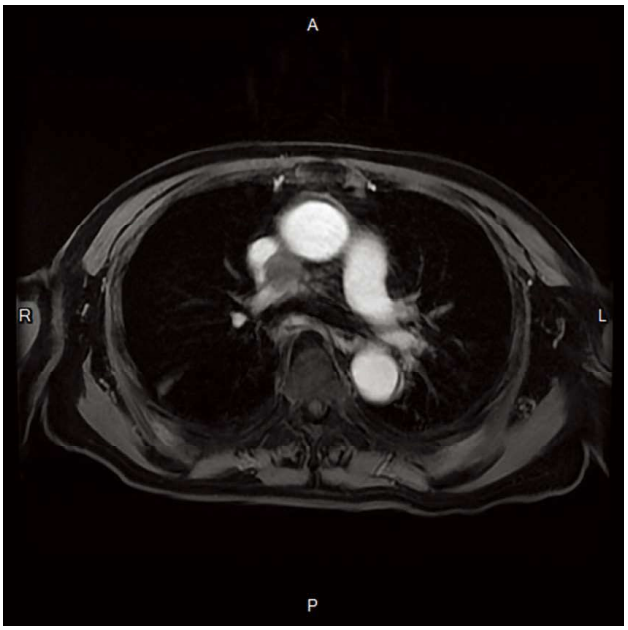

Fig. 2. Chest magnetic resonance imaging showed an enlarged lymph node with necrosis in the pretracheal retrocaval (PTRC) region.

100 mg q12h PO to cover a broad spectrum of pathogens for 5 days. Antiviral treatment with Paxlovid 1 tab BID PO, and steroid with methasone 6 mg QD IV for 5 days were prescribed for COVID-19 pneumonia. We also performed a computed tomography (CT) scan of the chest, abdomen, and pelvis for a survey, which revealed bronchial wall thickening and infiltrations in the right middle lobe, lingula, right lower lobe, and left lower lobe, suggesting an inflammatory process or pneumonia. Several enlarged lymph nodes (maximal size: approximately 2.3 cm) in the mediastinum were seen (Figure 1), suggesting lymphadenopathy or metastasis. We discharged the patient under stable conditions and scheduled an outpatient department (OPD) follow-up.

At the OPD, magnetic resonance imaging (MRI) for several enlarged lymph nodes (maximal size: about 2.3 cm) in the mediastinum was performed. The image showed a necrotic node (size: about 2.1 cm) in the pretracheal retrocaval (PTRC) space (Figure 2). The patient was admitted again considering his complex medical history. A comprehensive medical examination was carried out and the general appearance of the patient was noted, with specific observations including normal skin turgor without signs of petechiae or ecchymosis, and no abnormalities in the head, eyes, ears, nose, and throat examination. The neck was supple without jugular vein engorgement, carotid bruits, lymphadenopathy, or goiter. No swelling or lesion of the inguinal and axilla region was noted. Chest examination showed symmetrical expansion, clear bilateral breathing sounds, and no wheezing or crackles. The patient had no history of TB.

After admission, the patient underwent endobronchial ultrasound-guided transbronchial needle aspiration (EBUS-TBNA) for biopsy of the mediastinal lymphadenopathy. The EBUS-TBNA was performed (Figures 3–4) on the

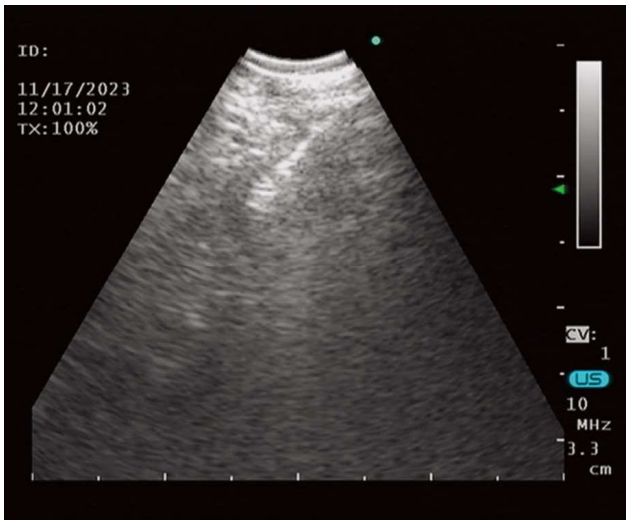

Fig. 3. Endobronchial ultrasound and transbronchoscopic needle aspiration (EBUS-TBNA) was performed for the pretracheal retrocaval (PTRC) node.

Fig. 4. Black fluid was drained from the PTRC node by EBUS-TBNA.

enlarged lymph node in the PTRC region. The EBUS image showed an ovoid and well-defined lymph node with heterogeneous echo texture indicating necrosis or granulomatous changes. The pathology showed cell debris with a few epithelial cells of the lymphoid tissue. TB polymerase chain reaction (PCR) of the specimen was positive, and TL was diagnosed. Because of the patient's chronic kidney disease (estimated glomerular filtration rate: 19.37 ml/min/1.73 m^2), we prescribed TB medication with a pyrazinamide tab 500 mg 2-tab TIW PO and Rina cap 300 mg/150 mg 2-tab QD PO for treatment of TL. However, the patient was lost to follow-up for personal reasons, so we could not check the post-treatment image.

Discussion

EPTB refers to TB infections that occur outside of the lungs. While pulmonary TB, which affects the lungs, is the most common form of the disease, TB bacteria can infect almost any part of the body, leading to extrapulmonary manifestations. EPTB accounts for approximately 20% of TB cases worldwide [3], and TL is the most common form of EPTB.

TL is a form of TB that affects the lymphatic system. TL occurs in any part of the body where lymph nodes are present. However, TB's widely varying locations often reflect the route of infection or the spread of M. tuberculosis within the body. TL is most commonly found in cervical—the most common involving lymph nodes in the neck, called "scrofula"--mediastinal, axillary, inguinal, and abdominal locations [4].

The prevalence of TL can vary significantly by region. TL is 1 of the most common forms of EPTB, and accounts for approximately 15–20% of all TB cases in immunocompetent patients, and a higher proportion in HIV-infected individuals [5]. The prevalence is higher in areas with high rates of TB and in populations with increased rates of HIV infection, as both condi-

tions are strongly interlinked.

Mediastinal tuberculous lymphadenitis (MTL) involves the lymph nodes located in the mediastinum. Patients with MTL may experience a range of symptoms owing to the infection and its impact on surrounding structures. Persistent cough that does not improve with conventional treatments, chest pain of varying intensity, and dyspnea, or difficulty breathing, are often reported. Fever, night sweats, and weight loss are typical symptoms of TB. Esophageal compression causes swallowing difficulty (dysphagia). In some cases, it can also cause swelling in the neck, face, and arms, indicating superior vena cava syndrome due to blocked blood flow [6]. General feelings of malaise and fatigue are also common among those affected.

Enlarged mediastinal lymph nodes of MTL are most readily detectable on CT or MRI. These nodes often exhibit central necrosis that is identifiable on CT or MRI as low-attenuation centers with possible rim enhancement post-contrast, indicating inflammation around necrotic areas. Chronic cases might show calcification within the lymph nodes, observed as high-density areas on CT scans. Large lymph nodes may compress nearby organs (esophagus, trachea, or vena cava), causing swallowing difficulties, dysphagia, dyspnea, or superior vena cava syndrome. Peripheral enhancement of the lymph nodes may be observed after contrast administration, highlighting active inflammation around a necrotic core. In severe cases, there may be a confluence of affected lymph nodes, forming large, irregular masses, which further complicates the clinical picture.

Diagnosing EPTB is more challenging owing to non-specific symptoms mimicking other illnesses. Diagnosing TL involves a comprehensive approach including detailed history-taking and physical examination. X-rays, ultrasounds, CT scans, and MRIs are key tools for spotting lesions [7]. Laboratory tests, including blood tests, cultures of body fluids (urine, cerebrospinal fluid, or ascitic fluid), and histopathological examination of biopsy specimens, further aid the diagnosis. Additionally, molecular tests like PCR can detect TB DNA in clinical specimens, offering a more specific approach to diagnosing TB.

Furthermore, EBUS-TBNA is crucial for diagnosing MTL. TBNA is a minimally invasive procedure that allows for the sampling of mediastinal lymph nodes via a bronchoscope inserted through the mouth into the lungs. TBNA is particularly useful for obtaining tissue samples from the mediastinum without the need for more invasive surgical procedures. TBNA biopsy for suspected MLT is best timed after imaging, but before starting antibiotics, considering clinical suspicion, patient health, and endobronchial ultrasound availability.

Diagnosing MTL relies heavily on EBUS-TBNA, which can reveal several distinctive characteristics. Lymph node enlargement in the mediastinum is notable, and EBUS provides real-time measurements for identifying abnormal lymph node enlargement. These lymph nodes often show a heterogeneous echo texture, indicating mixed echogenicity that could signify necrosis or granulomatous changes [8]. Hypoechoic areas within the nodes, suggestive of caseation necrosis, are prime targets for needle aspiration to improve diagnosis. Unlike malignant lymph nodes, tuberculous lymph nodes usually have well-defined margins. On ultrasound, central necrosis, a key indicator of TB, appears as areas of substantially lower echogenicity within the lymph node. In addition, EBUS can detect increased vascularity

around the lymph nodes using Doppler features, indicating inflammation, although this does not confirm TB. EBUS image findings provide crucial insights for diagnosing MTL, guiding the subsequent needle aspiration for tissue sampling and confirmation of the disease.

Conclusion

Historically, the diagnosis of MTL has been challenging due to the lack of systemic symptoms. The application of EBUS-TBNA offers a safe and effective way to diagnose asymptomatic lymph node enlargement in the mediastinum.

Acknowledgments

This study was supported through consultation with colleagues in the Division of Pulmonary and Critical Care Medicine, Department of Internal Medicine, Tri-Service General Hospital.

References

1. Hlokwe TM, Said H, Gcebe N. *Mycobacterium tuberculosis* infection in cattle from the Eastern Cape Province of South Africa. BMC Vet Res 2017; 13(1): 299.
2. Moule MG, Cirillo JD. *Mycobacterium tuberculosis* dissemination plays a critical role in pathogenesis. Front Cell Infect Microbiol 2020; 10: 65.
3. Mert A, Tabak F, Ozaras R, *et al*. Tuberculous lymphadenopathy in adults: a review of 35 cases. Acta Chir Belg 2002; 102(2): 118-21.
4. Mohapatra PR, Janmeja AK. Tuberculous lymphadenitis. J Assoc Physicians India 2009; 57: 585-90.
5. Sharma SK, Mohan A. Extrapulmonary tuberculosis. Indian J Med Res 2004; 120(4): 316-53.
6. Jang JH, Jeon D, Kim YS, *et al*. Superior vena cava syndrome due to mediastinal tuberculous lymphadenitis. Korean J Fam Med 2017; 38(3): 166-8.
7. Ferrer R. Lymphadenopathy: differential diagnosis and evaluation. Am Fam Physician 1998; 58(6): 1313-20.
8. Erer OF, Erol S, Anar C, *et al*. The diagnostic accuracy of endobronchial ultrasound-guided transbronchial needle aspiration (EBUS-TBNA) in mediastinal tuberculous lymphadenitis. Turk J Med Sci 2017; 47(6): 1874-9.

Pulmonary Nocardiosis with Multiple Brain Abscesses: A Case Report

Mei-Yuan Teo[1], Chen-Yiu Hung[1], Chun-Hua Wang[1], Horng-Chyuan Lin[1]

Nocardiosis is a rare but potentially life-threatening infectious disease, especially in immunocompromised individuals and those with central nervous system (CNS) involvement. We reported a case of pulmonary nocardiosis accompanied by multiple brain abscesses that was successfully managed in a young male diagnosed with anti-phospholipid syndrome. Following 12 weeks of combined antimicrobial treatment, significant improvement was observed in the right lung mass and multiple brain abscesses. Subsequent follow-up examinations showed no signs of recurrence or relapse. Nocardia infection can manifest as disseminated disease and central nervous system infection, particularly in immunocompromised patients. Combined antimicrobial therapy is necessary for these patients to improve their chances of survival. ***(Thorac Med 2024; 39: 369-374)***

Key words: *Nocardia* species, pulmonary nocardiosis, brain abscess

Introduction

Nocardia species are Gram-positive aerobic filamentous bacterium of *Actinomycetes*, which is a soilborne and airborne opportunistic pathogen in immunocompromised patients or in immunocompetent patients with chronic lung disease like chronic obstructive pulmonary disease, interstitial lung disease and bronchiectasis [1-4]. Primary lung infections are prevalent, often occurring via inhalation of aerosolized spores or mycelia, followed by primary cutaneous infections, and disseminated infections [3, 4]. Here, we describe a case of right upper lung nocardiosis with multiple brain abscesses in a 32-year-old male with anti-phospholipid syndrome.

Case Report

The patient was a 32-year-old Taiwanese male with a history of anti-phospholipid syndrome (APS) with thrombocytopenia for 3 years. The APS with thrombocytopenia had been successfully managed with hydroxychloroquine (200 mg daily), azathioprine (150 mg

[1]Department of Thoracic Medicine, Chang Gung Memorial Hospital, Chang Gung University College of Medicine, Taoyuan, Taiwan.
Address reprint requests to: Dr. Horng-Chyuan Lin, No. 5, Fu-Xing St. Kwei-Shan Dist. Taoyuan City, 33333 Taiwan.

daily) and prednisolone (7.5 mg daily) within the 3-year history of APS without any complication.

In mid-April 2022, the patient presented to an emergency department with the complaint of high fever of up to 39°C for 1 day. The accompanying symptoms were productive cough and right chest pain. He had no blood-tinged sputum, weight loss, or shortness of breath. The patient was alert and oriented. His respiratory rate was 16/min, blood pressure was 125/69 mmHg, pulse rate was 94/min, and his oxyhemoglobin saturation by pulse oximetry was 100% under room air. Physical examination revealed bilateral symmetric expansion during respiration and a normal breathing sound. There was no skin lesion, wound, or soft tissue erythematous change.

A chest X-ray (CXR) revealed soft tissue density without signs of collapse in the right upper lung (RUL) (Fig. 1(A)). Chest computed tomography (CT) showed a soft tissue mass measuring approximately 6.8 cm x 5.5 cm in the RUL, abutting the mediastinum, along with a necrotic lymph node in the right paratracheal space (Fig. 2 (A)). Laboratory findings indicated leukopenia (with a white blood cell count of 2.9 x 103/μL, segment count of 92.5%, and lymphocyte count of 5.0%), anemia (hemoglobin 9.4 g/dL), and thrombocytopenia (platelet count of 58 x 103/μL, with a baseline of 100 x 103/μL). Liver and renal function were normal, and electrolyte levels were within normal range. C-reactive protein (CRP) was markedly elevated at 107.3 mg/dL (normal range <5 mg/dL). Real-time polymerase chain reaction (PCR) tests for severe acute respiratory syndrome coronavirus 2 (SARS-CoV-2) and influenza revealed negative results.

During the initial hospitalization, the patient received amoxicillin-clavulanic acid (1 g every 8 hours). Due to persistent intermittent low-grade fever and lack of significant resolution on CXR, antibiotic therapy was escalated

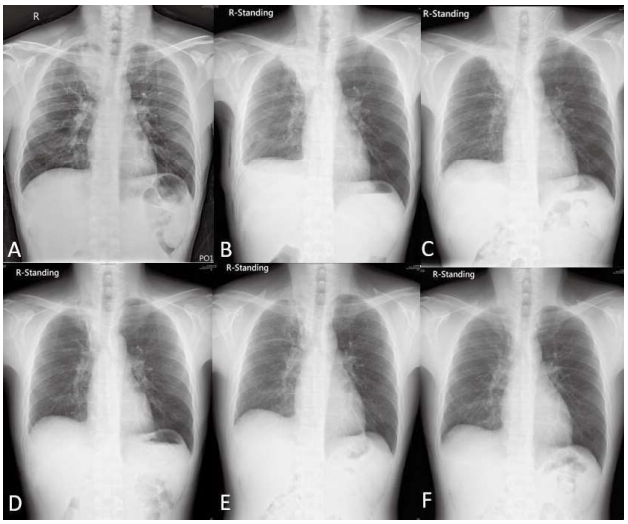

Fig. 1. The right upper lung soft tissue mass showed improvement on chest X-ray during follow-up. (A) Day 1 of hospitalization; (B) Day 32 of hospitalization; combination antimicrobial treatment for nocardiosis started at this point; (C) Day 44 of hospitalization; trimethoprim-sulfamethoxazole discontinued; (D) Day 101 of hospitalization; intravenous antimicrobial treatment switched to oral antimicrobial; (E) 12-week antimicrobial treatment completed; (F) Outpatient department follow-up 1 year later.

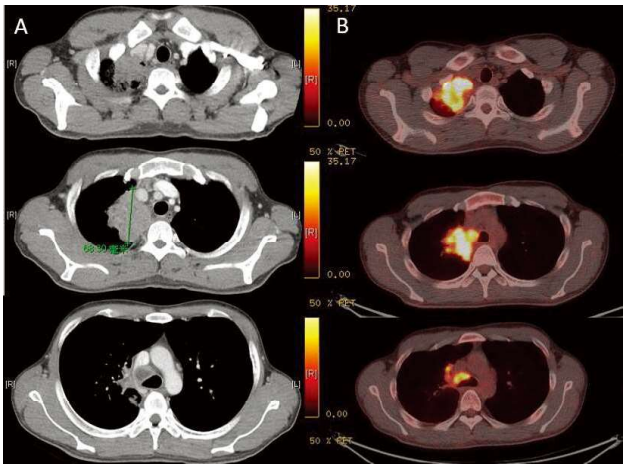

Fig. 2. (A) CT revealed a 6.8 cm x 5.5 cm soft tissue mass at the upper lobe of the right lung, which abutted the mediastinum, and necrotic lymph node at the right paratracheal space. (B) PET revealed a mass at the apex of the right upper lung and right mediastinal lymphadenopathy, with a maximum standardized uptake value (SUVmax) of 18.0 and 10.3, respectively.

to piperacillin-tazobactam (4.5 g every 6 hours) and teicoplanin (400 mg daily). Blood culture and sputum culture showed no growth for aerobes and anaerobes. Other microbiological cultures and examinations, including mycobacterial smear and culture, *Aspergillus galactomannan*, and fungal culture, were all negative. In addition, the human immunodeficiency virus (HIV) antibody and antigen combination assay revealed negative results.

A CT-guided biopsy of the soft tissue mass in the RUL was performed on the second day after admission. In addition, fine needle aspiration from the right paratracheal lymph node was carried out under endobronchial ultrasound (EBUS) guidance, yielding yellowish-white pus-like material with numerous neutrophils, but no tumor cells. A positron emission tomography (PET)/CT scan revealed a mass in the apex of the RUL and right mediastinal lymphadenopathy, with maximum standardized uptake values (SUVmax) of 18.0 and 10.3, respectively (Fig. 2 (B)). The patient underwent surgical lung tissue biopsy at the end of April, revealing acute on chronic inflammation with focal granuloma formation (Fig. 4 (A)). Staining with Grocott methenamine silver (GMS), periodic acid-Schiff (PAS), and acid-fast stains was negative.

On the 28th day of hospitalization, the patient developed symptoms of vomiting and headache, followed by weakness in the right-side extremity (muscle power score 4). Brain magnetic resonance angiography (MRA) revealed multiple ring-enhanced lesions with central necrosis and adjacent white matter edema in bilateral cerebral hemispheres, the left thalamus, midbrain, pons, and bilateral cerebellum, suggestive of brain abscess formation (Fig. 3 (A)).

The reports on both specimens obtained via CT-guided biopsy from the RUL mass and fine needle aspiration from the paratracheal lymph node confirmed *Nocardia* species. Considering

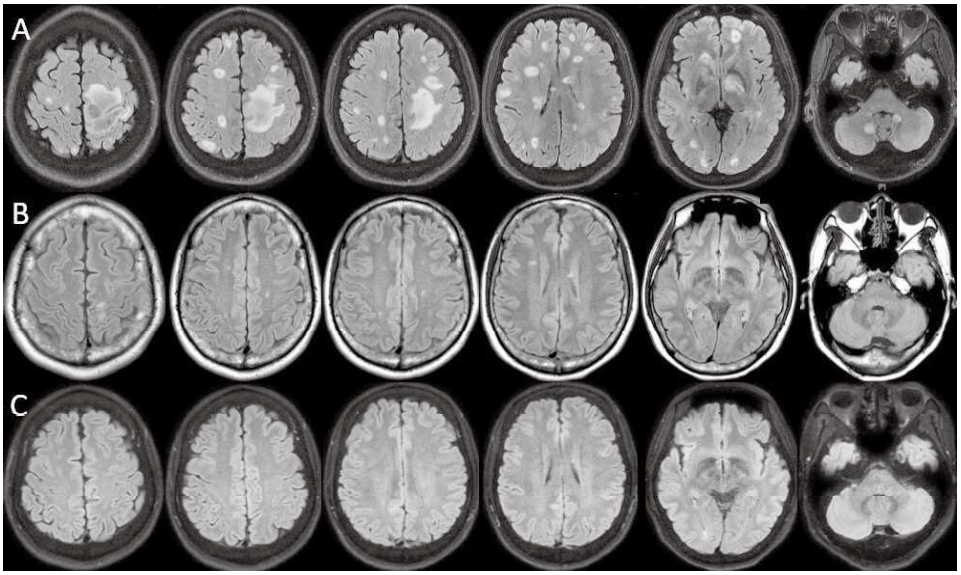

Fig. 3. Brain magnetic resonance angiography (MRA) T2/FLAIR; (A) Day 32 of hospitalization; brain MRA revealed multiple ring-enhanced lesions with central necrosis and adjacent white matter edema at the bilateral cerebral hemispheres, left thalamus, midbrain, pons, and bilateral cerebellum; (B) Day 85 of hospitalization; brain MRA revealed significant improvement in terms of abscess size and number; (C) 3 months after the completion of treatment; brain MRA revealed complete remission of the preexisting brain abscesses.

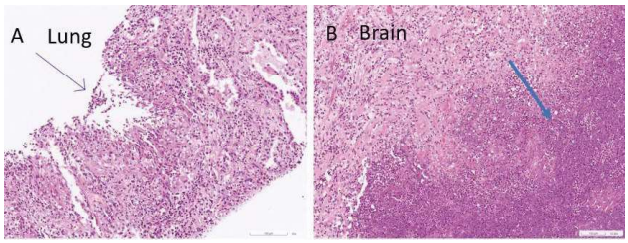

Fig. 4. (A) Hematoxylin & eosin (H&E) stain shows lung nocardiosis with focal granuloma formation (arrow); culture grew Nocardia; Original magnification: X20; (B) H&E shows brain nocardiosis with central abscess and neutrophil infiltrate (arrow); Original magnification: X12.

the patient's symptoms, medical history, radiological and histopathological findings, and positive specimen cultures, the primary diagnosis was established as *Nocardia* sp. infection with brain abscess formation. A left parietal craniotomy for brain tissue biopsy was performed, revealing brain tissue with necrotic debris, purulent exudates, and numerous neutrophils, consistent with a brain abscess (Fig. 4 (B)). No definite malignancy was observed.

Treatment involving intravenous administration of trimethoprim-sulfamethoxazole (TMP-SMX; 15 mg/kg daily), imipenem (500 mg every 6 hours), and amikacin (7.5 mg/kg every 12 hours) was started in mid-May 2022 (4th week of hospitalization). Additional treatment with ampicillin (2 g every 6 hours) was initiated, since *Enterococcus faecalis* was isolated from the brain abscess specimen. TMP-SMX was discontinued 2 weeks later due to progressive leukopenia and gradually increasing liver enzymes. Amikacin was also discontinued 10 days later to prevent ototoxicity and nephrotoxicity.

After completing 8 weeks of combined antimicrobial treatment, brain MRA revealed significant improvement in the brain abscess in terms of size and number, coinciding with an improvement in the weakness of the right-side extremity (the muscle power score improved from 4 to 5) (Fig. 3 (B)). In addition, the RUL mass was gradually improving on the CXR (Fig. 1 (B-E). Antibiotics with imipenem and ampicillin were switched to oral antibiotic monotherapy with amoxicillin-clavulanate (875 mg twice daily) after completing a 10-week treatment course. The patient was discharged after 15 weeks hospitalization and continued oral antibiotic treatment for an additional 2 weeks. The last brain MRA in November 2022 (3 months after the completion of treatment) showed complete remission of the preexisting brain abscess (Fig. 3, Panel C). The entire treatment course is summarized in Fig. 5.

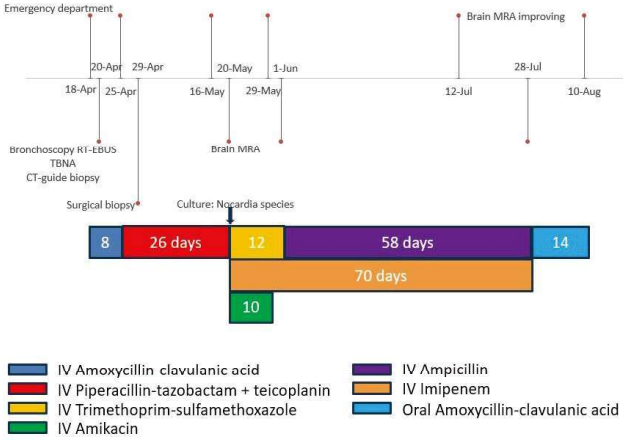

Fig. 5. Summary of the entire treatment course.

Discussion

We reported a case of pulmonary nocardiosis with multiple brain abscesses that was successfully treated with a 12-week combination of antimicrobial therapy. Nocardiosis typically presents with an acute onset and inflammatory response, potentially progressing to granulomatous inflammation or necrotic abscess formation [1, 5-6]. However, its diagnosis is challenging

due to nonspecific radiographic findings, varied pathological features, and clinical manifestations [7]. Prompt diagnosis and treatment are crucial given the high mortality rate, ranging from 16.2% to 60% in disseminated infections, especially in those with central nervous system (CNS) involvement or in immunocompromised patients [3, 7-10].

CNS infection is a significant complication of disseminated nocardiosis, occurring in 44% of cases [4, 11]. Brain imaging typically reveals ring-enhanced nodules with vasogenic edema, mostly in the frontal and parietal lobes; cerebellar involvement is rare [5, 10]. Our case showed multiple brain abscesses in various regions, including the midbrain and cerebellum, with a co-infection of *Enterococcus faecalis*. Though rare, CNS co-infections with *Nocardia* and other pathogens, such as *Toxoplasma gondii* and *Salmonella enteritidis*, have been documented [5, 12].

Traditionally, *Nocardia* identification relied on observing microscopic characteristics and macroscopic inspection for colony morphology, which can be time-consuming and challenging due to slow growth [1, 6]. Molecular identification methods, such as gene sequencing and mass spectrometry, have become the gold standard for accurate and rapid species identification, as well as determining antimicrobial susceptibility profiles [1, 6]. Unfortunately, these methods were not commonly utilized in our hospital. Moreover, without antimicrobial susceptibility profiles, empirical treatment was based on common *Nocardia* species found in Taiwan.

There are no standardized recommendations for the treatment and duration of nocardiosis, which necessitates personalized approaches based on disease severity, underlying conditions, and antimicrobial susceptibility testing [1, 15]. Previous studies in Taiwan and in our hospital identified *N. brasiliensis*, *N. farcinica* and *N. cyriacigeorgica* as predominant species, with high susceptibility to TMP-SMX, linezolid, and amikacin (>98%) [6-7, 13-14]. Empirical combination therapy is advised for severe or disseminated cases, especially those involving the CNS [10]. Given the high susceptibility of *N. brasiliensis*, *N. farcinica* and *N. cyriacigeorgica* to TMP-SMX and amikacin, these were our initial choices for combination therapy. Imipenem is recommended as an alternative or part of a combined treatment if TMP-SMX resistance, allergy, or adverse effects occur [15-16]. We discontinued TMP-SMX due to intolerance, and amikacin to prevent nephrotoxicity and ototoxicity. Ampicillin served as an alternative therapy, and is also effective against *Enterococcus faecalis* in brain abscesses [6]. Combined therapy with imipenem and ampicillin proved effective for our patient, as evidenced by the gradual improvement in the RUL mass on CXR, and significant improvement in the brain abscesses on MRA. Although our case had a relatively shorter duration of treatment, no recurrence or relapse was observed on follow-up CXR and brain MRA 3 months after treatment cessation.

We encountered several limitations during the treatment of this case. The first was the lack of an accurate and rapid method of *Nocardia* identification. The appropriate antimicrobial therapy was administered after a delay of nearly a month, due to our awaiting the culture results. The second limitation was the use of empirical antimicrobial treatment without having any results of the antibiotic susceptibility profile. There is a lack of consensus on the optimal antimicrobial therapy and treatment duration for

nocardiosis, necessitating larger cohort studies and systemic reviews in the future.

Conclusion

In conclusion, nocardiosis is a rare but potentially life-threatening infectious disease, especially in immunocompromised individuals and those with CNS involvement. Its lack of specificity and slow growth often lead to delayed diagnosis and treatment. Early diagnosis and appropriate management are essential to improve outcomes in patients with nocardiosis.

References

1. Traxler RM, Bell ME, Lasker B, *et al.* Updated Review on *Nocardia* Species: 2006-2021. Clin Microbiol Rev 2022; 35(4): e0002721.
2. Han Y, Cheng M, Li Z, *et al.* Clinical characteristics and drug resistance of *Nocardia* in Henan, China, 2017-2023. Ann Clin Microbiol Antimicrob 2024; 23(1): 23.
3. Woodworth MH, Saullo JL, Lantos PM, *et al.* Increasing *Nocardia* Incidence Associated with Bronchiectasis at a Tertiary Care Center. Ann Am Thorac Soc 2017; 14(3): 347-54.
4. Steinbrink J, Leavens J, Kauffman CA, *et al.* Manifestations and outcomes of *nocardia* infections: Comparison of immunocompromised and nonimmunocompromised adult patients. Medicine 2018; 97(40): e12436.
5. Kisiel M, Bass VM, Fong C, *et al.* Clinicopathologic characteristics of *Nocardia* brain abscesses: Necrotic and non-necrotic foci of various stages. J Neurol Sci 2024; 456: 122850.
6. Brown-Elliott Barbara A, Brown June M, Conville Patricia S, *et al.* Clinical and Laboratory Features of the *Nocardia* spp. Based on Current Molecular Taxonomy. Clinical Microbiology Reviews 2006; 19(2): 259-82.
7. Yang CH, Kuo SF, Chen FJ, *et al.* Clinical manifestations and outcome of nocardiosis and antimicrobial susceptibility of *Nocardia* species in southern Taiwan, 2011-2021. J Microbiol Immunol Infect 2023; 56(2): 382-91.
8. TORRES HA, REDDY BT, RAAD II, *et al.* Nocardiosis in Cancer Patients. Medicine 2002; 81(5): 388-97.
9. Lebeaux D, Freund R, van Delden C, *et al.* Outcome and Treatment of Nocardiosis After Solid Organ Transplantation: New Insights From a European Study. Clin Infect Dis 2017; 64(10): 1396-405.
10. Corsini Campioli C, Castillo Almeida NE, O'Horo JC, *et al.* Clinical Presentation, Management, and Outcomes of Patients With Brain Abscess due to *Nocardia* Species. Open Forum Infect Dis 2021; 8(4): ofab067.
11. Beaman BL, Beaman L. *Nocardia* species: host-parasite relationships. Clinical Microbiology Reviews 1994; 7(2): 213-64.
12. Bishburg E, Eng RHK, Slim J, *et al.* Brain Lesions in Patients With Acquired Immunodeficiency Syndrome. Archives of Internal Medicine 1989; 149(4): 941-3.
13. Lai CC, Liu WL, Ko WC, *et al.* Multicenter study in Taiwan of the in vitro activities of nemonoxacin, tigecycline, doripenem, and other antimicrobial agents against clinical isolates of various *Nocardia* species. Antimicrob Agents Chemother 2011; 55(5): 2084-91.
14. Lao CK, Tseng M-C, Chiu C-H, *et al.* Clinical manifestations and antimicrobial susceptibility of *Nocardia* species at a tertiary hospital in Taiwan, 2011–2020. Journal of the Formosan Medical Association 2022;121(10): 2109-22.
15. Wilson JW. Nocardiosis: Updates and Clinical Overview. Mayo Clinic Proceedings 2012; 87(4): 403-7.
16. Ameen M, Arenas R, Vásquez del Mercado E, *et al.* Efficacy of imipenem therapy for *Nocardia* actinomycetomas refractory to sulfonamides. Journal of the American Academy of Dermatology 2010; 62(2): 239-46.

Treatment of Iatrogenic Cervical Esophageal Transection Following Thyroidectomy – A Case Report

Kai-Yun Hsueh[1], En-Kuei Tang[1]

Iatrogenic cervical esophageal transection after thyroidectomy is an extremely rare condition that requires prompt diagnosis and surgical intervention. We reported a case of iatrogenic cervical esophageal transection following thyroidectomy for goiter in a 54-year-old woman. Primary repair was not achievable because of loss of a long segment of the cervical esophagus. A modified diversion was performed by inserting a T-tube into the remnant esophagus, followed by gastrostomy and jejunostomy. The next day, mediastinal abscess was detected on chest computed tomography; therefore, thoracoscopic mediastinotomy was performed, with placement of 2 drains. After 6 months, thoracoscopic esophagectomy, alimentary reconstruction with gastric pull-up, and cervical esophagogastrostomy anastomosis were performed. The patient was discharged without complications. Iatrogenic cervical esophageal transection following thyroidectomy can be successfully managed with a series of treatments, including a modified diversion procedure, prompt drainage of mediastinitis, alimentary reconstruction with gastric pull-up, and cervical esophagogastrostomy anastomosis. ***(Thorac Med 2024; 39: 375-379)***

Key words: Iatrogenic esophageal injury, goiter, thoracoscopic mediastinotomy, thyroidectomy, reconstructive surgery, modified diversion procedure

Background

Iatrogenic esophageal injury, a serious complication of thyroidectomy, may result in deep neck infection, subcutaneous emphysema, pneumomediastinum, mediastinal abscess, and even death. Most complications of iatrogenic esophageal injuries are identified and repaired during surgery. Cervical esophageal transection following thyroidectomy is an extremely rare condition that requires prompt intervention. We report a case of iatrogenic cervical esophageal transection following thyroidectomy, which was successfully managed with a series of treatments, including a modified diversion procedure, prompt drainage of mediastinitis, alimentary reconstruction with gastric pull-up, and cervical esophagogastrostomy anastomosis.

[1]Division of Thoracic Surgery, Department of Surgery, Kaohsiung Veterans General Hospital, Kaohsiung, Taiwan.
Address reprint requests to: Dr. Kai-Yun Hsueh, Division of Thoracic Surgery, Department of Surgery, Kaohsiung Veterans General Hospital, Kaohsiung, Taiwan.

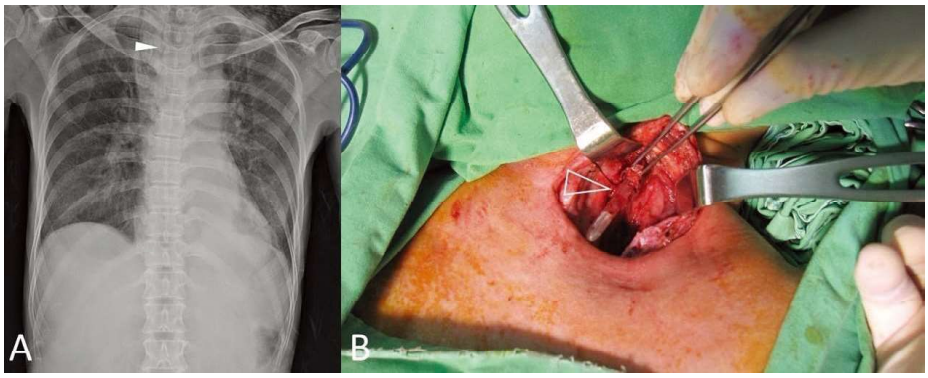

Fig. 1. (A) Chest roentgenogram revealing massive subcutaneous emphysema extending from the neck to the chest wall (white arrowhead). (B) An intraoperative image showing transection of the cervical esophagus, with only a short proximal stump (hollow arrowhead).

Case Presentation

A 54-year-old woman underwent thyroidectomy for goiter at a regional institute. After surgery, she experienced neck swelling, dysphagia, and drainage of a copious amount of saliva from the surgical wound. Therefore, on her request, she was referred to our hospital for further treatment. Upon arrival at the emergency room, physical examination revealed crepitation from the neck to the chest wall, with redness and swelling of the neck. A chest roentgenogram revealed massive subcutaneous emphysema extending from the neck to the chest wall (Fig. 1A). Due to a high index of suspicion of esophageal injury, an urgent surgery (neck exploration) was performed, during which we noted much purulent discharge accumulation beneath the neck wound. A nasogastric tube was used to verify the location of the esophagus, and transection of the cervical esophagus with a short proximal stump was identified (Fig. 1B). The distal stump of the esophagus was not visualized; therefore, primary anastomosis could not be achieved. During the diversion procedure, 1 limb of the T-tube was inserted into the proximal stump of the esophagus (with ligation of the other limb) to drain the saliva and to maintain the patency of the esophageal lumen. Median laparotomy with gastrostomy for decompression and jejunostomy for enteral feeding were also performed.

The day after surgery, she developed dyspnea with accompanying symptoms of neck swelling and tenderness. Chest computed tomography (CT) revealed a massive pneumomediastinum and mediastinal abscess (Fig. 2). An urgent video-assisted thoracoscopic surgery mediastinotomy for drainage of the mediastinal abscess was performed (Fig. 3A). The pleura of

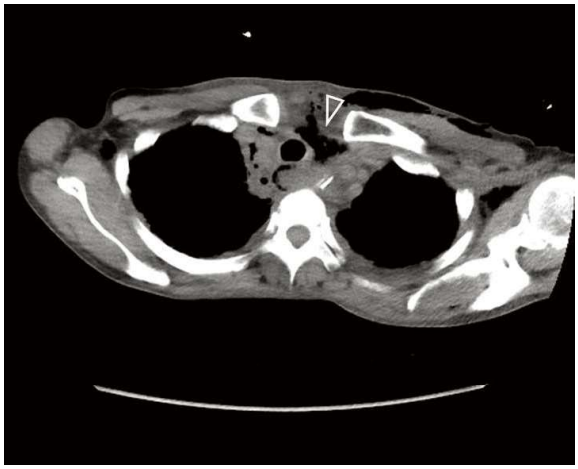

Fig. 2. Chest computed tomography scan showing massive pneumomediastinum (hollow arrowhead).

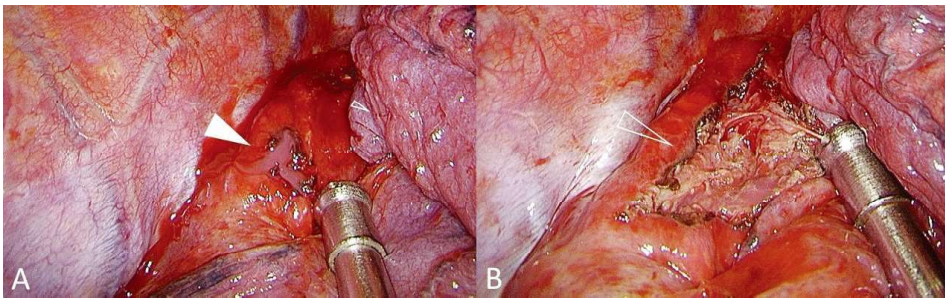

Fig. 3. (A) An intraoperative image showing accumulation of purulent discharge around the upper third of the esophagus (white arrowhead). (B) An intraoperative image showing the opened mediastinal pleura, with drainage of the purulent discharge (hollow arrowhead).

the mediastinum was incised, the purulent discharge was drained out (Fig. 3B), and 2 chest tubes were placed.

The patient was transferred to the intensive care unit for postoperative care. After a few days of antibiotic treatment, follow-up chest CT revealed complete resolution of the pneumomediastinum and a significant regression of the mediastinal abscess. The patient was discharged uneventfully, 4 weeks after surgery. Six months later, the patient underwent esophageal reconstruction with thoracoscopic esophagectomy, gastric pull-up via a substernal route, and cervical esophagogastrostomy anastomosis. She was then discharged on postoperative day 18, with no complications.

Discussion

Esophageal transection is a life-threatening condition that requires early diagnosis and prompt surgical intervention to prevent serious morbidities or even mortality. There are different etiologies of esophageal injuries, including iatrogenic injury, spontaneous perforation [1], trauma, foreign body ingestion, and malignancy. Most esophageal injuries are iatrogenic, occurring especially during endoscopy or echocardiography. Intraoperative esophageal injury accounts for only a small proportion of the iatrogenic type. Esophageal transection during total thyroidectomy is an extremely rare condition, as experienced surgeons carefully dissect periesophageal soft tissues to avoid complications during the procedure.

The most common presenting complaints following esophageal injury include pain, fever, dysphagia, odynophagia, and subcutaneous emphysema; leakage of intraluminal content from the esophagus into the mediastinum causes a serious inflammatory reaction. A chest roentgenogram in such a patient will possibly reveal a widened mediastinum, diffuse pneumomediastinum, pneumothorax, or pleural effusion. Chest CT scans are also usually obtained to survey the extent and location of esophageal injury, and may show mediastinal abscess, dilated esophagus, or pneumomediastinum. Modalities commonly used for direct evaluation by the surgeons are endoscopy and esophagography. Contrasts such as barium and water-soluble agents are used to evaluate extravasation of the intraluminal esophageal content. However, if esophageal transection is highly suspected, exploration is strongly recommended to visualize, diagnose, and control infection by placing drains around the injury site.

Treatment for esophageal injury mainly

depends on the location and timing of the symptoms. Nonoperative management may be successful in some patients who meet certain strict criteria. A hemodynamically stable patient with a new-onset local esophageal injury could be managed nonoperatively with antimicrobial agents and adequate drainage [2]. However, emergency surgical intervention is provided with the first sign of clinical deterioration. Most complications of esophageal surgeries can be immediately observed and managed during surgery by an experienced surgeon [3]. Primary surgical repair of esophageal injury is usually performed with interrupted, absorbable sutures for the mucosal layer and nonabsorbable sutures for the muscular layer.

However, primary repair or anastomosis was not indicated in our case because the distal stump of the esophagus could not be visualized. The space between the proximal and distal portions of the esophagus was significant; therefore, the 2 ends of the esophagus could not be approximated [4]. Surgical treatment of cervical esophageal transection includes a diversion procedure and esophagectomy, followed by esophageal reconstruction after 6 months [4]. Diversion procedures involve proximal diversion of the esophagus with cervical esophagostomy, gastric diversion with gastrostomy, and jejunostomy for decompression, as well as nutritional support. In our patient, cervical esophagostomy for proximal diversion was extremely difficult to execute because of the friable nature and short length of the esophageal remnant. We adapted an alternative esophageal diversion, where we inserted a 1-limb T-tube (the other limb was ligated) into the lumen of the remaining esophagus for drainage of saliva. We recommend early recognition of mediastinitis and prompt mediastinotomy for drainage of mediastinal abscesses [3], to prevent sepsis and enhance postoperative recovery. Esophageal reconstruction is typically conducted half a year later, and the gastric conduit [5] is commonly used for alimentary reconstruction owing to its sufficient length and blood supply. The colon, jejunum or even a forearm free flap may be used for reconstruction if the stomach is unavailable owing to a previous gastric surgery [6-7].

Conclusion

Iatrogenic cervical esophageal transection following thyroidectomy is a rare, but fatal complication. It can be successfully managed with a series of treatments, including a modified diversion procedure, prompt drainage of mediastinitis, alimentary reconstruction with gastric pull-up, and cervical esophagogastrostomy anastomosis.

References

1. Ashrafian H, Sanchez AN, Thanos A, *et al*. Thoracoscopic esophageal repair of a spontaneous Barrett's ulcer perforation. Ann Thorac Surg 2015; 99: 331-333. doi: 10.1016/j.athoracsur.2014.02.067.
2. Roro GM, Folvik G, Louis L, *et al*. Drug-induced esophageal injuries with an atypical presentation mimicking acute coronary syndrome. BMC Gastroenterol 2021; 21: 486. doi.org/10.1186/s12876-021-02063-2.
3. Al-Mufarrej F, Badar J, Gharagozloo F, *et al*. Spontaneous pneumomediastinum: diagnostic and therapeutic interventions. J Cardiothorac Surg 2008; 3: 59. doi.org/10.1186/1749-8090-3-59.
4. Chirica M, Kelly MD, Siboni S, *et al*. Esophageal emergencies: WSES guidelines. World J Emerg Surg 2019; 14:26. doi.org/10.1186/s13017-019-0245-2.
5. Akiyama H, Miyazono H, Tsurumaru M, *et al*. Use of the stomach as an esophageal substitute. Ann Surg 1978 Nov; 188(5): 606-10. doi: 10.1097/00000658-197811000-

00004. PMID: 718285; PMCID: PMC1396768.
6. Hanwei P, Steven JW, Weixiong L. Rare complication after thyroidectomy-cervical esophageal stenosis: a case report and literature review. World J Surg Oncol 2014; 12:308. doi: 10.1186/1477-7819-12-308.
7. Ma L, Chengwu L, Jiandong M, *et al*. Successful cervical esophageal reconstruction using gastric conduit without gastroepiploic artery. Ann Thorac Surg 2019; 107: e409-e410. doi: 10.1016/j.athoracsur.2018.09.068.

Resistance Transformation in Lung Adenocarcinoma Following Targeted Therapy: A Case Study

Yi-Chen Shao[1], Wan-Shan Li[2], Chang-Yao Chu[2,3], Sheng-Tsung Chang[2]
Shu-Farn Tey[1,3]

This report presents the case of a 61-year-old female with advanced non-small cell lung cancer (NSCLC), initially treated with afatinib, a second-generation epidermal growth factor receptor (*EGFR*)-tyrosine kinase inhibitor, after an *EGFR* exon 21 L858R mutation was identified. Despite initial tumor regression, the patient developed resistance, as indicated by disease progression and histological transformation to small cell lung cancer. The subsequent treatment regimen included a combination of chemotherapy and osimertinib, targeting both the original *EGFR* mutation and a later emerging T790M mutation. This case exemplifies the intricate relationship of genetic mutations, treatment responses, and the evolution of resistance in the management of NSCLC. Furthermore, this case underscores the critical need for ongoing research and the development of novel treatments to address NSCLC. ***(Thorac Med 2024; 39: 380-388)***

Key words: Adenocarcinoma, resistance, small cell transformation, epidermal growth factor receptor, T790M

Introduction

According to Taiwan Cancer Registry Annual Reports from 2015 to 2021, the prevalence of lung cancer in Taiwan increased from 12.44% to 13.86% of all cancer cases during that period, indicating a rising incidence of this malignancy. Conversely, mortality rates have remained relatively stable, fluctuating around 19%, despite the increased prevalence. In response, targeted therapies have been refined, offering greater specificity for non-small cell lung cancer (NSCLC) with epidermal growth factor receptor (*EGFR*) mutations, and reducing systemic toxicity compared to traditional chemotherapy [22].

In NSCLC, *EGFR* signaling is a crucial determinant of tumor growth and progression. [[These pathways of *EGFR* signaling serve as positive regulators of proliferation and progression, and negative regulators of apoptosis [21]. The most common *EGFR* mutations, which ac-

[1]Department of Pulmonary Medication, Chi-Mei Medical Center, Tainan, Taiwan, [2]Department of Pathology, Chi-Mei Medical Center, Tainan, Taiwan, [3]School of Medicine, College of Medicine, National Sun Yat-sen University, Kaohsiung, Taiwan.
Address reprint requests to: Dr. Shu-Farn Tey, Department of Pulmonary Medication, Chi-Mei Medical Center, No. 901, Zhonghua Rd., Yongkang Dist., Tainan City 71004, Taiwan (R.O.C.).

count for approximately 90% of cases, include deletions in exon 19 and the L858R point mutation in exon 21; less prevalent *EGFR* mutations include G719X, S768I, and L861Q. The use of tyrosine kinase inhibitors (TKIs) in these patients has significantly improved progression-free survival (PFS) [23].

Unfortunately, many patients experience relapse due to the development of resistance mechanisms such as phenotypic transformations, activation of alternative pathways, and *EGFR* T790M mutations. It is important to note that *EGFR* T790M resistance typically develops after using first and second-generation *EGFR*-TKIs. Third-generation *EGFR*-TKIs have been engineered with heightened specificity for the common *EGFR* mutations, and also the T790M mutation. Overcoming this advanced level of resistance is critical, prompting the development of the next generation of TKIs. The standard treatment for small cell lung cancer (SCLC) is used to manage transformations to small cell carcinoma (SCC).

Case Report

A 61-year-old female presented with a 1-day history of left chest pain and hemoptysis, accompanied by a chronic cough persisting for 2 months. Her medical history included uterine prolapse, with no significant past surgical, familial, or medication-related findings contributing to her current condition.

During the physical examination, the patient exhibited symptoms indicative of respiratory pathology, specifically showing mildly decreased breathing sounds in the left upper lobe (LUL). Diagnostic imaging played a crucial role in her assessment. A chest computed tomography (CT) scan revealed a mass with central necrosis in the LUL. A CT-guided biopsy of this mass identified scant atypical cells with extensive necrosis, immunoreactive for thyroid transcription factor-1 (TTF-1), suggesting a primary lung origin. Further confirmation came from a surgical lymph node biopsy, which diagnosed metastatic adenocarcinoma (Fig. 1A).

Clinically, the patient was determined to have stage IV adenocarcinoma, due to distant metastases involving the brain and the right acetabulum. The discovery of an *EGFR* exon 21 L858R mutation prompted the initiation of targeted therapy with afatinib, combined with radiotherapy for brain metastasis. Initially, the patient responded to this regimen, as evidenced by tumor regression on follow-up imaging.

However, 6 months into the afatinib treatment, the disease progressed, characterized by an increase in the size of the LUL tumor with mediastinal invasion and lymph node metastasis, coupled with regression of prior bone metastases and stability of brain metastases. A re-biopsy revealed transformation to SCC, an aggressive form of lung cancer that tested positive for chromogranin A and synaptophysin, and focally positive for AE1/AE3, but negative for TTF-1 and CD45 (Fig. 1B, 1C, 1D). This posed a significant challenge due to the aggressive nature and rapid progression of SCLC.

Given these new histopathological findings, the treatment strategy was revised to include a regimen of platinum-based chemotherapy with cisplatin and etoposide; however, continuing afatinib due to combined SCC or small cell transformation could not be totally excluded after further discussion with the pathologist. This approach resulted in a dramatic reduction in the size of the lung tumor within a month, as indicated by a follow-up chest X-ray (Fig. 2).

Over the next 8 months, the patient com-

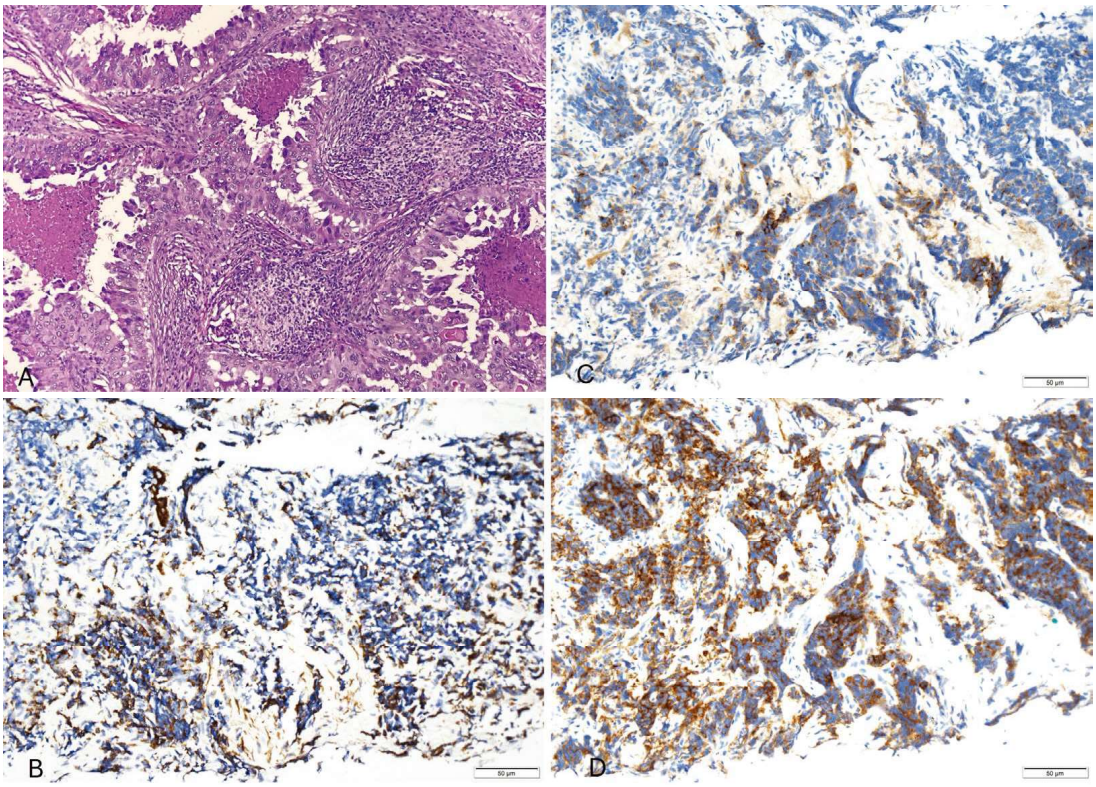

Fig. 1. (A) Before treatment, lymph node biopsy shows metastatic adenocarcinoma. (B) Recurrent tumor showed positive staining for AE1/AE3. (C) Positive staining for chromogranin A. (D) Positive staining for synaptophysin.

pleted 6 cycles of chemotherapy while continuing on afatinib, and maintained a stable condition. Despite this, her health declined, leading to her presenting at the emergency department with persistent coughing, production of yellowish and blood-streaked sputum, and increased difficulty breathing. A subsequent chest CT scan showed growth of the lung tumor, with new spreading to the mediastinal and cervical lymph nodes, extension to the opposite lung, and possible metastasis in the right adrenal gland. This growth led to obstructive pneumonitis in the left lung and was further complicated by the discovery of left vocal cord paralysis during a bronchoscopy.

Upon admission, the patient was treated with antibiotics for suspected infections, then received bronchial stent insertion and radiotherapy to alleviate the tumor-caused obstruction in her LUL. During her hospital stay, she tested positive for COVID-19 and was treated with the antiviral medication molnupiravir. Once her condition stabilized, chemotherapy with pemetrexed and cisplatin was initiated. To manage her pancytopenia, a side effect of the chemotherapy, she received blood transfusions and filgrastim.

The persistence of the L858R mutation along with the newly identified T790M mutation in the lung tumor biopsy led to a crucial change in her treatment plan. With these new genetic findings, her treatment was switched to osimertinib. These comprehensive adjustments in her treatment regimen allowed her to stabilize sufficiently to be discharged from the hospital (Fig. 3A, 3B, 3C).

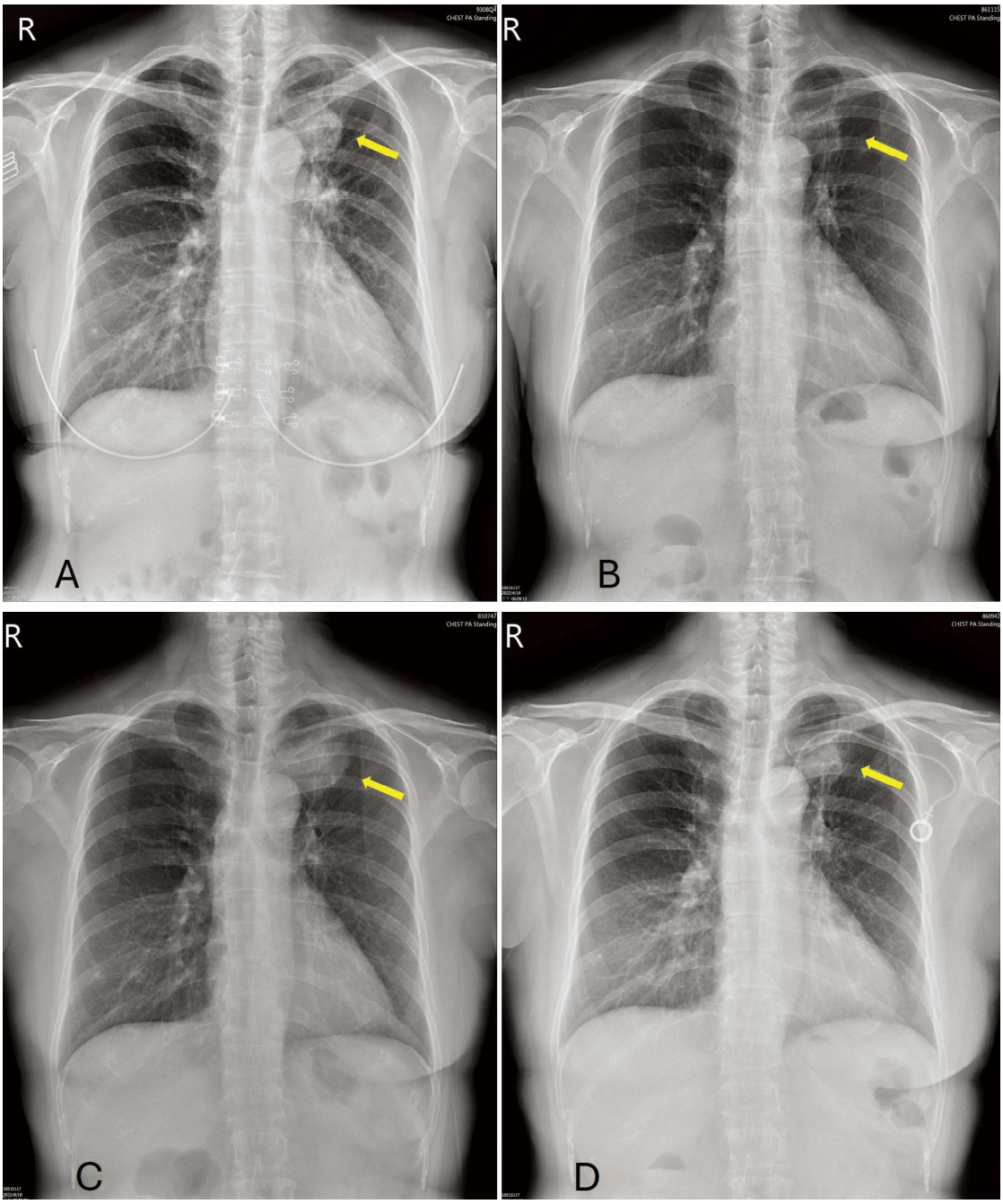

Fig. 2. Chest X-ray showing (A) Baseline adenocarcinoma (B) Partial remission after 2 months of afatinib treatment (C) Recurrent LUL tumor after treatment for 6 months, and (D) Tumor size shrinkage after 1 month of chemotherapy with cisplatin plus etoposide, and afatinib treatment.

Despite initial improvement, the patient was readmitted 2 months after discharge due to suspected tumor progression (Fig. 3D). Imaging studies confirmed new metastases, and an echo-guided biopsy from the right back muscle revealed adenocarcinoma with the L858R mutation, but without the T790M variant, *KRAS* mutation, *MET* amplification, or *EGFR* C797S mutation. Deterioration in imaging and clinical respiratory status suggested potential resistance to osimertinib.

The patient's health continued to decline

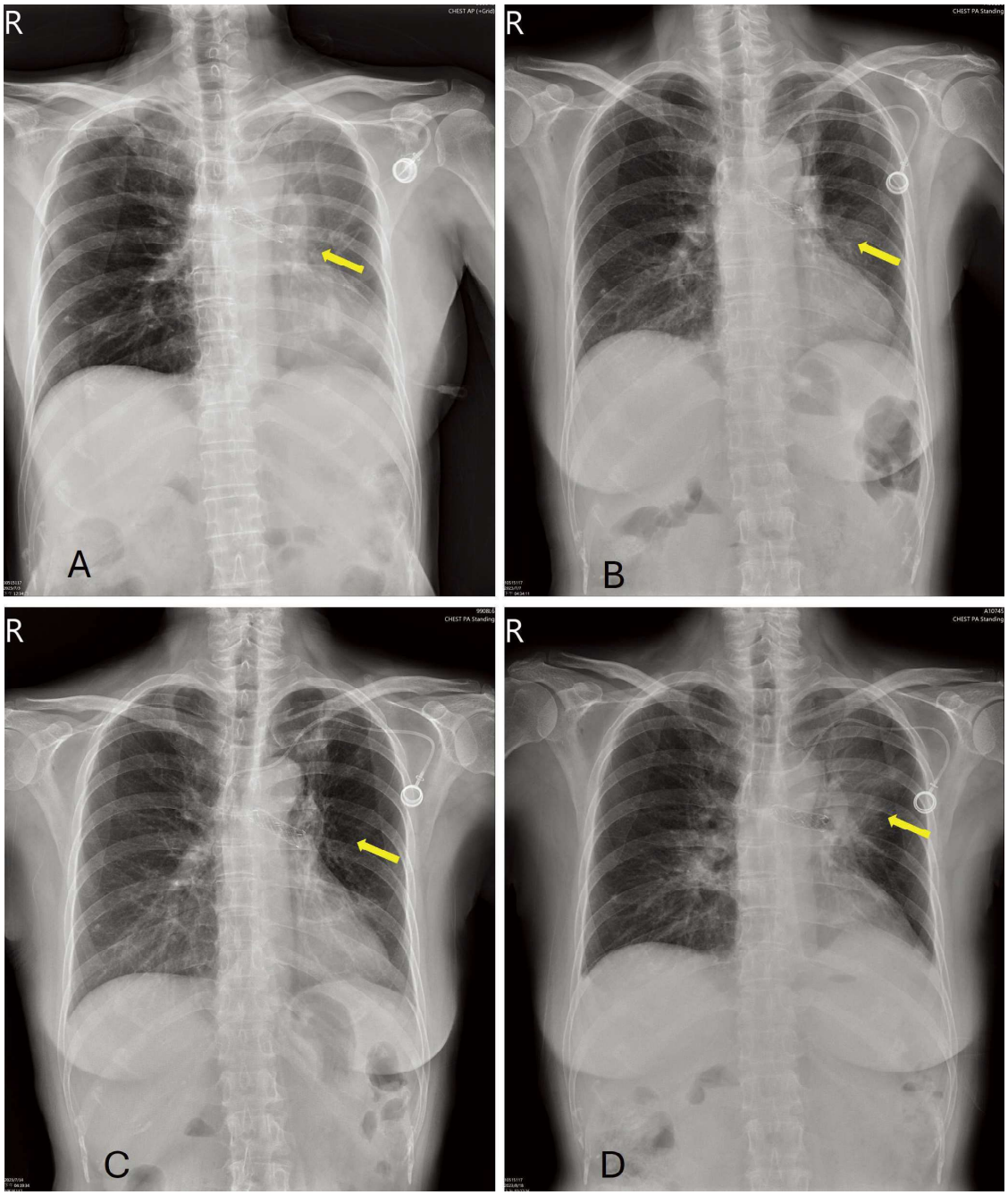

Fig. 3. Series of follow-up chest X-rays (CXR), as follows: (A) Post-stenting in the left bronchus, with suspected re-expansion of the obstructive left lung. (B) Stable lung cancer in the left upper lobe (LUL) with lung-to-lung metastasis. (C) One-week outpatient follow-up; minimal change in LUL lung cancer with lung-to-lung metastasis. (D) Nearly 2 months later, suspected progression of lung cancer with signs of obstructive pneumonitis.

due to the progression of pneumonia, despite treatment with antibiotics and antifungals. We discussed her worsening condition and limited treatment options with her family, given her advanced cancer and complications from pneumonia. Unfortunately, her condition continued to deteriorate, possibly due to sepsis, making further cancer treatment unfeasible. Twenty days after her readmission, the patient passed away.

This case illustrates the challenges of man-

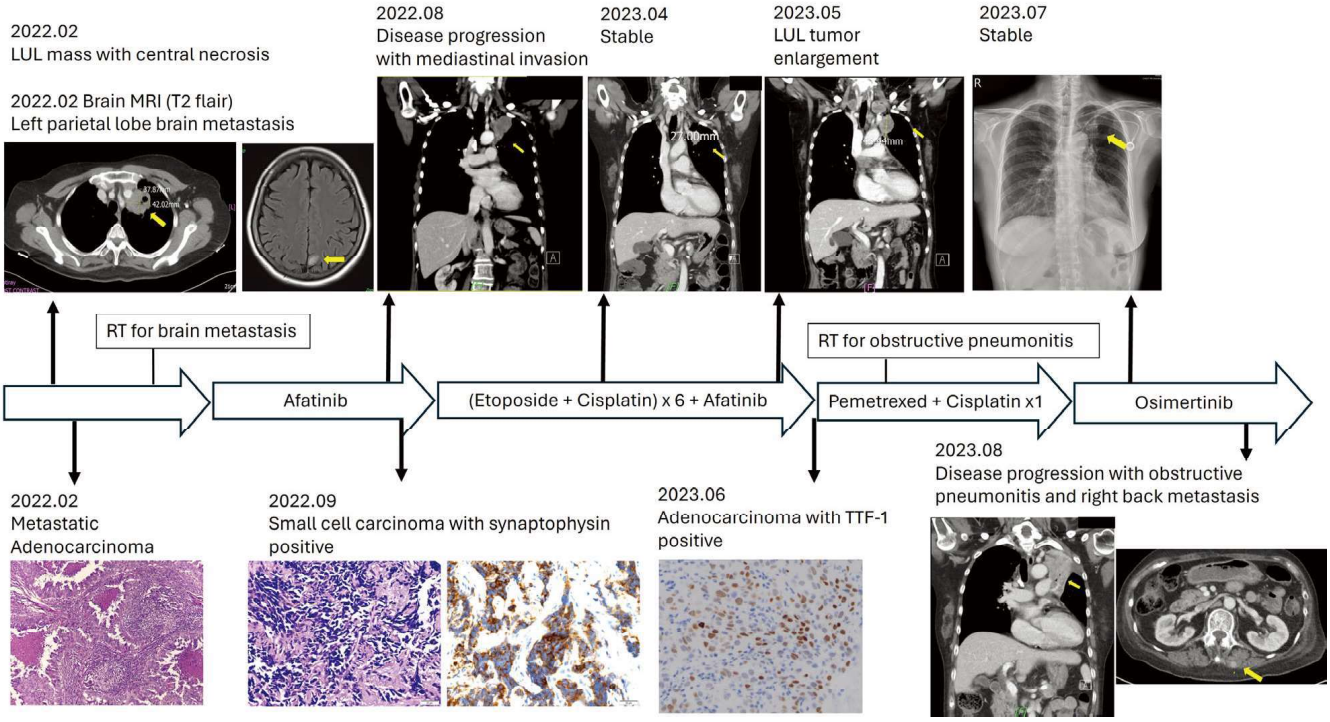

Fig. 4. Summary chart of this case's treatment process, and histological and imaging changes.

aging advanced NSCLC, particularly when faced with resistance to targeted therapy and the phenomenon of histologic transformation or even when combined with SCLC. Furthermore, this case underscores the necessity for vigilant attention to and adaptation with therapeutic strategies to optimize patient outcomes in the face of evolving disease.

Discussion

The World Health Organization's 2020 report underscores the significant global health impact of lung cancer, noting approximately 2.2 million new cases. While breast cancer has slightly surpassed lung cancer in incidence, lung cancer continues to be the deadliest cancer worldwide, with nearly 1.8 million deaths—almost double the mortality rate of colorectal cancer, the second most common cancer.

A retrospective observational study published in 2021 [5] reveals that about 1.6 million of the new lung cancer cases diagnosed annually are classified as NSCLC, with 60%-70% diagnosed at an advanced stage, specifically stage IV. The prognosis for these patients remains poor, with 2-year and 5-year survival rates of approximately 50% and 20%, respectively. These outcomes are influenced by multiple factors, including performance status, TNM staging, histological type, number of chemotherapy cycles, and the use of targeted therapy.

The introduction of TKIs has revolutionized the treatment of NSCLC, particularly for cases with *EGFR* mutations. However, acquired resistance mechanisms [1], such as phenotypic transformation to SCLC and the development of secondary *EGFR* mutations, pose significant challenges. The first documented case of small cell transformation was reported in 2006 [7],

with subsequent studies [6] reporting a transformation rate of 14% in patients harboring sensitive *EGFR* mutations who underwent TKI treatment.

Studies of mice [9,10,11,12] indicate that alveolar type II cells, which are precursors to adenocarcinoma, may also undergo transformation into SCLC. This finding contrasts with the genetic analysis from our patient, where the original *EGFR* mutation persisted despite the phenotypic transformation, suggesting a mechanism of resistance transformation rather than the emergence of a new primary cancer. This observation challenges established theories of tumor heterogeneity that have been based on limited biopsy samples. Importantly, it raises questions about clinical progression, as patients typically respond to *EGFR* inhibitors for an extended period before experiencing a significant decline in health, marked by disease progression, worsening symptoms, reduced overall health, and decreased treatment efficacy following the diagnosis of SCLC [2].

In a Korean study [15], 1.5% of patients with lung adenocarcinoma showed transformation to SCLC morphology on the second biopsy, with all retaining the same *EGFR* mutation. In addition, the T790M mutation, which accounts for 50-60% of resistance cases, is associated with an improved median overall survival of 26.8 months when treated with osimertinib [13-14]. This highlights the critical importance of ongoing genetic testing in managing resistance.

Challenges associated with resistance patterns are well-documented. Historical reports from as early as 2007 [16] have noted cases where patients' adenocarcinoma transformed into SCLC following treatment with gefitinib. This transformation was confirmed by positive synaptophysin staining during immunohistochemical analysis. Despite this phenotypic change, the response to subsequent chemotherapy was only partial. Follow-up CT scans showed continued tumor growth and a reversion to the original adenocarcinoma subtype, which tested negative for synaptophysin.

Further illustrating these challenges, a 2018 case from Japan [17] described a patient with an *EGFR* L858R mutation who received treatment with both first and third-generation *EGFR*-TKIs, along with chemotherapy. This patient revealed 2 forms of drug resistance: a transformation to SCLC still harboring the L858R mutation following gefitinib treatment, and the subsequent emergence of an unexpected *EGFR* T790M mutation during chemotherapy. These cases underscore the critical importance of regular biopsies for accurately identifying resistance mechanisms and tailoring treatment strategies effectively.

The evolution of resistance mechanisms to osimertinib [14], despite the absence of evidence for related mutations in this case, underscores the need for further research into genetic modifications, such as the C797S mutation, and other alterations including MET gene amplification, epithelial-mesenchymal transition, and histological transformation. Research in these areas is crucial for developing more effective strategies to combat resistance in cancer treatment.

Ongoing clinical trials are evaluating fourth-generation TKIs that have been structurally modified [17] to specifically target mutations such as the previously mentioned C797S mutation. One study [18] has demonstrated early clinical efficacy and safety in mouse models. These investigations [17,18,19,20] are critical for advancing our understanding and management of tumor progression in the presence of

multiple resistance mechanisms.

In this case of advanced NSCLC, the patient initially responded to treatment with the *EGFR*-TKI afatinib, but subsequently developed resistance, manifested by disease progression and histological transformation to SCLC. Notably, genetic testing was not performed on the SCLC specimen initially. Considering that the founder *EGFR* mutation is usually retained at the moment of SCLC transformation [24], the tumor might contain both the initial *EGFR* mutation and histological changes or the possibility of combined SCLC. Therefore, afatinib treatment was maintained.

Based on the histological transformation, chemotherapy was added to the treatment strategy, combining afatinib with chemotherapy to target both the *EGFR* mutation and the aggressive nature of SCLC.

Clinical and radiological deterioration prompted a re-biopsy, which unexpectedly revealed a reversion to adenocarcinoma. This tissue was then subjected to genetic testing, where the T790M mutation was identified alongside the original *EGFR* mutation. This crucial finding informed the shift to osimertinib, targeting the T790M mutation.

However, the patient experienced further disease progression with a notably short PFS. In reviewing the patient's clinical course and investigating potential causes, it is possible that the tumor's complex resistance pattern, including sequential resistance transformations, combined with 2 histologic types of cancer cells, contributed to the short PFS. While no additional mutations such as C797S or MET amplification, which are known to cause resistance, were detected, the potential for other mechanisms remains.

One study indicated that approximately 10-12% of patients using osimertinib might develop resistance due to cell cycle gene alterations [25], which can also shorten PFS. Although we found no evidence to confirm this in our patient, it remains a plausible explanation. Furthermore, due to the small biopsy sample, it was challenging to fully analyze the tumor's morphology. There may still be a mixed histological component, such as SCLC, which could also contribute to the shortened PFS.

These findings underscore the need for comprehensive genetic and histological analysis in understanding resistance mechanisms. Further research is essential to develop effective strategies for managing such complex cases of lung cancer.

Conclusion

This case highlights the complexity of treating NSCLC amid various resistance mechanisms. It underscores the necessity for ongoing research to develop effective strategies to overcome these challenges. Our study contributes to a deeper understanding of NSCLC's clinical behavior and its management, emphasizing the crucial role of personalized treatment strategies in oncology. This study also reinforces the importance of meticulous monitoring and periodic biopsies to detect resistance after treatment.

References

1. Suda K, Murakami I, Sakai K, *et al*. Small cell lung cancer transformation and T790M mutation: complimentary roles in acquired resistance to kinase inhibitors in lung cancer. Sci Rep 2015; (5)1: 14447.
2. Oser MG, Niederst MJ, Sequist LV, *et al*. Transformation from non-small- cell lung cancer to small-cell lung cancer: molecular drivers and cells of origin. Lancet Oncol 2015 April; 16(4): e165-e172.

3. Chen YJ, Roumeliotis T, Chang, YH, *et al*. Proteogenomics of non-smoking lung cancer in East Asia delineates molecular signatures of pathogenesis and progression. Cell 2020 July; 182: 226-44.
4. Tseng CH, Tsuang BJ, Chiang CJ, *et al*. The relationship between air pollution and lung vancer in nonsmokers in Taiwan. J Thorac Oncol 2019 May; 14(5): 784-92.
5. Guo H, Li H, Zhu L, *et al*. "How long have I got?" in stage IV NSCLC patients with at least 3 months up to 10 years survival, accuracy of long-, intermediate-, and short-term survival prediction is not good enough to answer this question. Front Oncol 2021 Dec; 11: 761042.
6. Sequist LV, Waltman BA, Dias-Santagata D, *et al*. Genotypic and histological evolution of lung cancers acquiring resistance to *EGFR* inhibitors. Sci Transl Med 2011 Mar; 3(75): 75ra26.
7. Zakowski MF, Ladanyi M, Kris MG. *EGFR* mutations in small-cell lung cancers in patients who have never smoked. N Engl J Med 2006 July; 355(2): 213-5.
8. Sutherland KD, Proost N, Brouns I, *et al*. Cell of origin of small cell lung cancer: inactivation of Trp53 and Rb1 in distinct cell types of adult mouse lung. Cancer Cell 2011; 19: 754-64.
9. Mainardi S, Mijimolle N, Francoz S, *et al*. Identification of cancer initiating cells in K-Ras driven lung adenocarcinoma. Proc Natl Acad Sci USA 2014; 111: 255-60.
10. Sutherland KD, Song JY, Kwon MC, *et al*. Multiple cells-of-origin of mutant K-Ras-induced mouse lung adenocarcinoma. Proc Natl Acad Sci USA 2014; 111: 4952-57.
11. Lin C, Song H, Huong C, *et al*. Alveolar type II cells possess the capability of initiating lung tumor development. PLoS One 2012; 7(12): e53817.
12. Wang S, Cang S, Liu D. Third-generation inhibitors targeting *EGFR* T790M mutation in advanced non-small cell lung cancer. J Hematol Oncol 2016 Apr 12; 9:34.
13. Leonetti A, Sharma S, Minari R, *et al*. Resistance mechanisms to osimertinib in *EGFR*-mutated non-small cell lung cancer. Br J Cancer 2019; 121(9): 725-37.
14. Ahn S, Hwang SH, Han J, Transformation to small cell lung cancer of pulmonary adenocarcinoma: clinicopathologic analysis of six cases. J Pathol Transl Med 2016 Jul; 50(4): 258-263.
15. Morinaga R, Okamoto I, Furuta K, *et al*. Sequential occurrence of non-small cell and small cell lung cancer with the same *EGFR* mutation. Lung Cancer 2007; 58(3): 411-413.
16. Sonoda T, Nishikawa S, Sakakibara R, *et al*. *EGFR* T790M mutation after chemotherapy for small cell lung cancer transformation of *EGFR*-positive non-small cell lung cancer. Respir Med Case Rep 2018; 24: 19-21.
17. Mansour MA, AboulMagd AM, Abbas SH. Insights into fourth generation selective inhibitors of (C797S) *EGFR* mutation combating non-small cell lung cancer resistance: a critical review. RSC Adv 2023; 13(277): 18825-18853.
18. Lim SM, Fujino T, Kim C, *et al*. BBT-176, a novel fourth-generation tyrosine kinase inhibitor for osimertinib-resistant *EGFR* mutations in non–small cell lung cancer. Clin Cancer Res 2023; 29(16): 3004-3016.
19. Xu L, Xu B, Wang J, *et al*. Recent advances of novel fourth generation *EGFR* inhibitors in overcoming C797S mutation of lung cancer therapy. Eur J Med Chem 2023 Jan; 245(Pt 1): 114900.
20. Lucas M, Merchant M, O'Connor M, *et al*. BDTX-1535, a fourth generation *EGFR* inhibitor, targeting intrinsic and acquired resistance mutations in NSCLC. Eur J Cancer 2022 Oct; 174(1):S22.
21. Kobayashi K. Primary resistance to *EGFR* tyrosine kinase inhibitors (TKIs): contexts and comparisons in *EGFR*-mutated lung cancer. J. Respir 2023; 3(4): 223-36.
22. Rafael Sierra J, Cepero V, Giordano S. Molecular mechanisms of acquired resistance to tyrosine kinase targeted therapy. Mol Cancer 2010 Apr 12; 9: 75.
23. Johnson M, Garassimo MC, Mok T, *et al*. Treatment strategies and outcomes for patients with *EGFR*-mutant non-small cell lung cancer resistant to *EGFR* tyrosine kinase inhibitors: focus on novel therapies. Lung Cancer 2022 Aug; 170: 41-51.
24. Passaro A, Janne PA, Mok T, *et al*. Overcoming therapy resistance in *EGFR*-mutant lung cancer. Nat Cancer 2021 Apr; 2(4): 377-391.
25. Fu K, Xie F, Wang F Therapeutic strategies for *EGFR*-mutated non-small cell lung cancer patients with osimertinib resistance. J Hematol Oncol 2022 Dec 8; 15(1): 173.